APPLICATION OF HUMAN LIVER STEM CELLS FOR RECEPTOR-MEDIATED TOXICOGENOMIC STUDY

By

Suntae Kim

A DISSERTATION

Submitted to
Michigan State University
in partial fulfillment of the requirements
for the degree of

DOCTOR OF PHILOSOPHY

Biochemistry and Molecular Biology - Environmental Toxicology

2011

ABSTRACT

APPLICATION OF HUMAN LIVER STEM CELLS FOR RECEPTOR-MEDIATED TOXICOGENOMIC STUDY

By

Suntae Kim

The high drug development failure rates, the large response discrepancy among test animal species to evaluate drug efficacy, and the lack of mechanism-based high-throughput screening recently prompted US and EU legislation recommend the development of reliable human *in vitro* models for toxicity testing to replace, reduce and refine animal testing. I*n vitro* models are widely used, but the abnormality of continuous cell lines and restricted acquisition, source inconsistency and instability of primary cells limit their use. Adult stem cells derived from intact human tissue provides an innovative alternative that may more accurately predict *in vivo* toxicity.

The objective of this research was to evaluate HL1-1 human hepatic stem cell line as a viable model for receptor-mediated toxicogenomic studies using the aryl hydrocarbon receptor (AhR) and peroxisome proliferator-activated receptor α (PPARα) as prototypical ligand activated transcription factors for comparative toxicogenomic investigation. AhR and PPARα are targets for environmental contaminants and pharmaceutical reagents and complementary species-specific hepatic responses are currently being studied.

Comprehensive time course and dose-response gene expression studies were conducted in HL1-1 cells to assess the differential gene expression elicited by AhR and PPARα ligands in comparison to other *in vitro* and *in vivo* models. Some conserved responses with overlapping biological functions were identified. Although subsets of conserved differentially expressed genes are consistent with the known *in vivo* responses, the results suggest that species- and model-specific gene expression profiles are linked to species-specific physiology.

HL1-1 cell were also immortalized by hTERT stable transfection (HLhT1) to overcome cell senescence and life span limitations. Immortalized HLhT1 cells maintain pluripotency characteristics as defined by stem cell and oval cell marker protein expression. The expression of functional AhR and PPARα and their ligand responsiveness is also comparable to the parental cell line. Collectively, human liver stem cells are viable models and warrant further development for mechanistic investigation of receptor-mediated hepatic toxicity and high throughput screening.

To my wife and family

ACKNOWLEDGMENTS

I received an invaluable life experience while obtaining by PhD degree at Michigan State University. Without the help and support from numerous outstanding individuals, I could not have accomplished it. I would like to thank all people who have offered encouragement and support and inspired me throughout my graduation program.

First, I would like to express my sincere and most heartfelt thanks to my advisor and mentor, Dr. Tim Zacharewski. He has provided me extraordinary opportunity to study in genomics, stem cell research and bioinformatics which are very advanced and promising field in biomedical research. He has been understanding and encouraging and has helped me to develop scientifically, intellectually and professionally. I could not complete this research without his tremendous supports.

I would also like to thank my Graduate Committee members, Drs. Kristina Chan, John LaPres, James Pestka and Kevin Walker for their availability, insight and unique perspectives in contributing to the success of my project during our meetings.

I would like to express my special thanks to Drs. CC Chang and Trosko and their lab for all supports and guidance in stem cell research with resources, techniques and advices.

I would like to thank all current and previous my lab members, Ania Kopec, Michelle Angrish, Agnes Forgacs, Rance Nault, Qi Ding, Lyle Burgoon, Ed Dere, Naoki Kiyosawa, Josh Kwekel, Bryan Mets, Cora Fong, Jeremy Burt, Darrell Boverhof and many others, including co-operative education students for their friendship, advice and support inside and outside of the lab.

I also owe my deepest gratitude to everyone who provides me tremendous efforts to review and help editing my humble English writing and presentations.

Also I would like send my gratitude to all Korean friends who work in biology fields and were met in Christian community at Michigan State University and University of Michigan. They are great fellows in both academically and socially, and make me and my family feel like at home country.

Finally, I wish to thank my family for their love and support. My parents, Jongkook Kim and Kyungbok Lee, my wife's parents, Youngsoo Bae and Kiok Ryu, and my brothers and their family gave me endless supports and encouragement for my study and taking care of our children. Thank you for encouraging me in the right direction and always supporting my choices. And to my wife Heekyong Bae who is outstanding researcher and the most faithful supporter, and my children, Ayn and Younghoo, you are the most precious gift I got through my PhD years.

TABLE OF CONTENTS

LIST OF TABLES

LIST OF FIGURES

LIST OF ABBREVIATIONS

ADMET	Absorption, distribution, metabolism, elimination and toxicity
AhR	Aryl hydrocarbon receptor
ANOVA	Analysis of variance
ARNT	Aryl hydrocarbon receptor nuclear translocator
Asc-2P	L-ascorbic acid 2-phosphate
bHLH/PAS	Basic helix-loop-helix/PER-ARNT-SIM
BP	Biological process
BW	Body weight
CC	Cellular component
cDNA	Complementary deoxyribonucleic acid
ChIP	Chromatin immunoprecipitation
CHX	Cycloheximide
CLO	Clofibrate
cpdl	Cumulative population doubling level
CV	Central vein
DAVID	Database for Annotation, Visualization and Integrated Discovery
dNTP	Deoxynucleotide triphosphate
DRE	Dioxin response element
DTT	Dithiothreitol
ED50	Effective dose 50
EDC	Endocrine disrupting chemical

EDSP	Endocrine disruptor screening program
EPA	Environmental Protection Agency
ES cell	Embryonic stem cell
EU	European Union
FBS	Fetal bovine serum
FN	Fibronectin
FNF	Fenofibrate
GO	Gene ontology
HGF	Hepatocyte growth factor
HSP	Heat shock protein
hTERT	Human telomertase reverse transciptase
IARC	International Agency for Research on Cancer
iPS cell	Induced pluripotent stem cell
KEGG	Kyoto Encyclopedia of Genes and Genomes
LDB	Ligand-binding domain
MCD	Methionine and choline deficient
MEM	Modified Eagle's minimum essential medium
MeV	Multiexperiment Viewer
MSC	Mesenchymal stem cells
MSS	Matrix similarity score
MTT	3-(4,5-dimethyl-2-thiazolyl)-2,5-diphenyl-2H tetrazorium bromide
NAC	N-acetyl-L-cysteine
NAFLD	Non-alcoholic fatty liver disease

NGS	Next generation sequencing
NR	Nuclear receptor
NRC	National Research Council
PCA	Principal component analysis
PND	Postnatal day
PP	peroxisome proliferator
PPARα	Peroxisome proliferator-activated receptor α
PPRE	Peroxisome proliferator response elements
PV	Portal vein
PWM	Position weight matrix
PXR	Pregnane X receptor
QRT-PCR	Quantitative real-time PCR
REACH	the Registration, Evaluation, Authorization, and Restriction of Chemicals
RLW	Relative liver weight
RXR	Retinoid X receptor
SD	Standard deviation
SDS	Sodium dodecyl sulfate
SE	Standard error
SNP	Single-nucleotide polymorphism
T	2,3,7,8-Tetrachlorodibenzo-p-dioxin
TCDD	2,3,7,8-Tetrachlorodibenzo-p-dioxin
TIMS	Toxicogenomic information management system
TSS	Transcription start sites

UCSC	University of California Santa Cruz
UTR	Untranslated region
V	Vehicle
VEH	Vehicle
WHO	World Health Organization
WY	Wy-14,643

CHAPTER 1

CHAPTER 1

REVIEW OF THE LITERATURE: APPLICATION OF HUMAN STEM CELL IN RECEPTOR MEDIATED TOXICITY

CURRENT NEEDS OF ALTERNATIVE METHODS FOR TOXICITY TESTS

Development of mechanism based alternative methods and *in vitro* models to replace/reduce/refine animal testing are a current issue to pharmaceutical and chemical industries and government. Pharmaceutical industries invest more than 20 billion US dollars annually for the development of novel drugs [1, 2]. New drug candidates must pass a series of preclinical tests and clinical trials in order to launch but less than 10% survive to reach the market [3]. Failures typically include safety problems and lack of effectiveness which are not predicted by tests in animal models before entering clinical trials. Toxicity of drug candidates is one of the most significant causes of attrition [4]. In many cases, the toxicity of candidate drugs is not detected until clinical trials and late stage failures contribute substantial costs of drug development. In order to improve success and reduce late stage attrition, earlier more accurate high throughput toxicity prediction is needed [5, 6].

Recent legislations in the European Union (EU) and US have bolstered alternative animal testing efforts. In 2006, the EU developed the Registration, Evaluation, Authorization, and Restriction of Chemicals (REACH) legislation which established provisions for improved identification of intrinsic properties of chemical substances. REACH places greater responsibility on industry to manage chemical risks and to provide additional safety information.

Estimated costs for registration and testing range from 2.3-100 billion Euro during the first 11 years [7]. Moreover, testing on animals for cosmetic purposes has been banned effective 2009, and requires the use of alternative methods [8]. In the US, the National Research Council (NRC) report "Toxicity Testing in the 21st Century: A Vision and a Strategy" recommends the development of novel tools and approaches including high-throughput *in vitro* methods, systems biology, and computer-based modeling for toxicity testing [9-11].

Endocrine disrupting chemicals (EDCs) are exogenous substances that alter functions of the endocrine system and consequently cause adverse health effects. EDCs include a wide variety of chemicals, such as natural and synthetic hormones, pesticides, industrial by-products, consumer products, and pollutants [12]. EDCs were declared a high research priority by the World Health Organization (WHO) in 2010 [13]. The US EPA has developed the Endocrine Disruptor Screening Program (EDSP), consisting of Tier 1 screening and Tier 2 testing, in order to be compliant with the Food Quality Protection Act and Safe Drinking Water Act amendments [14, 15]. Screening deficits for selected toxicities has prompted the need to develop new toxicity testing and assay methods approaches.

Traditional toxicological tests typically involve animal experiments including multi-generation studies which require a large number of animals, are time-consuming and result in high costs. As an alternative, *in vitro* systems are used to gain mechanistic understanding of the health effects for preclinical safety testing and i*n vivo* studies are then used to establish dose-limiting toxicity and identify target organs [16]. Alternative i*n vitro* methods have many advantages for toxicity testing including small set-ups minimal test substance requirements, lower costs, high numbers of replicates, miniaturization, and automation. In addition, emerging

novel technologies including imaging and comprehensive 'omic' technologies also stimulate developments of alternative methods.

TOXICOGENOMIC APPROACHES

Toxicogenomics is the study of the response of a genome to environmental stressors and toxicants. The ability to probe thousands of genes simultaneously has made genomics a prime technology for toxicology. Microarrays and other methods of gene expression profiling have served as useful tools for identifying the responses of toxicologically relevant genes and discerning the mechanisms invoking toxic effects. Moreover, toxicogenomics can identify biomarkers of disease and exposure to toxic substances. Toxicogenomic approaches are also highly sensitive and detect toxic responses at earlier time points and at lower doses than conventional approaches such as histopathology and clinical chemistry [17, 18]. Toxicogenomic studies are usually designed to correlate expression profiles with phenotype defined by conventional measures of toxicity. Phenotypic anchoring of molecular expression data involves determining the relationship between a particular expression profile and the pharmacological or toxicological phenotype of the organism.

A key goal in toxicogenomics is to integrate data from different studies and analytical platforms to produce a richer and biologically more refined understanding of the toxicological response [19]. It integrates genetics, genomic-scale mRNA expression (transcriptomics), protein expression (proteomics), metabolite profiling (metabonomics) and bioinformatics with conventional toxicology to identify molecular changes and elucidate molecular mechanisms of toxicity and disease causation [20-24]. Integration of data can provide a more complete picture of the expression profiles that are associated with a particular treatment. There are a number of

public repositories available that provide combined profile data with associated biological, chemical and toxicological endpoints (Table 1).

The rapid accumulation of genomic-sequence data and associated gene and protein annotation has catalyzed the application of gene-expression analysis to understanding the modes of action of chemicals and other environmental stressors on biological systems. Improvements of bioinformatics related on statistical analysis and presentation of microarray data make it easier to interpret 'omic' data. Prior to the current advances in bioinformatics, the most common way of reporting results of microarray studies involved listing differentially expressed genes, with little information about the statistical significance or biological pathways. New mathematical and graphical approaches have been developed to improve data presentation and interpretation. Furthermore, curated web-based tools and software applications have been developed to provide information on cellular location, physiological function, or disease association of a given gene (Table 1). These approaches for analysis of microarray data, initiate "pathway mapping" provide more biological relevance to the analyses. Moreover, predictive systems toxicology will gradually evolve, aided by knowledge that is systematically generated through literature mining, comparative analysis and iterative modeling of expression datasets.

Nuclear receptors (NRs) regulate numerous interacting biological processes, which confound the identification of key events and molecular targets related to toxicity [17]. Global genomic profiling approaches are required to comprehensively decipher intricate NRs regulation mechanisms.

NUCLEAR RECEPTORS AND ARYL HYDROCARBON RECEPTOR MEDIATED TOXICITY

Nuclear receptors are ligand-activated transcription factors involved in the regulation of specific target genes associated with metabolism, development, and cell differentiation [17].

Table 1. Online resources for toxicogenomic studies

Online Resource Name	URLs
Omic Data Resources	
GEO	http://www.ncbi.nlm.nih.gov/geo/
ArrayExpress	http://www.ebi.ac.uk/arrayexpress/
CEBS	http://www.niehs.nih.gov/research/resources/databases/cebs/
TG-GATES	http://toxico.nibio.go.jp/
SMD	http://smd.stanford.edu/
Gene Signature Resources	
DrugMatrix	https://ntp.niehs.nih.gov/drugmatrix/index.html
NextBio	http://www.nextbio.com/b/nextbio.nb
GeneSigDB	http://compbio.dfci.harvard.edu/genesigdb/
ArrayExpress	http://www.ebi.ac.uk/arrayexpress/
Connectivity Map	http://www.broadinstitute.org/genome_bio/connectivitymap.html
Toxicity Data Resources	
TOXNET	http://toxnet.nlm.nih.gov/
NTP database	http://ntp-apps.niehs.nih.gov/ntp_tox/index.cfm
Comparative Toxicogenomics Database (CTD)	http://ctd.mdibl.org/
ACToR	http://actor.epa.gov/actor/faces/ACToRHome.jsp
ToxRefDB	http://www.epa.gov/ncct/toxrefdb/
ExpoCast	http://www.epa.gov/ncct/expocast/
ToxCast	http://www.epa.gov/ncct/toxcast/
DssTox	http://www.epa.gov/ncct/dsstox/index.html
Carcinogen Potency Database	http://potency.berkeley.edu/

Table 1 (cont'd)

Online Resource Name	URLs
Gene Annotation Information	
UCSC Genome browser	http://www.genome.ucsc.edu/
NCBI Entrez Gene	http://www.ncbi.nlm.nih.gov/gene
OmicBrowser	http://omicspace.riken.jp/db/genome.html
Biological Ontology	
DAVID Bioinformatics	http://david.abcc.ncifcrf.gov/
Gene Ontology Database	http://www.geneontology.org/
Ingenuity	http://www.ingenuity.com/
GSEA	http://www.broadinstitute.org/gsea/index.jsp
GeneGo	http://www.genego.com/
Open Biomedical Ontologies	http://www.obofoundry.org/
CoPub	http://services.nbic.nl/copub/portal/
PantherDB	http://www.pantherdb.org/panther/ontologies.jsp
ToppGene	http://toppgene.cchmc.org/
Pathway Resources	
KEGG Pathway	http://www.genome.jp/kegg/pathway.html
Biocarta	http://www.biocarta.com/genes/allPathways.asp
GenMapp	http://www.genmapp.org/
Pathway Interaction Database	http://pid.nci.nih.gov/
Reactome	http://www.reactome.org/ReactomeGWT/entrypoint.html
NetPath	http://www.netpath.org/
WikiPathways	http://www.wikipathways.org/index.php/WikiPathways
SMPDB	http://www.smpdb.ca/
PantherDB	http://www.pantherdb.org/pathway/index.jsp

Endogenous or xenobiotic ligands bind the ligand-binding domain (LDB) at the carboxy terminus resulting in receptor activation. The activated receptor binds to recognition elements and recruits accessory proteins such as co-activators, co-repressors, and basal transcriptional factors to regulate target gene expression. NRs are attractive drug targets due to their regulatory role of a wide range of physiologic responses. In addition, many pharmaceutical agents along with environmental chemicals are NR ligands. Most adverse effects of EDCs are mediated by nuclear receptors and a number of therapeutic compounds including antibiotics, anticonvulsants, hypolipidemics, and cancer therapies target these receptors [25].

The peroxisome proliferator-activated receptors (PPARs) and pregnane X receptor (PXR) are members of the nuclear receptor superfamily that dimerize with the retinoid X receptor (RXR) and bind to specific regions on the DNA of target genes to modulate their expression. PPARs are known for their role in fatty acid metabolism and glucose homeostasis [26] and are useful drug targets for hyperlipidemia, diabetes and obesity. Additionally, the PXR plays an important role in xenobiotic sensing and regulation of genes involved in expression of phase I and II metabolizing enzymes to protect the liver and other organs from potentially harmful compounds [27-29]. PXR has a large number of exogenous ligands, many of which have been identified as endocrine-disrupting chemicals [17].

NRs and the aryl hydrocarbon receptor (AhR), a basic helix-loop-helix/PER-ARNT-SIM (bHLH/PAS) transcription factor, share similar modes of action as ligand-activated transcription factors which regulates the expression of genes involved in pleiotropic responses [17]. 2,3,7,8-Tetrachlorodibenzo-*p*-dioxin (TCDD) is the prototypical AhR ligand. It is a ubiquitous, bioaccumulative environmental contaminant that causes various effects including endocrine, immunotoxicity, hepatotoxicity, teratogenesis, and multi-site tumor promotion [30]. A variety of

studies have demonstrated the carcinogenicity of TCDD which acts as a multi-site carcinogen and liver tumor promoter in rodents [31]. TCDD was also listed as an established human carcinogen by the International Agency for Research on Cancer (IARC) in 1997 [32]. Most, if not all of these effects are mediated by the AhR [33].

Receptor-mediated effects are attractive targets for toxicity screening and drug development, due to their role as drug and environmental toxicant targets and their high association with the human diseases. Despite numerous studies assessing NR and AhR-mediated toxicity using animal models, extrapolation to humans has identified a significant number of discordances [34]. Although the AhR is evolutionary conserved, responses elicited by TCDD and related compounds vary widely across species [35-38]. Induction of PPARα by chronic exposure to the peroxisome proliferators (PPs) fibrate drugs resulted in peroxisome proliferation and the development of hepatocarcinomas in mice. However, primates and humans appear to be non-responsive to these adverse effects. Species differences in PPARα function, particularly between mice and humans, are attributed to the level of PPARα expression, ligand activation, and biological responses [39-42]. PPARα humanized mice results suggest that species differences in the receptor only partially explain the differential susceptibility [43].

CURRENT MODELS FOR RECEPTOR MEDIATED HEPATOTOXICITY

The liver is a vital organ essential for metabolism. It receives venous blood from the small intestine, stomach, pancreas and spleen containing high levels of nutrients, xenobiotics and other compounds. Due to reactive metabolite formation resulting from metabolism, the liver is a frequent target of toxicity. Most toxicogenomics studies so far have examined hepatotoxicants as the liver is the primary source of xenobiotic metabolism and detoxification and because liver injury is the principal reason for withdrawal of new drugs from the market. Notably, liver

toxicity and alterations of hepatic function are the most frequent reasons for pre-clinical drug development failure.

To assess the risk of specific compounds in humans, many toxicity studies are performed by animal tests. However, it is difficult to accurately predict the hepatotoxicity of new compounds in humans and is often observed only in the clinical trials. The underlying reason for this may be related to marked species differences and is due to extensive use of animal models. Due to species differences and to reduce animal use, there is a need for a reliable human *in vitro* hepatotoxicity test systems. Significant effort has been devoted to establish predictive human hepatic cell models that could be assayed *in vitro*. *In vitro* models such as continuous cell lines, primary cells and organ slices, have been used to investigate ADMET (absorption, distribution, metabolism, elimination and toxicity) properties[44]. The principle approach of *in vitro* models is to assess the mode of action, including toxicant-target interaction and dose/time dependent responses [45]. In general, the more similar the model system is to a human target tissue, the more likely the results will predict *in vivo* human responses. Therefore, mechanism-based approach using an *in vitro* model system derived from human target tissue will provide more accurate predictive models of *in vivo*, responses relevant to efficacy and safety [46]. Although *in vitro* models do not always replicated *in vivo* responses, human based *in vitro* models are more likely to predict *in vivo* human responses and are preferred to predict mechanism of action of the chemicals [6, 45, 47, 48].

Hepatocytes constitute 60% of the liver cell population (80% of the volume) and are the major functional cells performing metabolic, endocrine and secretory functions [49]. Typical available models are based on human cancer cell lines or primary cells isolated from biopsies, but these have significant drawbacks. For example, human hepatoma cell lines such as HepG2,

poorly replicate phenotypic and functional native hepatocytes [50-53]. Cancer cells may also have mutations that result in the loss of significant portions of a chromosome. The preferred option, with respect to functional differentiation, is human primary hepatocytes. However, availability, viability and variability limit their usefulness. Furthermore, the purity of the primary isolations is also a point of concern as related non-parenchymal cells contaminate the final cell preparations [45, 47, 54]. Primary hepatocytes also do not proliferate and gradually lose their metabolic activity after maintaining in the cell culture media several weeks [51].

Hence, there is a need for novel models for human hepatocytes. Since mature hepatocytes are difficult to maintain and grow *in vitro*, liver stem or precursor cells derived from adult liver are potential alternatives. Limitation of mature hepatocytes may be overcome by the generation of differentiated hepatocytes from adult or embryonic stem cells or immortalization of differentiated hepatocytes.

APPLICATION OF HUMAN STEM CELLS FOR TOXICOLOGY

Stem cells are undifferentiated cells with the capacity for unlimited or prolonged self-renewal and the ability to give rise to differentiated cells. The regenerative capacity of the liver is well established in models of partial hepatectomy or hepatotoxic injury [55, 56]. Evidence from several studies indicates the presence of resident stem cells in the adult liver [49, 57-59] and the oval cells located in the canals of Herring or Cholangioles appear to represent the progeny of pluripotential liver stem cells which are capable of generating hepatic lineages.

Stem cells have the capacity of self-renewal and differentiation into virtually any cell type making them an attractive *in vitro* model. Human stem cells provide an attractive *in vitro* alternative and a potentially unlimited source of human cells [60, 61]. Normal adult human stem cells isolated from liver tissue might provide an alternative system which can proliferate and

closely mimics human responses [60, 62, 63]. Another advantage is the use of cells derived from a single stem cell line which would minimize donor and preparation variability. Moreover, there is increasing evidence that the origin of cancer is the adult stem cell population and their derivatives, which are targets for transforming mutations/epigenetic changes [64, 65].

Genomic profiling of nuclear receptor-mediated responses following toxicant exposure has confirmed the role of nuclear receptors in maintaining homeostatic conditions and mediating toxicity, distinguishing chemicals with similar or diverse mechanisms of toxicity and identifying potential gene expression markers of toxicity [17, 18]. Genomics can effectively be used *in vitro* and across non-rodent animal models to confirm pathways of toxicity. Mechanism-based approaches for *in vitro* model system may also lead to predictive models for toxicity screening [66]. The application of a toxicogenomic approach to human liver stem cells will provide global gene expression profiles leading to species comparison and the identification of species specific molecular mechanisms of toxicity. Taken together, toxicogenomic approach to human liver stem cells is a novel toxicity screening assay to identify mechanistically-based mode of action for early nuclear receptor-mediated toxicity. The use of human stem cells technologies could aid in toxicity testing during drug development and reduce the need for *in vivo* testing.

REFERENCES

REFERENCES

1. Morgan, S., et al., *The cost of drug development: a systematic review.* Health Policy, 2011. **100**(1): p. 4-17.

2. Dimasi, J.A., *Risks in new drug development: approval success rates for investigational drugs.* Clin Pharmacol Ther, 2001. **69**(5): p. 297-307.

3. DiMasi, J.A., et al., *Trends in risks associated with new drug development: success rates for investigational drugs.* Clin Pharmacol Ther, 2010. **87**(3): p. 272-7.

4. Watkins, P.B., *Drug safety sciences and the bottleneck in drug development.* Clin Pharmacol Ther, 2011. **89**(6): p. 788-90.

5. Dalgetty, D.M., et al., *Progress and future challenges in stem cell-derived liver technologies.* Am J Physiol Gastrointest Liver Physiol, 2009. **297**(2): p. G241-8.

6. Pritchard, J.F., et al., *Making better drugs: Decision gates in non-clinical drug development.* Nat Rev Drug Discov, 2003. **2**(7): p. 542-53.

7. Williams, E.S., J. Panko, and D.J. Paustenbach, *The European Union's REACH regulation: a review of its history and requirements.* Crit Rev Toxicol, 2009. **39**(7): p. 553-75.

8. Taylor, K., C. Casalegno, and W. Stengel, *A critique of the EC's expert (draft) reports on the status of alternatives for cosmetics testing to meet the 2013 deadline.* ALTEX, 2011. **28**(2): p. 131-48.

9. Gibb, S., *Toxicity testing in the 21st century: a vision and a strategy.* Reprod Toxicol, 2008. **25**(1): p. 136-8.

10. Krewski, D., et al., *Toxicity testing in the 21st century: implications for human health risk assessment.* Risk Anal, 2009. **29**(4): p. 474-9.

11. Dix, D.J., et al., *The ToxCast program for prioritizing toxicity testing of environmental chemicals.* Toxicol Sci, 2007. **95**(1): p. 5-12.

12. Soto, A.M. and C. Sonnenschein, *Environmental causes of cancer: endocrine disruptors as carcinogens.* Nat Rev Endocrinol, 2010. **6**(7): p. 363-70.

13. Alonso-Magdalena, P., I. Quesada, and A. Nadal, *Endocrine disruptors in the etiology of type 2 diabetes mellitus.* Nat Rev Endocrinol, 2011.

14. Stokes, W.S., *Selecting appropriate animal models and experimental designs for endocrine disruptor research and testing studies.* ILAR J, 2004. **45**(4): p. 387-93.

15. Willett, C.E., P.L. Bishop, and K.M. Sullivan, *Application of an integrated testing strategy to the U.S. EPA endocrine disruptor screening program.* Toxicol Sci, 2011. **123**(1): p. 15-25.

16. Hartung, T., *From alternative methods to a new toxicology.* Eur J Pharm Biopharm, 2011. **77**(3): p. 338-49.

17. Woods, C.G., J.P. Heuvel, and I. Rusyn, *Genomic profiling in nuclear receptor-mediated toxicity.* Toxicol Pathol, 2007. **35**(4): p. 474-94.

18. Morgan, K.T., et al., *The hepatic transcriptome as a window on whole-body physiology and pathophysiology.* Toxicol Pathol, 2005. **33**(1): p. 136-45.

19. Waters, M.D. and J.M. Fostel, *Toxicogenomics and systems toxicology: aims and prospects.* Nat Rev Genet, 2004. **5**(12): p. 936-48.

20. Tennant, R.W., *The National Center for Toxicogenomics: using new technologies to inform mechanistic toxicology.* Environ Health Perspect, 2002. **110**(1): p. A8-10.

21. Mattes, W.B., et al., *Database development in toxicogenomics: issues and efforts.* Environ Health Perspect, 2004. **112**(4): p. 495-505.

22. Gant, T.W. and S.D. Zhang, *In pursuit of effective toxicogenomics.* Mutat Res, 2005. **575**(1-2): p. 4-16.

23. Boverhof, D.R. and T.R. Zacharewski, *Toxicogenomics in risk assessment: applications and needs.* Toxicol Sci, 2006. **89**(2): p. 352-60.

24. Carlson, E.A. and J.B. Silkworth, *Toxicogenomics in human health risk assessment.* Toxicol Appl Pharmacol, 2009. **236**(2): p. 254-6; author reply 257-60.

25. Moore, J.T., J.L. Collins, and K.H. Pearce, *The nuclear receptor superfamily and drug discovery.* ChemMedChem, 2006. **1**(5): p. 504-23.

26. Dreyer, C., et al., *Control of the peroxisomal beta-oxidation pathway by a novel family of nuclear hormone receptors.* Cell, 1992. **68**(5): p. 879-87.

27. Kretschmer, X.C. and W.S. Baldwin, *CAR and PXR: xenosensors of endocrine disrupters?* Chem Biol Interact, 2005. **155**(3): p. 111-28.

28. Timsit, Y.E. and M. Negishi, *CAR and PXR: the xenobiotic-sensing receptors.* Steroids, 2007. **72**(3): p. 231-46.

29. Matic, M., et al., *Pregnane X receptor: promiscuous regulator of detoxification pathways.* Int J Biochem Cell Biol, 2007. **39**(3): p. 478-83.

30. Denison, M.S. and S. Heath-Pagliuso, *The Ah receptor: a regulator of the biochemical and toxicological actions of structurally diverse chemicals.* Bull Environ Contam Toxicol, 1998. **61**(5): p. 557-68.

31. Knerr, S. and D. Schrenk, *Carcinogenicity of 2,3,7,8-tetrachlorodibenzo-p-dioxin in experimental models.* Mol Nutr Food Res, 2006. **50**(10): p. 897-907.

32. McHale, C.M., et al., *Microarray analysis of gene expression in peripheral blood mononuclear cells from dioxin-exposed human subjects.* Toxicology, 2007. **229**(1-2): p. 101-13.

33. Okey, A.B., *An aryl hydrocarbon receptor odyssey to the shores of toxicology: the Deichmann Lecture, International Congress of Toxicology-XI.* Toxicol Sci, 2007. **98**(1): p. 5-38.

34. Olson, H., et al., *Concordance of the toxicity of pharmaceuticals in humans and in animals.* Regul Toxicol Pharmacol, 2000. **32**(1): p. 56-67.

35. Silkworth, J.B., et al., *Comparison of TCDD and PCB CYP1A induction sensitivities in fresh hepatocytes from human donors, sprague-dawley rats, and rhesus monkeys and HepG2 cells.* Toxicol Sci, 2005. **87**(2): p. 508-19.

36. Boverhof, D.R., et al., *Comparative toxicogenomic analysis of the hepatotoxic effects of TCDD in Sprague Dawley rats and C57BL/6 mice.* Toxicol Sci, 2006. **94**(2): p. 398-416.

37. Nohara, K., et al., *Comparison of the 2,3,7,8-tetrachlorodibenzo-p-dioxin (TCDD)-induced CYP1A1 gene expression profile in lymphocytes from mice, rats, and humans: most potent induction in humans.* Toxicology, 2006. **225**(2-3): p. 204-13.

38. Kransler, K.M., B.P. McGarrigle, and J.R. Olson, *Comparative developmental toxicity of 2,3,7,8-tetrachlorodibenzo-p-dioxin in the hamster, rat and guinea pig.* Toxicology, 2007. **229**(3): p. 214-25.

39. Lawrence, J.W., et al., *Differential gene regulation in human versus rodent hepatocytes by peroxisome proliferator-activated receptor (PPAR) alpha. PPAR alpha fails to induce peroxisome proliferation-associated genes in human cells independently of the level of receptor expresson.* J Biol Chem, 2001. **276**(34): p. 31521-7.

40. Klaunig, J.E., et al., *PPARalpha agonist-induced rodent tumors: modes of action and human relevance.* Crit Rev Toxicol, 2003. **33**(6): p. 655-780.

41. Ammerschlaeger, M., et al., *Characterization of the species-specificity of peroxisome proliferators in rat and human hepatocytes.* Toxicol Sci, 2004. **78**(2): p. 229-40.

42. Gonzalez, F.J. and Y.M. Shah, *PPARalpha: Mechanism of species differences and hepatocarcinogenesis of peroxisome proliferators.* Toxicology, 2007.

43. Morimura, K., et al., *Differential susceptibility of mice humanized for peroxisome proliferator-activated receptor alpha to Wy-14,643-induced liver tumorigenesis.* Carcinogenesis, 2006. **27**(5): p. 1074-80.

44. Li, A.P., *Screening for human ADME/Tox drug properties in drug discovery.* Drug Discov Today, 2001. **6**(7): p. 357-366.

45. MacGregor, J.T., et al., *In vitro human tissue models in risk assessment: report of a consensus-building workshop.* Toxicol Sci, 2001. **59**(1): p. 17-36.

46. Burczynski, M.E., et al., *Toxicogenomics-based discrimination of toxic mechanism in HepG2 human hepatoma cells.* Toxicol Sci, 2000. **58**(2): p. 399-415.

47. Abbott, A., *Cell culture: biology's new dimension.* Nature, 2003. **424**(6951): p. 870-2.

48. MacGregor, J.T., *SNPs and chips: genomic data in safety evaluation and risk assessment.* Toxicol Sci, 2003. **73**(2): p. 207-8.

49. Tanaka, M., et al., *Liver stem/progenitor cells: their characteristics and regulatory mechanisms.* J Biochem, 2011. **149**(3): p. 231-9.

50. Harris, A.J., S.L. Dial, and D.A. Casciano, *Comparison of basal gene expression profiles and effects of hepatocarcinogens on gene expression in cultured primary human hepatocytes and HepG2 cells.* Mutat Res, 2004. **549**(1-2): p. 79-99.

51. Wilkening, S., F. Stahl, and A. Bader, *Comparison of primary human hepatocytes and hepatoma cell line Hepg2 with regard to their biotransformation properties.* Drug Metab Dispos, 2003. **31**(8): p. 1035-42.

52. Zhang, Z.Y., et al., *Preferential inducibility of CYP1A1 and CYP1A2 by TCDD: differential regulation in primary human hepatocytes versus transformed human cells.* Biochem Biophys Res Commun, 2006. **341**(2): p. 399-407.

53. Guillouzo, A., et al., *The human hepatoma HepaRG cells: a highly differentiated model for studies of liver metabolism and toxicity of xenobiotics.* Chem Biol Interact, 2007. **168**(1): p. 66-73.

54. Boess, F., et al., *Gene expression in two hepatic cell lines, cultured primary hepatocytes, and liver slices compared to the in vivo liver gene expression in rats: possible implications for toxicogenomics use of in vitro systems.* Toxicol Sci, 2003. **73**(2): p. 386-402.

55. Alison, M.R., S. Islam, and S. Lim, *Stem cells in liver regeneration, fibrosis and cancer: the good, the bad and the ugly.* J Pathol, 2009. **217**(2): p. 282-98.

56. Michalopoulos, G.K. and M.C. DeFrances, *Liver regeneration.* Science, 1997. **276**(5309): p. 60-6.

57. Herrera, M.B., et al., *Isolation and characterization of a stem cell population from adult human liver.* Stem Cells, 2006. **24**(12): p. 2840-50.

58. Gaudio, E., et al., *New insights into liver stem cells.* Dig Liver Dis, 2009. **41**(7): p. 455-62.

59. Zhang, L., et al., *The stem cell niche of human livers: symmetry between development and regeneration.* Hepatology, 2008. **48**(5): p. 1598-607.

60. Rohwedel, J., et al., *Embryonic stem cells as an in vitro model for mutagenicity, cytotoxicity and embryotoxicity studies: present state and future prospects.* Toxicol In Vitro, 2001. **15**(6): p. 741-53.

61. Davila, J.C., et al., *Use and application of stem cells in toxicology.* Toxicol Sci, 2004. **79**(2): p. 214-23.

62. Rolletschek, A., P. Blyszczuk, and A.M. Wobus, *Embryonic stem cell-derived cardiac, neuronal and pancreatic cells as model systems to study toxicological effects.* Toxicol Lett, 2004. **149**(1-3): p. 361-9.

63. Carere, A., A. Stammati, and F. Zucco, *In vitro toxicology methods: impact on regulation from technical and scientific advancements.* Toxicol Lett, 2002. **127**(1-3): p. 153-60.

64. Ahuja, Y.R., V. Vijayalakshmi, and K. Polasa, *Stem cell test: a practical tool in toxicogenomics.* Toxicology, 2007. **231**(1): p. 1-10.

65. Alison, M.R. and M.J. Lovell, *Liver cancer: the role of stem cells.* Cell Prolif, 2005. **38**(6): p. 407-21.

66. Suk, W.A., K. Olden, and R.S. Yang, *Chemical mixtures research: significance and future perspectives.* Environ Health Perspect, 2002. **110 Suppl 6**: p. 891-2.

CHAPTER 2

CHAPTER 2

RATIONALE, HYPOTHESIS AND SPECIFIC AIMS

RATIONALE

Receptor-mediated toxicity is an attractive target for toxicity test and drug development, since receptors are a major drug and toxicant target and due to their high association with human diseases. Numerous studies to assess nuclear receptor and AhR-mediated toxicity have used animal models. However, extrapolating animal model data to humans has limited success [1]. Alternatively, the use of *in vitro* human-based model systems has focused more attention in toxicity tests [2]. Even though human-derived continuous cells, primary cells and tissue slice have been used toxicity testing, they are limited by abnormalities introduced into continuous cell lines, and the cost, instability and availability of primary cells/tissue model systems [3-5]. Therefore, more efficient and reliable, high throughput human-derived *in vitro* model system to assess the human toxicity warrant developed. This study will focus on developing a novel *in vitro* model system for receptor-mediated toxicity screening employing normal human liver stem cells isolated from adult liver tissue, an attractive alternative that provides high proliferative capacity and an origin from normal liver tissue.

HYPOTHESIS

Normal adult human liver stem cells are a viable *in vitro* model for receptor-mediated human gene response study related with toxicity.

SPECIFIC AIMS

To address this hypothesis, the following specific aims with human liver stem cell characterization and engineering, and cross-model & cross-species comparative toxicogenomic analysis will be used:

1. Evaluate HL1-1 cells as an *in vitro* receptor-mediated toxicity model system by determining the expression and functionality of AhR and PPARα and cell engineering for its practical application.
2. Establish baseline quantitative temporal and dose-dependent data on global gene expression in HL1-1 human cells elicited by AhR agonists and evaluate the model-specific and model-conserved gene expression responses.
3. Establish baseline quantitative temporal data on the hepatic effects elicited by PPARα agonists in an *in vivo* mouse model and on gene expression in HL1-1 human cells and evaluate the model-specific and model-conserved gene expression responses.

REFERENCES

REFERENCES

1. Olson, H., et al., *Concordance of the toxicity of pharmaceuticals in humans and in animals.* Regul Toxicol Pharmacol, 2000. **32**(1): p. 56-67.

2. Li, A.P., *Screening for human ADME/Tox drug properties in drug discovery.* Drug Discov Today, 2001. **6**(7): p. 357-366.

3. MacGregor, J.T., et al., *In vitro human tissue models in risk assessment: report of a consensus-building workshop.* Toxicol Sci, 2001. **59**(1): p. 17-36.

4. Abbott, A., *Cell culture: biology's new dimension.* Nature, 2003. **424**(6951): p. 870-2.

5. Boess, F., et al., *Gene expression in two hepatic cell lines, cultured primary hepatocytes, and liver slices compared to the in vivo liver gene expression in rats: possible implications for toxicogenomics use of in vitro systems.* Toxicol Sci, 2003. **73**(2): p. 386-402.

CHAPTER 3

CHAPTER 3

EVALUATION OF HUMAN ADULT HEPATIC STEM CELLS AS AN *IN VITRO* RECEPTOR-MEDIATED TOXICOGENOMIC MODEL AND THEIR CELL ENGINEERING FOR IMMORTALIZATION

ABSTRACT

Primary and continuous cell lines are valuable *in vitro* models that have been widely used to provide insights into mechanisms of toxicity. However the abnormality of continuous cell lines and a high cost and instability of primary cells limit their use as ideal model systems. The availability of human adult stem cells provides an innovative *in vitro* model that may more accurately predict *in vivo* toxicity. In this study, the human hepatic adult stem cell line, HL1-1, was assessed as a viable model for receptor-mediated toxicogenomic studies. Furthermore, HL1-1 cell were immortalized by hTERT stable transfection (HLhT1) to overcome its limited application due to cell senescence and limited life span. The mRNA and protein expression levels of the Aryl hydrocarbon receptor (AhR) and nuclear receptors (PPARα and γ, ERα and PXR) were measured using QRT-PCR and Western blots, respectively in HL-1 and HLhT1 cells. The functionality of each receptor was assessed by treatment with prototypical agonist for each receptor and monitoring gene expression changes with QRT-PCR. TCDD, clofibrate and rifampicin were used as prototypical agonists and changes in mRNA expression of CYP1A1 (AhR), CPT1A (PPARα), and CYP3A4 (PXR) were evaluated. Expression level and responsiveness of the AhR and PPARα was confirmed in HL1-1 cells, however no changes were observed for the PXR. The immortalized HLhT1 cell maintains comparable expression of stem

cell and oval cell marker proteins (OCT4, AFP, VIM and THY1) relative to the parental cells. In addition, HLhT1 cell express functional AhR and PPAR and their responsiveness is also comparable to the parental cell line. Collectively, human liver stem cells, HL1-1 and HLhT1, are promising toxicogenomic models for mechanistic investigation of receptor-mediated hepatic toxicity.

INTRODUCTION

The liver is a central organ essential for the metabolism. The blood entering the liver consists of 75% of venous blood from the portal vein and 25% of arterial blood from the hepatic artery. All of the venous blood returning from the small intestine, stomach, pancreas and spleen converge into the portal vein and the liver receive all absorbed nutrients and xenobiotics. Hepatic metabolism leads to formation of reactive metabolites and it make liver as a frequent toxicity target. Liver toxicity and alterations of liver function are the most frequently occurring reasons for toxicology among drug molecules. However, it is difficult to predict hepatotoxic actions of new compounds in humans, because it is mainly related to distinct species differences and toxicity tests are based on the extensive use of animal models. Consequently, there is a demand for a reliable human test system and much effort has been directed to establish predictive human hepatic cell populations. The preferred human *in vitro* models are primary hepatocytes and hepatoma cell lines, but these have significant demerits. Continuous cell lines, while convenient for assessing the mechanistic toxicity, are mostly derived from diseased tissue or are transformed, which may lead to abnormal responses [1, 2]. The best option today, regarding functional aspect, is isolated human primary hepatocytes, but issues related to their acquisition, instability and variability from various source cause practical constraints that limit their application. Hence, there is a great need for novel improved models for human hepatocytes.

Liver stem cells derived from the human liver tissue are a valuable for novel human *in vitro* hepatic models and a potentially unlimited source of human cells [3, 4]. Stem cells are generally defined as clonogenic cells capable of both self-renewal and multilineage differentiation. In the adult organism, stem cells mediate tissue homeostasis and repair, e.g. the regenerative capacity of the liver is well established in models of partial hepatectomy or hepatotoxic injury [5, 6]. The isolation and culture of liver stem cells from various sources have been reported [7-11]. Human liver stem cells have lot of advantages including the fact that they are non-transformed intact cells from human tissue with proliferating and differentiation ability. Moreover, there is an increasing evidence on the origin of cancer in adult stem cell populations and their derivatives, which are the target of transforming mutations and epigenetic changes [12, 13]. Thus, they could be a potential direct target for certain toxic end points, such as tumor development.

Receptor-mediated toxicity is an attractive target for toxicity screening assays and drug development, due to the role of receptors as a major drug and environmental toxicant target and their high association with the human diseases. A number of therapeutic compounds including hypolipidemic agents, antibiotics, cancer therapies, and anticonvulsants target nuclear receptor [15]. Nuclear receptors are members of a superfamily of ligand-activated transcription factors, which are involved in the regulation of specific target genes associated with metabolism, development, and cell differentiation [14]. Endogenous or xenobiotic ligands bind the ligand-binding domain of the receptor resulting in activation of the receptor. Activated receptor binds to recognition elements, recruits accessory proteins such as co-activators, co-repressors, and basal transcriptional factors to regulate the expression of target genes.

The peroxisome proliferator-activated receptors (PPARs) are known for their role in fatty acid metabolism and glucose homeostasis [16] and have been identified as useful drug targets for hyperlipidemia, diabetes and obesity. Long-term treatment of peroxisome proliferators (PPs) in rodents results in the formation of hepatocellular tumors by a non-genotoxic mechanism, while humans appear to be non-responsive to these adverse effects. The pregnane X receptor (PXR) plays an important role in xenobiotic sensing and regulation of genes involved in phase I and II metabolizing enzymes to protect the liver and other organs from potentially harmful compounds [17-19]. PXR has a large number of exogenous ligands, many of which have been identified as endocrine-disrupting chemicals [14]. NRs and the aryl hydrocarbon receptor (AhR) share similar mode of action as ligand-activated transcription factors. 2,3,7,8-Tetrachlorodibenzo-*p*-dioxin (TCDD) is the prototypical AhR ligand [20]. TCDD is ubiquitous and bioaccumulates in the environment causing various adverse and biological effects in experimental animals and humans including endocrine, immuno- and hepato- toxicity, teratogenesis, and multi-site tumor promotion [21, 22].

In this study, HL1-1 human adult liver stem cells are evaluated as a novel model for receptor-mediated toxicogenomic studies. Also, a clonal population of immortalized cells, referred to as immortalized HL1-1 (HLhT1) cells, was obtained and characterized. These liver stem cells isolated from adult liver tissue could be served as novel human *in vitro* models to elucidate molecular mechanism of receptors-mediated conserved and divergent responses between species.

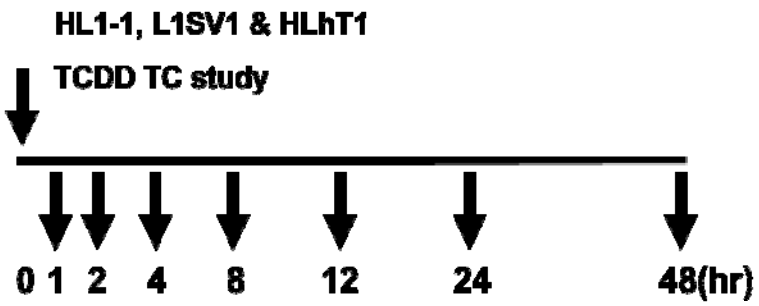

Figure 1. TCDD time course study design for cell line comparison.
Cells were treated with either 10 nM TCDD or 0.1% DMSO and harvested at 1, 2, 4, 8, 12, 24, or 48 hrs post-treatment. N = 3.

MATERIALS & METHODS

CULTURE AND TREATMENT OF CELL LINE

HL1-1, L1SV1 and HLhT1 cells were maintained in a modified MCDB 153 media (Keratinocyte-SFM, Invitrogen Corporation, Carlsbad, CA) supplemented with *N*-acetyl-*L*-cysteine (NAC) (2 mM), L-ascorbic acid 2-phosphate (Asc-2P) (0.2 mM), nicotinamide (5 mM) (referred to as K-NAC medium) [23]. The calcium concentration of this medium is 0.09 mM. The growth factors/hormones in the culture medium include rEGF (5 ng/mL), bovine pituitary extract (50 mg/mL) and 10% fetal bovine serum (FBS) (Hyclone, Logan, UT). NAC, a potent antioxidant, found to promote the self-renewal of glial precursor cells [24]. Asc-2P is a stable precursor to provide a constant concentration of ascorbate in the culture medium and ascorbate promotes cell growth and cell viability maintenance [25]. Nicotinamide is the poly (ADP-ribose) polymerase inhibitor and is known to prolong survival of primary cultured hepatocyte [26, 27]. D medium is utilized for cell life span expanding study and is a modified Eagle's minimum essential medium (MEM) medium supplemented with 5% FBS, NAC (2mM), Asc-2P (0.2mM). HepG2 cell lines were maintained in phenol-red free DMEM/F12 media (Invitrogen) supplemented with 5% FBS (Hyclone). Combined antibiotics (50 μg/mL gentamycin (Invitrogen), 100 U/mL penicillin and 100 μg/mL streptomycin (Invitrogen)) were applied for all cell culture media. For the chemical treatment, 1×10^6 cells were seeded into a 25 cm^2 cell culture flask (#430639, vent cap) (Corning Inc., Corning, NY) and incubated under standard conditions (5% CO_2, 37°C). For the receptor response studies, cells were treated with 10 nM TCDD, 50 μM Wy-14,643 (Sigma-Aldrich), 30 μM rifampicin (Sigma-Aldrich), or DMSO (Sigma-Aldrich) vehicle treatment and harvested at 24 or 48 h post-treatment. For the TCDD

time course studies, cells were treated with 10 nM TCDD or DMSO (Sigma-Aldrich) vehicle treatment and harvested at 1, 2, 4, 8, 12, 24 or 48 h post-treatment (Figure 1).

PROLIFERATION POTENTIAL OF HL1-1 CELL

The cumulative population doubling level (cpdl) determined to examine proliferation potential of HL1-1 cell. From the earliest passage of HL1-1 (cpdl = 26.5) stock, $1X10^5$ cells of were plated in 75 cm^2 flask (#431464, vent cap) (Corning Inc., Corning, NY) and grown in K-NAC medium containing 10% FBS until near confluence. To quantify the final cell yield they are subcultured continuously until no change in cpdl. The population doubling (pd) at each subculture was calculated by using the following equation: $pd = \ln (N_f / N_i)/\ln 2$, where N_i and N_f are initial and final cell numbers, respectively, and ln is the natural log. The pds of continuous subculture were added to obtain cpdl.

IMMORTALIZATION OF LIVER CELLS

Early passage HL1-1 cells were plated in three 60 mm plate ($5x10^5$ per plate). After overnight incubation, the cells were transfected with the human telomerase reverse transcriptase plasmid (pBabe-hygro-hTERT, a gift from Robert A. Weinberg, The Whitehead Institute for Biomedical Research, Department of Biology, Massachusetts Institute of Technology, Cambridge, MA) by Lipofectamine (Life Technologies, Inc., Gaithersburg, MD) (Figure 2). After 4 days incubation in the K-NAC medium, stably transfected clonal populations were selected in 100 mg/ml of hygromycin (Sigma-Aldrich). The surviving actively proliferating clonal cultures were established by the trypsin glass ring cloning of drug-resistant colonies and propagated to sufficient number of cells for storage in liquid nitrogen. After selection, these cells were used for determination of proliferation potential and further characterizations and were

compared with parental HL1-1 cells and the L1SV1 cells, another immortalized cell line transformed with simian virus 40 large T antigen (SV40T).

PROTEIN PREPARATION AND WESTERN BLOT

Cell and tissue lysates for Western blot analysis were prepared in RIPA buffer (1x PBS, 0.1% SDS, 1% IGEPAL CA-630 and 0.5% Na-Deoxycholate) with protease inhibitor cocktail tablet (Roche Diagnostics, Mannheim, Germany) and quantified using the modified Lowry assay (Bio-Rad, DC Protein Assay, Hercules, CA). Cell lysate proteins were electrophoretically separated on a denaturing 12% SDS-polyacrylamide gel and transferred onto nitrocellulose membrane (Amersham Biosciences Inc., Piscataway, NJ). The membranes were probed with anti-human AhR (N-19), PPAR-α (H-98), PPAR-γ (H-100), ER-α (H-184) and PXR (N-19) antibody followed by horseradish peroxidase-conjugated secondary antibodies (Santa Cruz Biotechnology Inc., Santa Cruz, CA). Immunochemical staining and fluorescence detection on X-ray film was performed using the SuperSignal West Dura substrate (Thermo Fisher Scientific, Inc., Waltham, MA).

RNA ISOLATION AND QUANTITATIVE REAL-TIME PCR ANALYSIS

Cells were harvested by scraping in the presence of TRIzol® Reagent (Invitrogen) and preserved at -80^{o}C until RNA isolation. Total RNA was isolated according to the manufacturer's protocol and resuspended in RNA Storage Solution (Ambion Inc., Austin, TX). The RNA samples were quantified spectrophotometrically (A_{260}) and assessed for purity by A_{260}/A_{280} ratio and by visual inspection on a denaturing agarose gel. Quantitative real-time PCR (QRT-PCR) was performed as verification of microarray data for selected genes. For each sample, 1.5 μg of total RNA was reverse transcribed by SuperScript II reverse transcriptase

(Invitrogen) using an anchored oligo-dT primer as described by the manufacturer's instructions. 1.5 μL of cDNA template was used in a 30 μL PCR reaction containing 0.1 μM of forward and reverse gene-specific primers designed using Primer3 [28] and SYBR Green PCR reaction mixture (Applied Biosystems, Foster City, CA). PCR amplification was conducted in MicroAmp Optical 96-well reaction plates (Applied Biosystems) on an Applied Biosystems PRISM 7500 Sequence Detection System. A dissociation protocol was performed to assess the specificity of the primers and the uniformity of the PCR products. Target gene cDNAs were quantified using a standard curve of log copy number versus threshold cycle (Ct). The copy number of each sample was standardized to the geometric mean of β-actin (ACTB) and glyceraldehyde-3-phosphate dehydrogenase (GAPDH), to control for differences in RNA loading, quality, and cDNA synthesis [29]. For graphing purposes, the relative gene expression levels were scaled such that the expression level of the time-matched vehicle treated control group was equal to 1. Official gene names and abbreviations, forward and reverse primer sequences, and product length for the genes verified by QRT-PCR are listed in Table 2.

RESULTS

RECEPTOR EXPRESSION AND FUNCTIONALITY OF IN HL1-1 CELLS

In order to assess HL1-1 cells as a feasible model for receptor-mediated toxicogenomic studies, basal expression levels of nuclear receptors and AhR were evaluated. Both mRNA and protein levels were analyzed by QRT-PCR and Western blotting, respectively. The basal transcripts of the AhR, ERα, PPARα and γ and PXR were measured in normal proliferating HL1-1 cells by QRT-PCR (Figure 3A). The purity of PCR product was inspected by the dissociation curve analysis and agarose gel electrophoresis (Figure 3B). The AhR expression was shown to be highest and the expression levels of ERα and PXR were the lowest based on

Table 2. Gene names and primer sequences for QRT-PCR

RefSeq	Gene name	Gene symbol	Entrez Gene ID	Forward Primer	Reverse Primer	Product Size (bp)
NM_001101	actin, beta	ACTB	60	CATCCCCCAA AGTTCACAAT	AGTGGGGTGG CTTTTAGGAT	125
NM_002046	glyceraldehyde-3-phosphate dehydrogenase	GAPDH	2597	GGCCTCCAAG GAGTAAGACC	AGGGGTCTAC ATGGCAACTG	147
NM_005036	peroxisome proliferative activated receptor, alpha	PPARA	65260	GCAGAAACCC AGAACTCAGC	ATGGCCCAGT GTAAGAAACG	141
NM_000778	cytochrome P450, family 4, subfamily A, polypeptide 11	CYP4A11	1579	GAGGAATGCC TTTCACCAGA	GTTGAGCCTTC CTCAGTTGG	125
NM_001122	adipose differentiation-related protein	ADFP	123	ACACCCTCCTG TCCAACATC	GCATTGCGGA ACACTGAGTA	103
NM_001621	aryl hydrocarbon receptor	AHR	157873	TGTTGGACGTC AGCAAGTTC	TGGTGCCCAG AATAATGTGA	197
NM_005037	peroxisome proliferative activated receptor, gamma	PPARG	109732	TGCAGGTGATC AAGAAGACG	TGGAAGAAGG GAAATGTTGG	117
NM_000125	estrogen receptor 1 (ERα)	ESR1	165444	TAAATGCTGCC ATGTTCCAA	AATGCAAAGG GGTCTGTGTC	113
NM_009992	cytochrome P450, family 1, subfamily A, polypeptide 1	CYP1A1	13076	AAGTGCAGAT GCGGTCTTCT	AAAGTAGGAG GCAGGCACAA	140

Table 2 (cont'd)

RefSeq	Gene name	Gene symbol	Entrez Gene ID	Forward Primer	Reverse Primer	Product Size (bp)
NM_000104	cytochrome P450, family 1, subfamily B, polypeptide 1	CYP1B1	1545	CACCAAGGCT GAGACAGTGA	GATGACGACT GGGCCTACAT	164
NM_000693	aldehyde dehydrogenase 1 family, member A3	ALDH1A3	220	GGTGGACCTG CTTACAGAGC	TCCACGGTATG CACTAACCA	165
NM_003486	solute carrier family member 5	SLC7A5	8140	AGGAGCCTTC CTTTCTCCTG	CTGCAAACCCT AAGGCAGAG	181
NM_017460	cytochrome P450, family 3, subfamily A, polypeptide 4	CYP3A4	1576	CAAGACCCCTT TGTGGAAAA	CGAGGCGACT TTCTTTCATC	187
NM_198253	telomerase reverse transcriptase	TERT	7015	GCGTTTGGTGG ATGATTTCT	CAGGGCCTCG TCTTCTACAG	151
NM_002701	POU class 5 homeobox 1	POU5F1 (OCT4)	5460	GTACTCCTCGG TCCCTTTCC	CAAAAACCCT GGCACAAACT	168
NM_001134	alpha-fetoprotein	AFP	174	CTTGTGAAGCA AAAGCCACA	CCCTCTTCAGC AAAGCAGAC	122
NM_003380	vimentin	VIM	7431	CCCTCACCTGT GAAGTGGAT	GCTTCAACGG CAAAGTTCTC	91
NM_006288	Thy-1 cell surface antigen	THY1	7070	GGACTGAGAT CCCAGAACCA	ACGAAGGCTC TGGTCCACTA	124

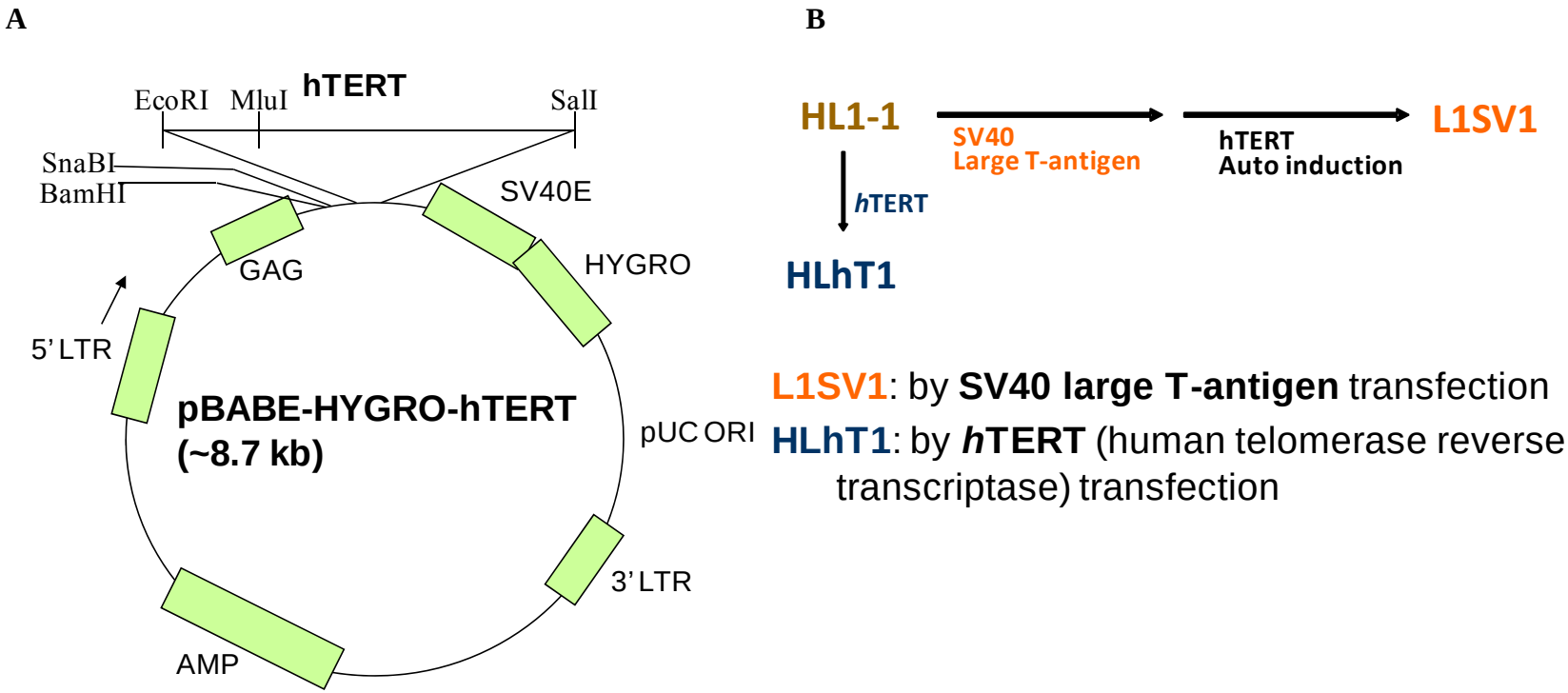

Figure 2. Immortalization of HL1-1 cells.
(A) Map of hTERT (human telomertase reverse transciptase) express plasmid (pBABE-HYGRO-hTERT) **(B)** HL1-1 cell immortalization strategy. L1SV1 cell: immortalized by SV40 large T-antigen transfection. HLhT1 cell: immortalized by hTERT transfection. Morphology of HL1-1 **(C)**, HLhT1 **(D)**, and L1SV1 cells **(E)**. The cultures contain serpiginous shaped cells for HL1-1 and HLhT1 cells and cuboid shaped cells for SV1C1 cells. For interpretation of the references to color in this and all other figures, the reader is referred to the electronic version of this dissertation.

Figure 2 (cont'd)

C

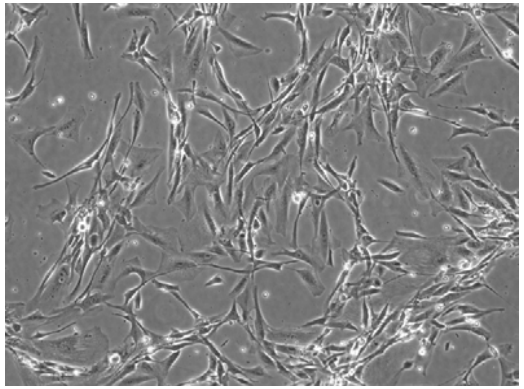

D

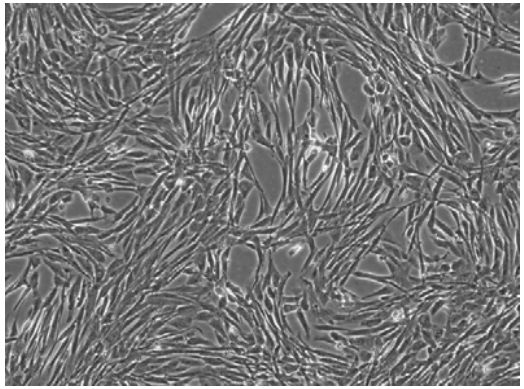

E

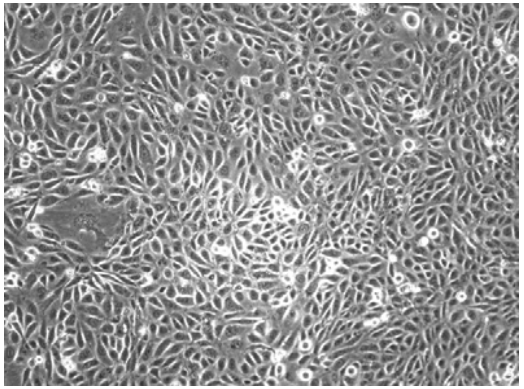

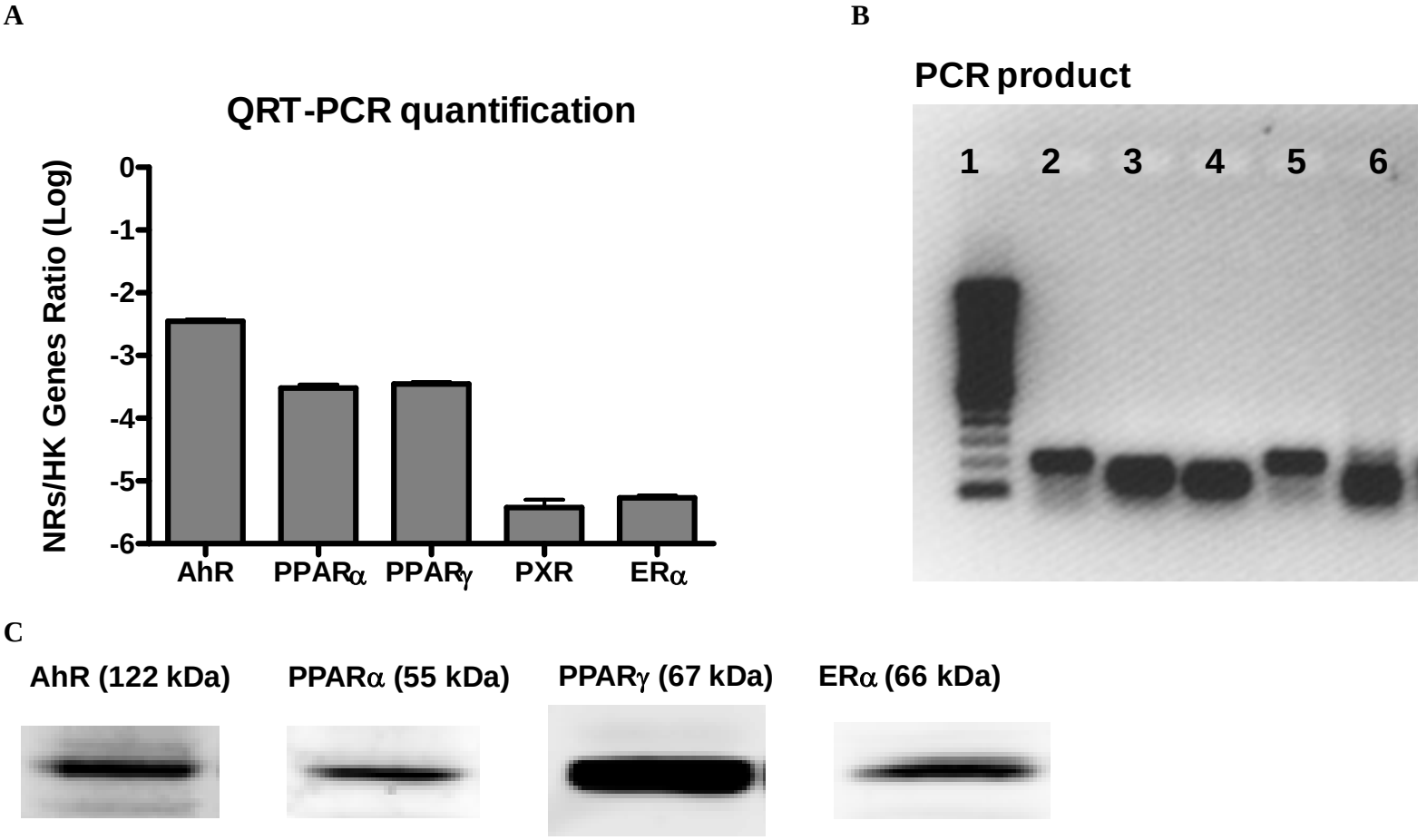

Figure 3. Basal mRNA and protein expression levels of AhR, PPARα and γ, ERα.
Various nuclear receptors detected by QRT-PCR and in protein levels by western blot. **(A)** The mRNA levels of the receptors were measured by QRT-PCR and normalized to several housekeeping genes (HK) and **(B)** PCR products were verified by agarose gel. 1. 100bp ladder, 2. AhR, 3. PPARα, 4. PPARγ, 5. PXR, 6. ERα. **(C)** Protein levels were determined by Western blots.

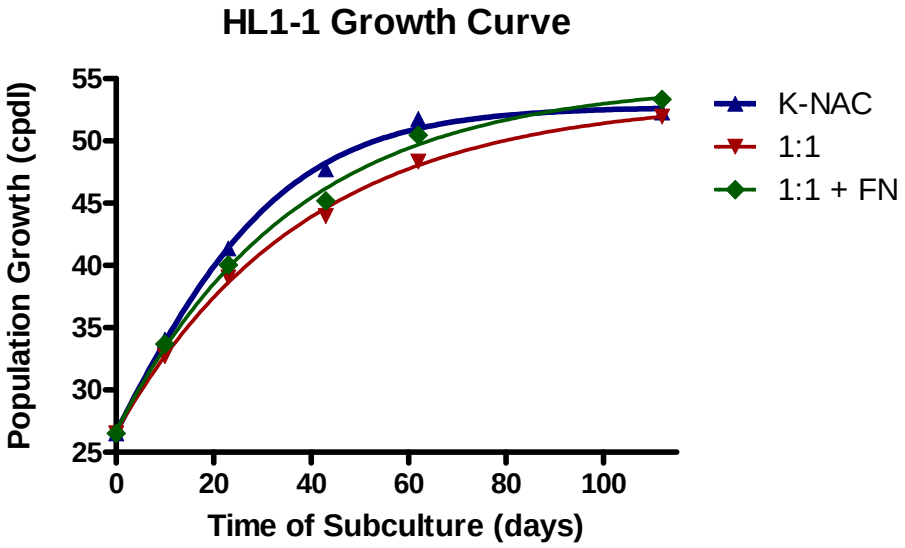

Figure 4. Proliferation potential of HL1-1 cell.
Cumulative pd of HL1-1 in K-NAC medium with 10% FBS (K-NAC), K-NAC:D (1:1) medium with 10% FBS (1:1) or 1:1 medium in fibronectin coated plate (1:1 + FN).

QRT-PCR results. The protein level of the AhR, ERα, PPARα and γ was confirmed by western blotting (Figure 3C). The PXR was not detected in western blotting because of the protein expression level was too low.

For investigation of the AhR and PPARα-responsiveness of the HL1-1 cells, TCDD and Wy-14,643 treatments were performed and induction of CYP1A1 and ADFP, proto-typical regulated genes, were measured by QRT-PCR, respectively. The functional responsiveness results are reported in Chapter 4 and 5, respectively.

PROLIFERATION POTENTIAL OF THE HL1-1 CELL AND THEIR IMMORTALIZATION

Several studies report on expanding cell life span by changing media conditions [30, 31]. Three media conditions, K-NAC medium with 10% FBS (K-NAC), the 1:1 mixture of K-NAC and D medium with 10% FBS (1:1), and fibronectin coated flask and K-NAC:D (1:1) with 10% FBS (FN), were tested for culture condition optimization for HL1-1 cell life span expansion. In 112 days after five passages, the lifespan of HL1-1 cells reached 52.3, 52.0, and 53.4 cpdl from initial 26.5 cpdl in the K-NAC, 1:1, and FN medium conditions, respectively (Figure 4A). Application of different media conditions did not expand the life span of HL1-1 cells significantly.

Previous reports have indicated that ectopic hTERT expression enables cells to circumvent senescence [32, 33]. For immortalization of HL1-1 cells, the cells were transfected with a plasmid carrying an hTERT cDNA (pBabe-hygro-hTERT) and selected with hygromycin (100 mg/ml). Ten days after the selection, surviving colonies were isolated and propagated. Among of them, the best proliferation ability and maintaining primitive cell morphology with high hTERT expression was selected (HLhT1). From continuous subculturing, HLhT1 cells maintain proliferation ability up to more than 6 months culturing with 18 passages without any

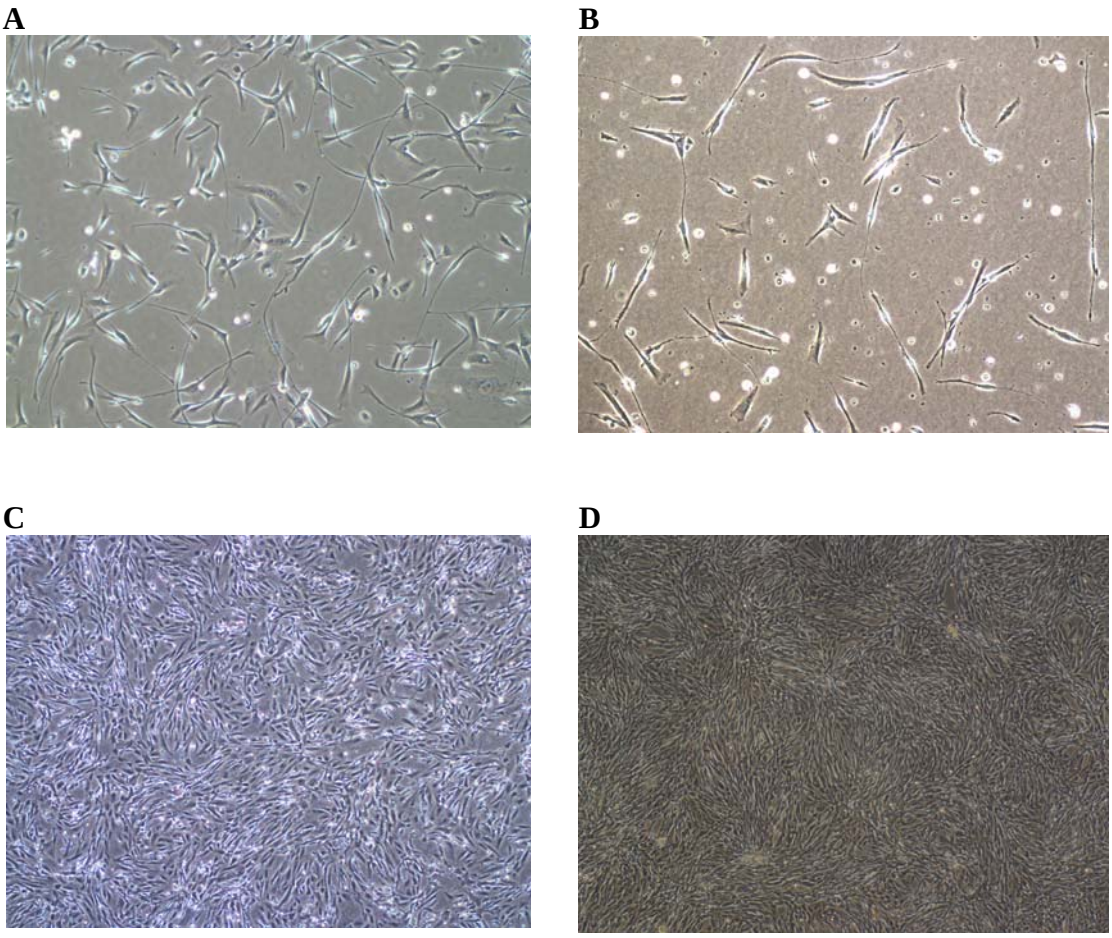

Figure 5. Morphology of HL1-1 and HLhT1 cells.
(A) HL1-1 cells at low cell densities. **(B)** HLhT1 cells at low cell densities. **(C)** HL1-1 cells at high cell densities. **(D)** HLhT1 cells at high cell densities.

sign of senescence or morphological change (Figure 5).

HLhT1 were compared with other three other cell lines, including parental HL1-1 cells, L1SV1 immortal liver cell line derived from HL1-1 transfected with SV40 large T-antigen and with human hepatoma HepG2 cells. Similar to the parental HL1-1 cells, immortalized HLhT1 and L1SV1 cells express comparable levels of stem cell marker (OCT4) and the oval cell markers (α-fetoprotein, AFP; vimentin, VIM; and Thy-1 cell surface antigen, THY1) (Figure 6). In contrast, compared to HepG2, HL1-1 cells and their immortalized derivatives (HLhT1 and L1SV1) showed lower expression of AFP, but higher expression of VIM and THY1. Basal expression levels of hTERT were the order of HLhT1, HepG2, L1SV1 and HL1-1 cells. Finally, expression of albumin (ALB), which is differentiated hepatocyte marker protein, was much higher in HepG2 cells compared to human liver stem cells.

RECEPTOR GENE EXPRESSION AND RESPONSE COMPARISON IMMORTALIZED CELL

For receptor-mediated response comparison between cell lines, basal expression levels of nuclear receptors and AhR were evaluated. The basal transcripts expression level of each receptor was measured in normal proliferating HL1-1, L1SV1 and HLhT1 cells by QRT-PCR (Figure 7A). The AhR expression level was comparable among all cells lines, the levels of PPARα were lower in L1SV1 and HLhT1 cells, and the expression of PPARγ was higher in HLhT1 compared to parental HL1-1 cells. Basal expression of PXR was very low in all three cell lines.

The AhR, PPARα and PXR receptor responsiveness was evaluated in HLhT1 cells using 10 nM TCDD, 50 μM Wy-14,643 and 30 μM rifampicin, respectively. After 12 h treatment, the induction of prototypical regulated genes, i.e. CYP1A1 (AhR) and ADFP (PPARα) was ~50-, and 3.5-fold, respectively, as measured by QRT-PCR (Figure 7B). However, rifampicin did not

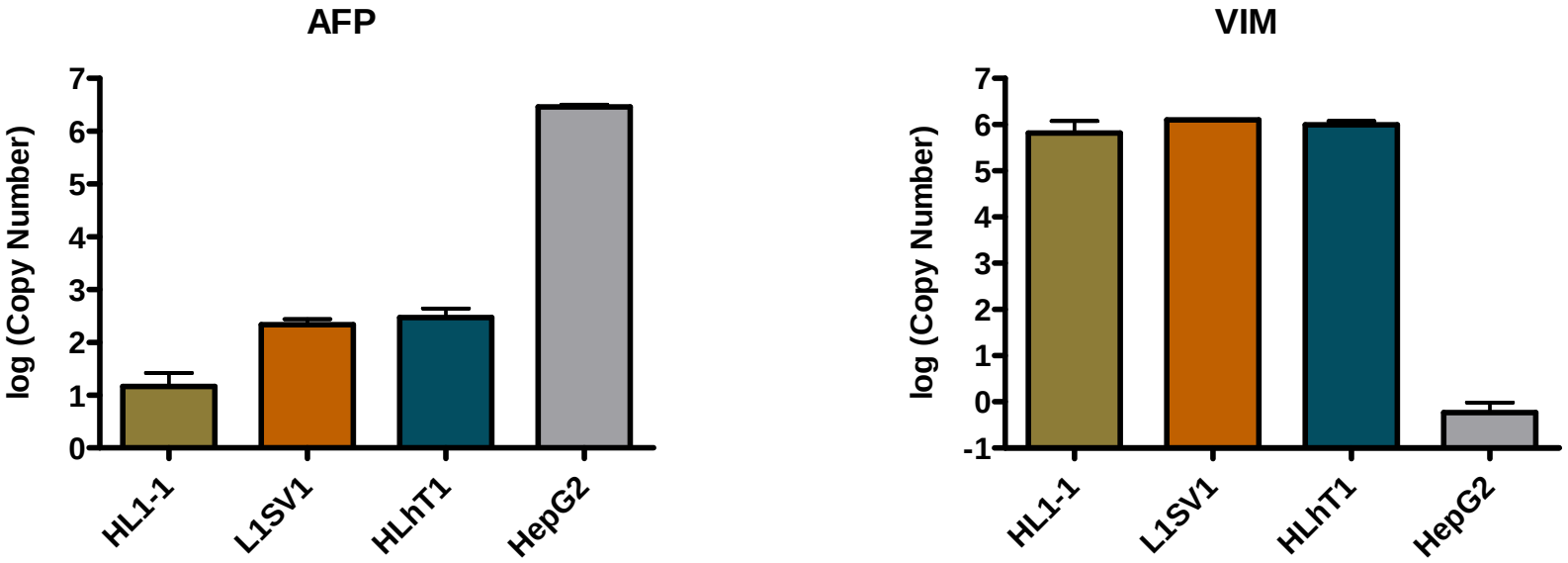

Figure 6. Basal stem cell marker and hepatocyte differentiation marker gene expression level comparison.
Stem cell marker (OCT4), liver oval cell marker (AFP, VIM and THY1), telomerase reverse transcriptase (hTERT) and hepatocyte differentiation marker (ALB) were examined by QRT-PCR and compared in HL1-1, L1SV1, HLhT1 and HepG2 cells. Bars are mean ± SE for the average log value of target gene copy number, N = 3.

Figure 6 (cont'd)

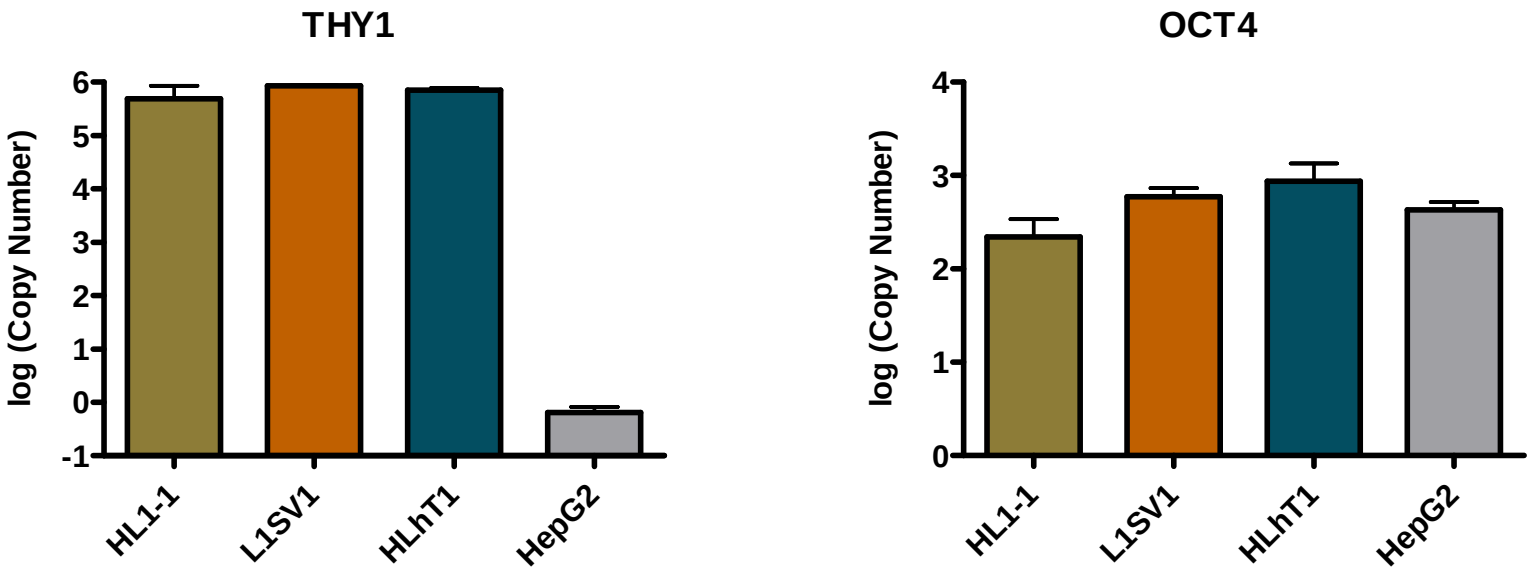

Figure 6 (cont'd)

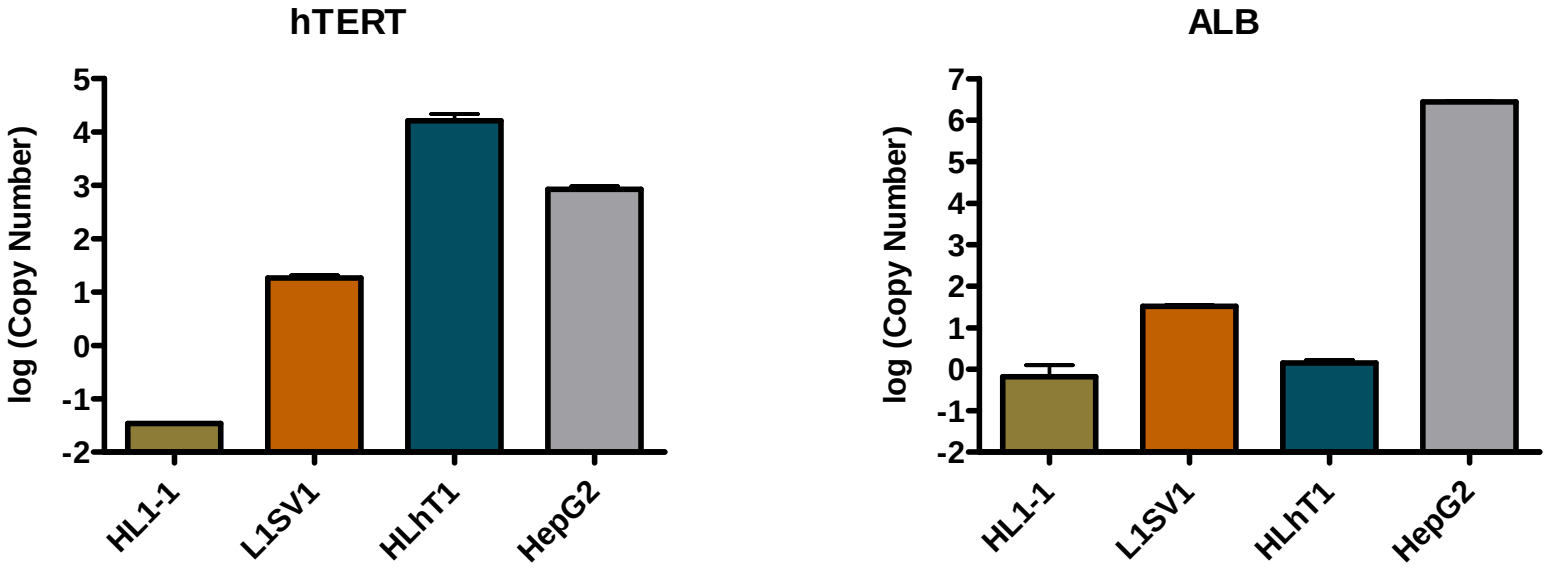

A

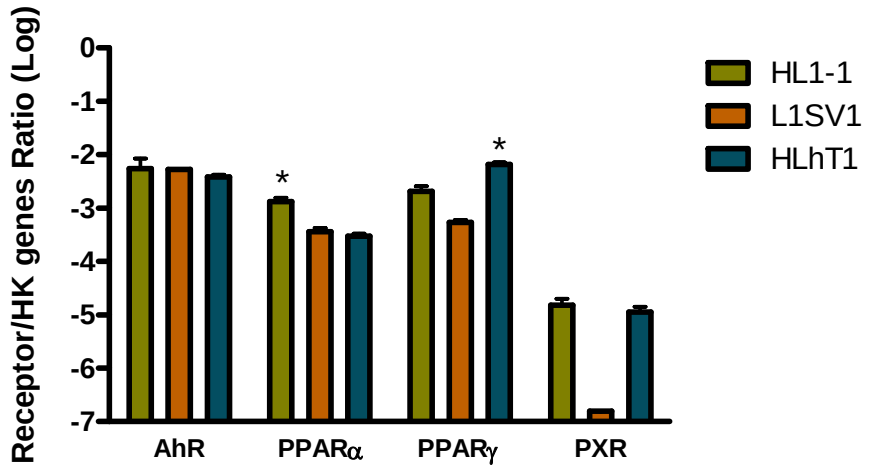

Figure 7. Basal AhR and NRs expression levels comparison in parental and immortalized cell lines and receptors response in HLhT1 cells.

(A) Comparison of basal mRNA expression levels of AhR, PPARα and γ, PXR in HL1-1, L1SV1 and HLhT1 cells. The gene expression ratio is represented by PPARα gene expression levels normalized to the housekeeping genes (HK) HPRT, GAPDH and ACTB. **(B)** Responsiveness of AhR, PPARα and PXR proteins in HLhT1 cells was determined by TCDD (CYP1A1), Wy-14,643 (ADFP) and rifampicin (CYP3A4) treatments, respectively. Bars are mean ± SE, N = 3.

Figure 7 (cont'd)

B

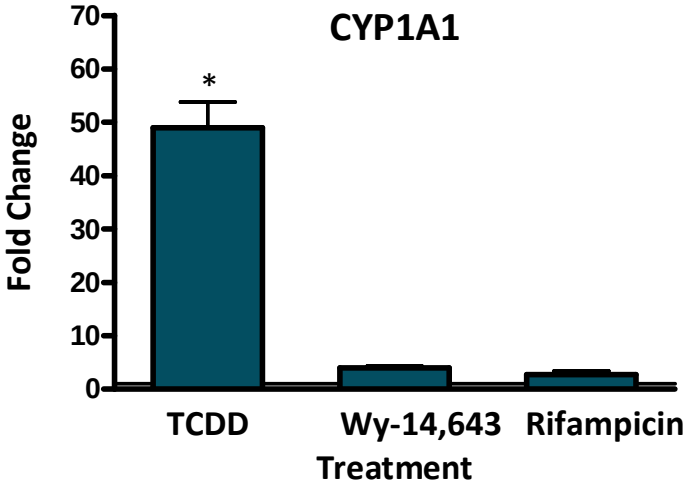

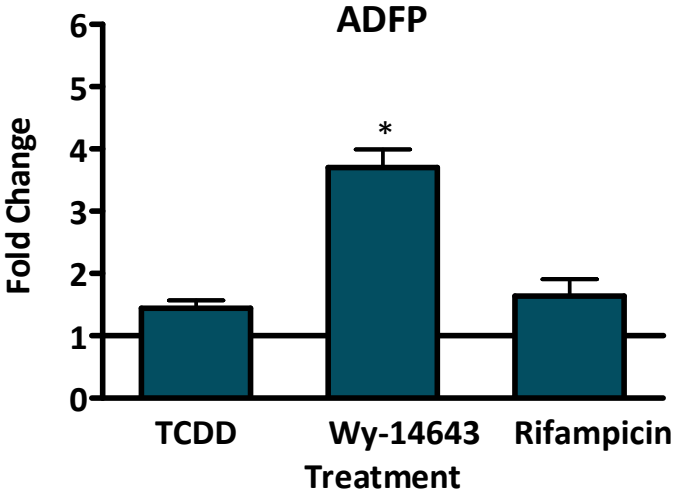

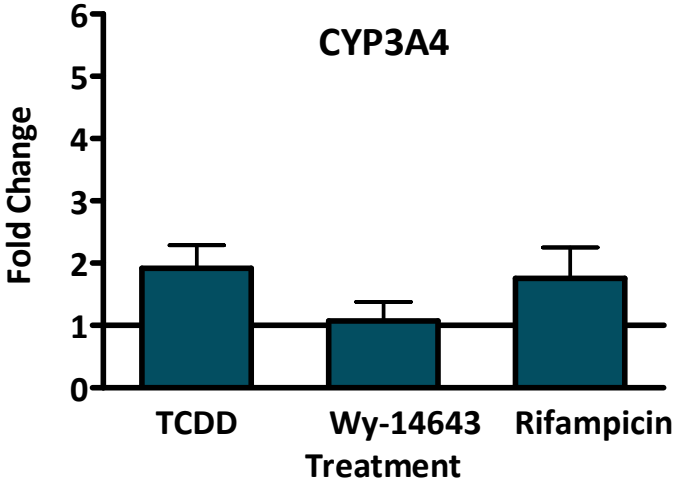

induce the PXR-regulated CYP3A4 expression. These results suggest that HLhT1 cells possess functional AhR and PPARα and are responsive to TCDD and Wy-14,643 treatment.

TCDD-INDUCIBLE TEMPORAL GENE EXPRESSION PROFILE COMPARISON

For AhR-mediated response comparison between cell lines, HL1-1, L1SV1 and HLhT1 cells were treated with 10 nM TCDD or DMSO vehicle and temporal changes in targeted gene expression were evaluated using QRT-PCR. Induction of CYP1A1, was confirmed all cell lines at all time points, however with different maximum responses between cells (L1SV1: ~27-fold, HL1-1: ~1,600-fold, HLhT1: ~5,000-fold) (Figure 8). In addition, the TCCD-regulated CYP1B1, SLC7A5 and ALDH1A3 were among the primary response genes with putative dioxin response elements (DREs) induced in the HL1-1 cells (discussed in Chapter 4). Temporal profile and induction level of these genes was comparable between immortalized HLhT and parental HL1-1 cells (Figure 9).

DISCUSSION

In the present study we characterized normal adult human liver stem cells (HL1-1) and their immortalized cell lines (L1SV1 and HLhT1) and evaluated their application for receptor mediated toxicogenomic studies. HL1-1 possesses stem cell characteristics such as high proliferation potential (cpdl = 49), multipotent differentiation and the ability of anchorage independent growth [8]. HL1-1 cells appear as serpiginous cells in morphology, especially when they are growing at low cell density or in growth factor-deprived medium, similar to cell morphologies observed in some stem cell from human bone marrow or precursor cells from rat and human pancreatic islets as well [34, 35]. Liver oval cells express vimentin, α-fetoprotein, thy-1 and the hematopoietic stem cell markers, CD34 and SCF/c-kit, which are not expressed in hepatocytes or bile duct cells [36]. HL1-1 express several mesenchymal and oval cell markers

(vimentin, α-fetoprotein and thy-1) and the embryonic stem cell marker (Oct-4) indicating a partial commitment to the hepatic lineage.

The basal expression of AhR, ERα, PPARα and γ mRNA and protein levels was confirmed in HL1-1 cells. However, PXR protein was not detected and treatment of the prototypical human PXR agonist (rifampicin) [37], failed to induce CYP3A4 expression. PXR, generally regarded as a sensor activated by exogenous and endogenous chemicals, regulates a large number of enzymes involved in oxidation, conjugation and transport of drug, xenobiotic and endobiotic molecules [38]. Due to its physiological role, PXR activation can affect drug-drug interactions and result in altered clinical responses [39]. Deficiency of functional PXR protein in HL1-1 cells could limit their application in testing of hepatocyte related functions.

Induction of PXR expression by differentiation has been previously reported in bipotential mouse embryonic liver cells [40]. Moreover, during mammalian hepatocyte differentiation, expression regulation of HNF1a and PXR by the transcription factor HNF4a has been reported [41, 42]. Accordingly, the PXR deficiency may be overcome by the generation of differentiated hepatocytes from liver stem cells. When growing in a modified Eagle's MEM (minimum essential medium) with high calcium (1.8 mM) and hepatocyte growth factor (HGF), most HL1-1 cells were morphologically changed into larger size with multiple nuclei and differentiated to albumin expressing hepatocytes [8]. The use of cells derived from monoclonal stem cell line would be beneficial compared to primary hepatocytes to minimize the donor and preparation variability.

HL1-1 cells maintained their proliferative ability for more than 50 cumulative population doublings over 10 to 15 sub-passages. Such proliferative capacity indicates that adult stem cells isolated from a human liver tissue could potentially generate trillions of cells.

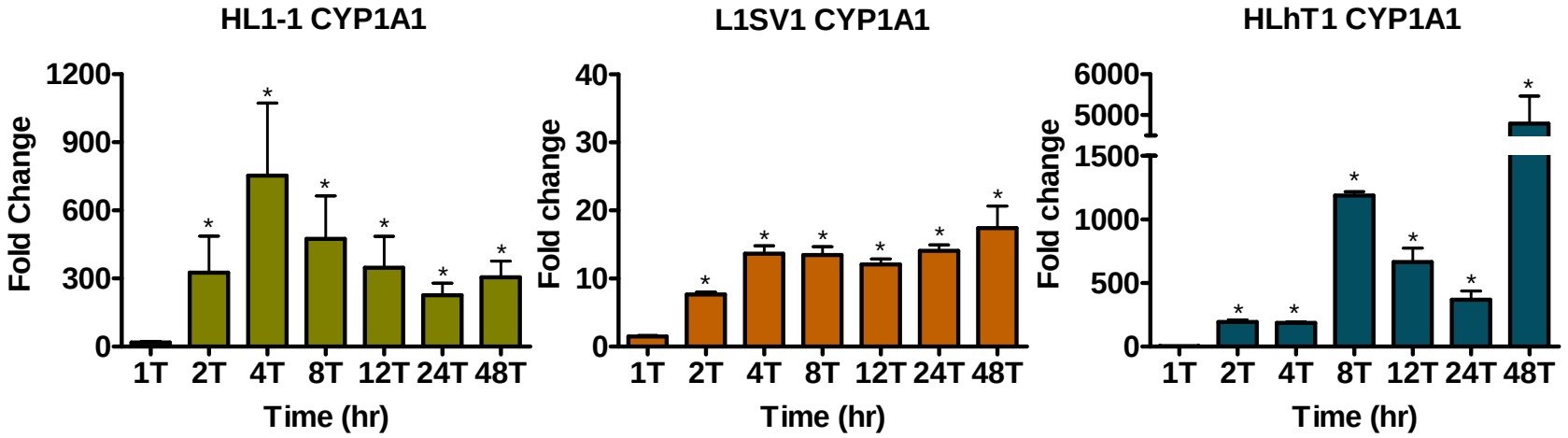

Figure 8. Temporal TCDD-mediated CYP1A1 induction profiles comparison.
Temporal TCDD-mediated CYP1A1 induction profiles in human liver stem cells (HL1-1) and immortalized liver cells (L1SV1 and HLhT1) measured by QRT-PCR. All fold changes were calculated relative to time-matched vehicle controls. Bars are mean ± SE for the average fold change, *$p < 0.05$ vs. control, N = 3.

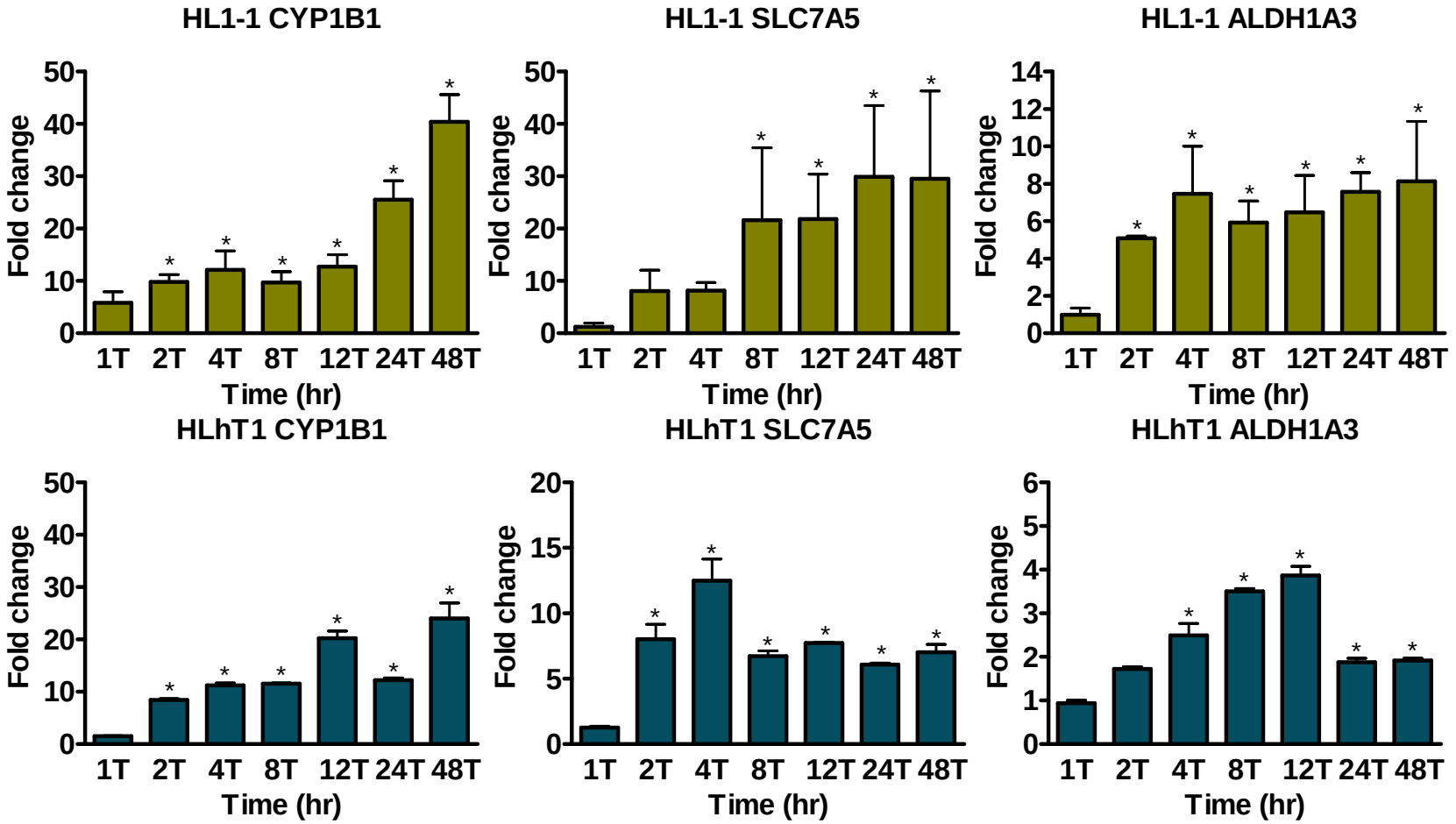

Figure 9. Temporal profiles of prototypical TCDD-responsive genes in human liver stem cell (HL1-1) and immortalized liver cells (HLhT1).

All fold changes were calculated relative to time-matched vehicle controls. Bars are mean ± SE for the average fold change, *$p < 0.05$ vs. control N = 3.

Although HL1-1 cells have high proliferation ability, they eventually become senescent. Normal somatic cells lose telomeric DNA at rates of 50 to 200 bp per cell division because of replication-associated attrition [43]. Critically shortened telomere which is incapable of looping leads to growth arrest signal activation and stops cell proliferation [44]. To overcome cellular senescence, genes related to cell cycle regulation and telomere maintenance were targeted for cell engineering. Human or primate hepatocytes have been previously immortalized using Simian virus 40 large T-antigen (SV40T) and the catalytic subunit of the telomerase (hTERT) and these immortalized cells are non-tumorigenic and express hepatocyte genes [45-47]. By means of transfection of a pBABE-hygro retroviral vector expressing hTERT, we isolated a transduced clone referred to as HLhT1 which grows as a continuous cell line *in vitro* and can be amplified and cryopreserved efficiently. QRT-PCR analysis of hTERT expression in HLhT1 cells demonstrated stable proviral integration. Prototypical gene responses in HLhT1 cells with transactivation of AhR and PPARα showed concordant responses with their parental cells. Hence, immortalized HLhT1 cells harbor a phenotype expected from the parental HL1-1 liver stem cells.

Compared to HLhT1 cells, L1SV1 cells immortalized by SV40T transduction appear morphologically different and exhibit lower level of CYP1A1 induction by TCDD treatment. SV40T is viral oncoprotein which targets, binds and inactivates tumor suppressor p53 and Rb proteins and drive cells into the cell cycle [48, 49]. The stabilization of p53 and subsequent transcription of p53-dependent genes results in cell cycle arrest and/or apoptosis. T antigen blocks this response by binding to p53 and preventing p53-dependent transcription in downstream of p53 pathway [50]. As a result, although infinite cell replication has been induced by expressing the SV40T, genetic transformation will lead to greater susceptibility for cancer by

blocking tumor suppressor p53 activity [46, 51]. Compared to SV40T, hTERT transduced immortalization has the advantage of being untransformed and non-tumorgenic after transplantation [47, 52, 53]. Telomerase reconstitution does not induce a transformed phenotype and is likely to be genoprotective throughout the expanded proliferative lifespan of immortalized cells.

There is increasing evidence that adult stem cells and their derivatives are targets for carcinogenesis [12, 13]. Oval cells are also involved in human liver disease condition caused by alcohol, hepatitis C virus and hemochromatosis which are also associated with increased incidence of hepatocellular carcinoma or cholangiocarcinoma [54, 55]. There is also evidence that oval cells give rise to hepatocellular carcinoma in mouse as well [56]. Since liver stem cells could be a potential direct target for carcinogenesis, these cells may be used to develop an *in vitro* model to study the mechanism of human liver carcinogenesis.

In summary, these results provide a novel *in vitro* model system for receptor-mediated toxicogenomic study employing human liver stem cells isolated from adult liver tissue. Human liver stem cells are an attractive alternative cell model, due to the high proliferative capacity, their intactness from normal liver tissue origin and differentiation ability. Furthermore, this study provides insight into cellular engineering approaches for the immortalization of human liver stem cells using hTERT transduction and their comparable AhR-mediated responsiveness with parental cells for extension of utilization. Further comparative studies with novel human liver stem cell model and conventional models may help elucidate the differences in the mechanisms of action of species-specific responses.

REFERENCES

REFERENCES

1. Abbott, A., *Cell culture: biology's new dimension.* Nature, 2003. **424**(6951): p. 870-2.

2. Wilkening, S., F. Stahl, and A. Bader, *Comparison of primary human hepatocytes and hepatoma cell line Hepg2 with regard to their biotransformation properties.* Drug Metab Dispos, 2003. **31**(8): p. 1035-42.

3. Rohwedel, J., et al., *Embryonic stem cells as an in vitro model for mutagenicity, cytotoxicity and embryotoxicity studies: present state and future prospects.* Toxicol In Vitro, 2001. **15**(6): p. 741-53.

4. Davila, J.C., et al., *Use and application of stem cells in toxicology.* Toxicol Sci, 2004. **79**(2): p. 214-23.

5. Alison, M.R., S. Islam, and S. Lim, *Stem cells in liver regeneration, fibrosis and cancer: the good, the bad and the ugly.* J Pathol, 2009. **217**(2): p. 282-98.

6. Michalopoulos, G.K. and M.C. DeFrances, *Liver regeneration.* Science, 1997. **276**(5309): p. 60-6.

7. Conigliaro, A., et al., *Isolation and characterization of a murine resident liver stem cell.* Cell Death Differ, 2008. **15**(1): p. 123-133.

8. Chang, C.C., Tsai,J.L., Kuo,K.K., Wang,K.H., Chiang,C.H., Kao,A.P., Tai,M.H. and Trosko,J.E., *Expression of Oct-4, alpha fetoprotein and vimentin and lack of gap-junctional intercellular communication (GJIC) as common phenotypes for human adult liver stem cells and hepatoma cells.* Proc. Am. Assoc. Cancer Res., 2004. **45**: p. 642.

9. Masson, N.M., et al., *Hepatic progenitor cells in human fetal liver express the oval cell marker Thy-1.* Am J Physiol Gastrointest Liver Physiol, 2006. **291**(1): p. G45-54.

10. Malhi, H., et al., *Isolation of human progenitor liver epithelial cells with extensive replication capacity and differentiation into mature hepatocytes.* J Cell Sci, 2002. **115**(Pt 13): p. 2679-88.

11. Suzuki, A., et al., *Clonal identification and characterization of self-renewing pluripotent stem cells in the developing liver.* J Cell Biol, 2002. **156**(1): p. 173-84.

12. Ahuja, Y.R., V. Vijayalakshmi, and K. Polasa, *Stem cell test: a practical tool in toxicogenomics.* Toxicology, 2007. **231**(1): p. 1-10.

13. Alison, M.R. and M.J. Lovell, *Liver cancer: the role of stem cells.* Cell Prolif, 2005. **38**(6): p. 407-21.

14. Moore, J.T., J.L. Collins, and K.H. Pearce, *The nuclear receptor superfamily and drug discovery.* ChemMedChem, 2006. **1**(5): p. 504-23.

15. Woods, C.G., J.P. Heuvel, and I. Rusyn, *Genomic profiling in nuclear receptor-mediated toxicity.* Toxicol Pathol, 2007. **35**(4): p. 474-94.

16. Dreyer, C., et al., *Control of the peroxisomal beta-oxidation pathway by a novel family of nuclear hormone receptors.* Cell, 1992. **68**(5): p. 879-87.

17. Kretschmer, X.C. and W.S. Baldwin, *CAR and PXR: xenosensors of endocrine disrupters?* Chem Biol Interact, 2005. **155**(3): p. 111-28.

18. Timsit, Y.E. and M. Negishi, *CAR and PXR: the xenobiotic-sensing receptors.* Steroids, 2007. **72**(3): p. 231-46.

19. Matic, M., et al., *Pregnane X receptor: promiscuous regulator of detoxification pathways.* Int J Biochem Cell Biol, 2007. **39**(3): p. 478-83.

20. Okey, A.B., *An aryl hydrocarbon receptor odyssey to the shores of toxicology: the Deichmann Lecture, International Congress of Toxicology-XI.* Toxicol Sci, 2007. **98**(1): p. 5-38.

21. Denison, M.S. and S. Heath-Pagliuso, *The Ah receptor: a regulator of the biochemical and toxicological actions of structurally diverse chemicals.* Bull Environ Contam Toxicol, 1998. **61**(5): p. 557-68.

22. Knerr, S. and D. Schrenk, *Carcinogenicity of 2,3,7,8-tetrachlorodibenzo-p-dioxin in experimental models.* Mol Nutr Food Res, 2006. **50**(10): p. 897-907.

23. Kim, S., et al., *Comparative analysis of AhR-mediated TCDD-elicited gene expression in human liver adult stem cells.* Toxicol Sci, 2009. **112**(1): p. 229-44.

24. Smith, J., et al., *Redox state is a central modulator of the balance between self-renewal and differentiation in a dividing glial precursor cell.* Proc Natl Acad Sci U S A, 2000. **97**(18): p. 10032-7.

25. Chepda, T., et al., *Monitoring of ascorbate at a constant rate in cell culture: effect on cell growth.* In Vitro Cell Dev Biol Anim, 2001. **37**(1): p. 26-30.

26. Inoue, C., et al., *Nicotinamide prolongs survival of primary cultured hepatocytes without involving loss of hepatocyte-specific functions.* J Biol Chem, 1989. **264**(9): p. 4747-50.

27. Mitaka, T., *The current status of primary hepatocyte culture.* Int J Exp Pathol, 1998. **79**(6): p. 393-409.

28. Rozen, S. and H. Skaletsky, *Primer3 on the WWW for general users and for biologist programmers.* Methods Mol Biol, 2000. **132**: p. 365-86.

29. Vandesompele, J., et al., *Accurate normalization of real-time quantitative RT-PCR data by geometric averaging of multiple internal control genes.* Genome Biol, 2002. **3**(7): p. RESEARCH0034.

30. Maheshwari, G., et al., *Cell adhesion and motility depend on nanoscale RGD clustering.* J Cell Sci, 2000. **113 (Pt 10)**: p. 1677-86.

31. Neupane, M., et al., *Isolation and characterization of canine adipose-derived mesenchymal stem cells.* Tissue Eng Part A, 2008. **14**(6): p. 1007-15.

32. Bodnar, A.G., et al., *Extension of life-span by introduction of telomerase into normal human cells.* Science, 1998. **279**(5349): p. 349-52.

33. Counter, C.M., et al., *Dissociation among in vitro telomerase activity, telomere maintenance, and cellular immortalization.* Proc Natl Acad Sci U S A, 1998. **95**(25): p. 14723-8.

34. Zulewski, H., et al., *Multipotential nestin-positive stem cells isolated from adult pancreatic islets differentiate ex vivo into pancreatic endocrine, exocrine, and hepatic phenotypes.* Diabetes, 2001. **50**(3): p. 521-33.

35. Lin, T.M., et al., *Accelerated growth and prolonged lifespan of adipose tissue-derived human mesenchymal stem cells in a medium using reduced calcium and antioxidants.* Stem Cells Dev, 2005. **14**(1): p. 92-102.

36. Alison, M., *Liver stem cells: a two compartment system.* Curr Opin Cell Biol, 1998. **10**(6): p. 710-5.

37. Bolt, H.M., *Rifampicin, a keystone inducer of drug metabolism: from Herbert Remmer's pioneering ideas to modern concepts.* Drug Metab Rev, 2004. **36**(3-4): p. 497-509.

38. Jones, S.A., et al., *The pregnane X receptor: a promiscuous xenobiotic receptor that has diverged during evolution.* Mol Endocrinol, 2000. **14**(1): p. 27-39.

39. Ma, X., J.R. Idle, and F.J. Gonzalez, *The pregnane X receptor: from bench to bedside.* Expert Opin Drug Metab Toxicol, 2008. **4**(7): p. 895-908.

40. Ochsner, S.A., et al., *Transcriptional profiling of bipotential embryonic liver cells to identify liver progenitor cell surface markers.* Stem Cells, 2007. **25**(10): p. 2476-87.

41. Li, J., G. Ning, and S.A. Duncan, *Mammalian hepatocyte differentiation requires the transcription factor HNF-4alpha.* Genes Dev, 2000. **14**(4): p. 464-74.

42. Kamiya, A., F.J. Gonzalez, and H. Nakauchi, *Identification and differentiation of hepatic stem cells during liver development.* Front Biosci, 2006. **11**: p. 1302-10.

43. Allsopp, R.C., et al., *Telomere length predicts replicative capacity of human fibroblasts.* Proc Natl Acad Sci U S A, 1992. **89**(21): p. 10114-8.

44. Hoare, M., T. Das, and G. Alexander, *Ageing, telomeres, senescence, and liver injury.* J Hepatol, 2010. **53**(5): p. 950-61.

45. Allain, J.E., et al., *Immortalization of a primate bipotent epithelial liver stem cell.* Proc Natl Acad Sci U S A, 2002. **99**(6): p. 3639-44.

46. Pfeifer, A.M., et al., *Simian virus 40 large tumor antigen-immortalized normal human liver epithelial cells express hepatocyte characteristics and metabolize chemical carcinogens.* Proc Natl Acad Sci U S A, 1993. **90**(11): p. 5123-7.

47. Wege, H., et al., *Telomerase reconstitution immortalizes human fetal hepatocytes without disrupting their differentiation potential.* Gastroenterology, 2003. **124**(2): p. 432-44.

48. Manfredi, J.J. and C. Prives, *The transforming activity of simian virus 40 large tumor antigen.* Biochim Biophys Acta, 1994. **1198**(1): p. 65-83.

49. Pipas, J.M., *SV40: Cell transformation and tumorigenesis.* Virology, 2009. **384**(2): p. 294-303.

50. Giono, L.E. and J.J. Manfredi, *The p53 tumor suppressor participates in multiple cell cycle checkpoints.* J Cell Physiol, 2006. **209**(1): p. 13-20.

51. Farwell, D.G., et al., *Genetic and epigenetic changes in human epithelial cells immortalized by telomerase.* Am J Pathol, 2000. **156**(5): p. 1537-47.

52. Jiang, X.R., et al., *Telomerase expression in human somatic cells does not induce changes associated with a transformed phenotype.* Nat Genet, 1999. **21**(1): p. 111-4.

53. Morales, C.P., et al., *Absence of cancer-associated changes in human fibroblasts immortalized with telomerase.* Nat Genet, 1999. **21**(1): p. 115-8.

54. Alison, M.R., *Liver stem cells: implications for hepatocarcinogenesis.* Stem Cell Rev, 2005. **1**(3): p. 253-60.

55. Lowes, K.N., et al., *Oval cell numbers in human chronic liver diseases are directly related to disease severity.* Am J Pathol, 1999. **154**(2): p. 537-41.

56. Dumble, M.L., et al., *Generation and characterization of p53 null transformed hepatic progenitor cells: oval cells give rise to hepatocellular carcinoma.* Carcinogenesis, 2002. **23**(3): p. 435-45.

CHAPTER 4

Kim S, Dere E, Burgoon LD, Chang CC, and Zacharewski TR: **Comparative analysis of AhR-mediated TCDD-elicited gene expression in human liver adult stem cells**. *Toxicol Sci* 2009, 112: 229-44.

CHAPTER 4

COMPARATIVE ANALYSIS OF AHR-MEDIATED TCDD ELICITED GENE EXPRESSION IN HUMAN LIVER ADULT STEM CELLS

ABSTRACT

Time course and dose-response studies were conducted in HL1-1 cells, a human liver cell line with stem cell-like characteristics, to assess the differential gene expression elicited by 2,3,7,8-tetrachlorodibenzo-p-dioxin (TCDD) compared to other established models. Cells were treated with 0.001, 0.01, 0.1, 1, 10 or 100 nM TCDD or DMSO vehicle control for 12 hrs for the dose response study, or with 10 nM TCDD or vehicle for 1, 2, 4, 8, 12, 24 or 48 hrs for the time course study. Elicited changes were monitored using a human cDNA microarray with 6,995 represented genes. Empirical Bayes analysis identified 144 genes differentially expressed at one or more time points following treatment. Most genes exhibited dose-dependent responses including CYP1A1, CYP1B1, ALDH1A3 and SLC7A5 genes. Comparative analysis of HL1-1 differential gene expression to human HepG2 data identified 74 genes with comparable temporal expression profiles including 12 putative primary responses. HL1-1 specific changes were related to lipid metabolism and immune responses, consistent with effects elicited *in vivo*. Furthermore, comparative analysis of HL1-1 cells with mouse Hepa1c1c7 hepatoma cell lines and C57BL/6 hepatic tissue identified 18 and 32 commonly regulated orthologous genes, respectively, with functions associated with signal transduction, transcriptional regulation, metabolism and transport. Although some common pathways are affected, the results suggest that TCDD elicits species- and model-specific gene expression profiles.

INTRODUCTION

2,3,7,8-Tetrachlorodibenzo-*p*-dioxin (TCDD) is a ubiquitous environmental contaminant that elicits a broad spectrum of responses including endocrine disruption, immunotoxicity, hepatotoxicity, teratogenesis, and tumor promotion [1]. It is a multi-site carcinogen and liver tumor promoter in rodents [2], and classified as a human carcinogen by the International Agency for Research on Cancer (IARC) [3]. The effects are mediated by the aryl hydrocarbon receptor (AhR) [4], a ligand activated basic helix-loop-helix/PER-ARNT-SIM (bHLH/PAS) transcription factor. Upon ligand binding, the cytosolic AhR undergoes a conformational change, which leads to the dissociation of chaperone proteins and translocation to the nucleus where it heterodimerizes with the aryl hydrocarbon receptor translocator (ARNT). The heterodimer complex binds to dioxin response elements (DREs) in the regulatory region of target genes to modulate gene expression. AhR-mediated changes in gene expression are believed to account for the toxicity of TCDD and related compounds.

In vivo and *in vitro* models have been used to investigate the mechanisms of action of TCDD and to assess its potential toxicity to humans and other environmentally relevant species. However, the relevance of data extrapolation from experimental models to target species has been questioned [5]. In general, minimizing the extrapolation between experimental models and the relevant species is expected to more accurately assess the potential toxicity to the target of concern. Although cell lines model may reflect some *in vivo* responses, their utility for predicting *in vivo* toxicity is limited. Nevertheless, human based *in vitro* models are expected to more accurately indicate potential *in vivo* human toxicity. For example, human based models are preferred in drug development to investigate the mechanisms of action and assess potential toxicities of drug candidates [6-9]. Immortalized cell lines, primary cells and organ slices have

been used as drug screening tools [10] and to assess potential mechanisms, including toxicant-target interaction and dose/time dependent responses [7]. However, while continuous cell lines are convenient, they are transformed or derived from diseased tissue, which may not accurately reflect normal tissue responses [6]. In contrast, the availability, use, cost, safety, and stability of primary cells and human tissue continues to be a factor.

Human stem cells provide an attractive alternative and potentially unlimited source of normal cells [11, 12]. They are defined by their self-renewal and differentiation capabilities, and classified as either embryonic or adult stem cells based on their developmental status. Normal adult human stem cells isolated from liver tissue is an alternative model for toxicity studies, that may more closely mimic human tissue [11, 13, 14]. Stem cells are also amenable to high throughput screening to rank and prioritize chemicals and drug candidates that warrant further investigation or development [12, 15, 16].

HL1-1 cells were derived from adult normal liver tissue. They exhibit high proliferation potential, express stem cell (Oct-4) and liver oval cell markers (AFP, vimentin and Thy-1), and have the ability to differentiate into hepatocytes [17]. In this study, HL1-1 cells were used to investigate the time- and dose-dependent gene expression changes elicited by TCDD. HL1-1 gene expression data were also compared to other *in vitro* (HepG2 and Hepa1c1c7 cells) and *in vivo* (C57BL/5 hepatic tissue) data sets treated with TCDD using comparable study designs and data analysis approaches. Although some common pathways are affected, the results suggest that TCDD elicits species- and model- specific gene expression profiles.

MATERIALS & METHODS

DERIVATION OF HL1-1 HUMAN LIVER CELL LINE

HL1-1 human liver cell line was derived from a normal healthy liver section obtained during the surgical resection of a male (age 49) with hemangioma. This cell line has been previously shown to possess liver stem cell characteristics [17, 18] including, (1**)** high self-renewal ability, cumulative population doubling level (cpdl) about 50, (2) deficiency in gap junctional intercellular communication, (3) expression of Oct 4, and liver stem cell markers, alpha-fetoprotein, vimentin and Thy-1, and (4) the ability to differentiate into albumin producing cells. The morphology and proliferation potential of HL1-1 cells are shown in Figure 10. The finite lifespan of HL1-1 cells and the non-tumorigenic nature of HL1-1 cells immortalized by SV40 large T-antigen (no tumor developed in 6 mice injected with 4 x 10^6 cells at 2 sites per mouse, our unpublished results) indicate that HL1-1 cells are normal non-tumorigenic cells. The cells at approximately passage 8 with cumulative population doubling level of about 40 were used for this study.

CULTURE AND TREATMENT OF CELL LINE

HL1-1 cells [17] were maintained in a low calcium (0.09mM) modified MCDB 153 medium (Keratinocyte-SFM, Invitrogen Corporation, Carlsbad, CA) supplemented with 2 mM N-acetyl-L-cysteine, 0.2 mM L-ascorbic acid 2-phosphate and 5 mM nicotinamide (referred to as K-NAC medium). The medium contains rEGF (5 ng/mL), bovine pituitary extract (50 ug/mL) and 10% fetal bovine serum (FBS) (Hyclone, Logan, UT). 1×10^6 cells were seeded into vented 25 cm^2 cell culture flasks (Corning Inc., Corning, NY) and incubated under standard conditions (5% CO_2, 37°C). For time course studies, cells were treated with 10 nM TCDD (S. Safe, Texas

A&M University, College Station, TX) or DMSO (Sigma, St. Louis, MO) and harvested at 1, 2, 4, 8, 12, 24 or 48 hrs (Figure 11). For dose-response studies HL1-1 cells were treated with DMSO (vehicle control) or TCDD (0.001, 0.01, 0.1, 1, 10, 100 nM) for 12 hrs (Figure 11). For the cycloheximide (CHX) study, HL1-1 cells were divided into four treatment groups: (1) 10 nM TCDD, (2) DMSO as a vehicle control, (3) pre-treatment with 10 μg/mL CHX(Sigma-Aldrich, St. Louis, MO) for 1 hr prior to treatment with DMSO, or (4) pre-treated with 10 μg/mL CHX for 1 hr prior to treatment with 10 nM TCDD, and then harvested at 4 and 12 hrs (Figure 11).

PROTEIN PREPARATION AND WESTERN BLOT

Cell lysates were prepared in RIPA buffer (1x PBS, 0.1% SDS, 1% IGEPAL CA-630 and 0.5% Na-Deoxycholate) containing a protease inhibitor cocktail (Roche Diagnostics, Mannheim, Germany). Protein concentrations were measured with a modified Lowry assay (Bio-Rad, DC Protein Assay, Hercules, CA). Cell lysates (20 ug) were separated on a 10% SDS-PAGE, transferred onto nitrocellulose membranes (Amersham Biosciences Inc., Piscataway, NJ), and probed with anti-human AhR (N-19) antibody followed by horseradish peroxidase-conjugated secondary antibodies (Santa Cruz Biotechnology Inc., Santa Cruz, CA). The blot was imaged by immunochemical staining and fluorescence detection on X-ray film by the ECL method (Amersham Biosciences Inc.).

RNA ISOLATION

All treatment groups were harvested in 1.0 mL Trizol Reagent (Invitrogen) and stored at -80^{o}C. Total RNA was isolated according to the manufacturer's protocol, resuspended in RNA Storage Solution (Ambion Inc., Austin, TX), and quantified spectrophotometrically (A_{260}). The purity and integrity of each sample was assessed by the A_{260}/A_{280} ratio and gel electrophoresis.

A

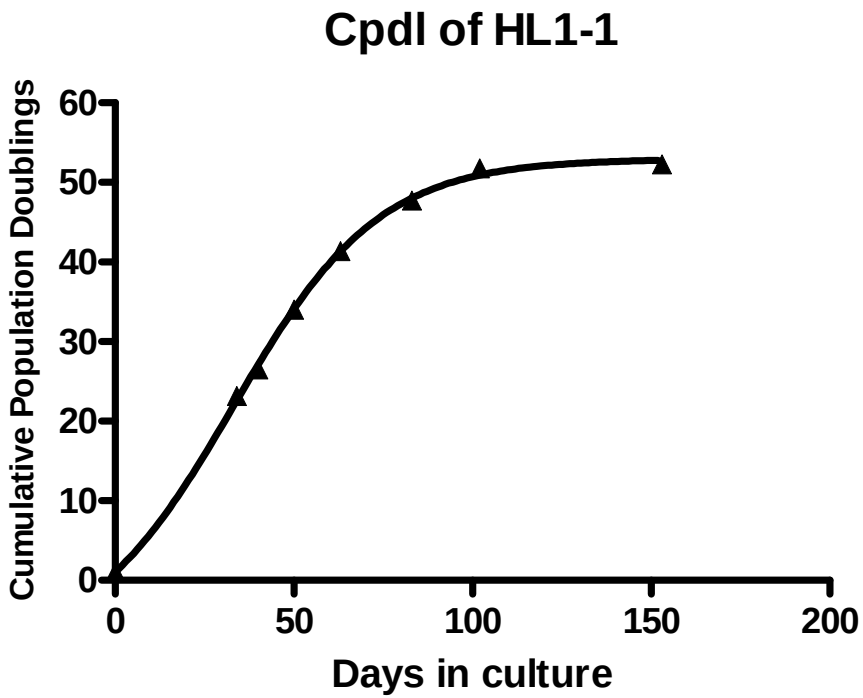

B

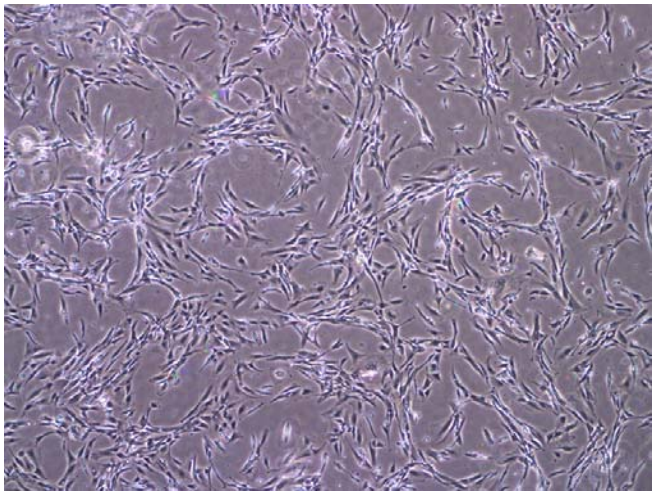

Figure 10. The proliferation potential and morphology of HL1-1 cell.
(A) The proliferation potential of HL1-1 cell clone as determined by cumulative population doubling level (cpdl) in continual growth and subculture from $1x10^5$ cells. (B) HL1-1 cell morphology.

MICROARRAY EXPERIMENTAL DESIGN

Gene expression changes were measured on custom human cDNA arrays containing 9,684 features representing 6,995 unique genes. For the time course study, an independent reference study design was used that included three replicates. Time-matched TCDD treated and vehicle samples were co-hybridized at each time point (Figure 12A). Dose-dependent changes in gene expression were analyzed using a spoke design with three replicates at 12 hrs (Figure 12B). Dye swaps were also performed for both time course and dose response studies to account for dye biases. For CHX studies, a 2X2 factorial design was used to facilitate appropriate statistical comparisons between all four treatment groups (Figure 12C) [19]. If TCDD-elicited gene response were sustained or enhanced by cycloheximide co-treatment, a direct effect independent of down stream translational activities was inferred and classified as a putative primary response. However, if the gene expression response was attenuated by CHX, it was assumed that the response was dependent on protein production(s), which were blocked by CHX, and therefore classified as putative secondary responses. Candidate genes that passed the first filter were further investigated by comparing CHX treatment alone to vehicle and co-treatment compared to CHX alone in order to exclude unclassified genes whose change in expression was affected by CHX.

ANALYSIS OF DIFFERENTIAL GENE EXPRESSION

PCR amplified cDNAs were robotically spotted onto epoxy-coated slides (Schott-Nexterion, Duryea, PA) by an Omnigrid arrayer (GeneMachines, San Carlos, CA) equipped with Chipmaker 3 pins in a CHP3 printhead (Telechem International Inc., Sunnyvale, CA) at the Research Technology Support Facility, Michigan State University (http://www.genomics.msu.edu). Selected clones were obtained from EPAMAC, Research

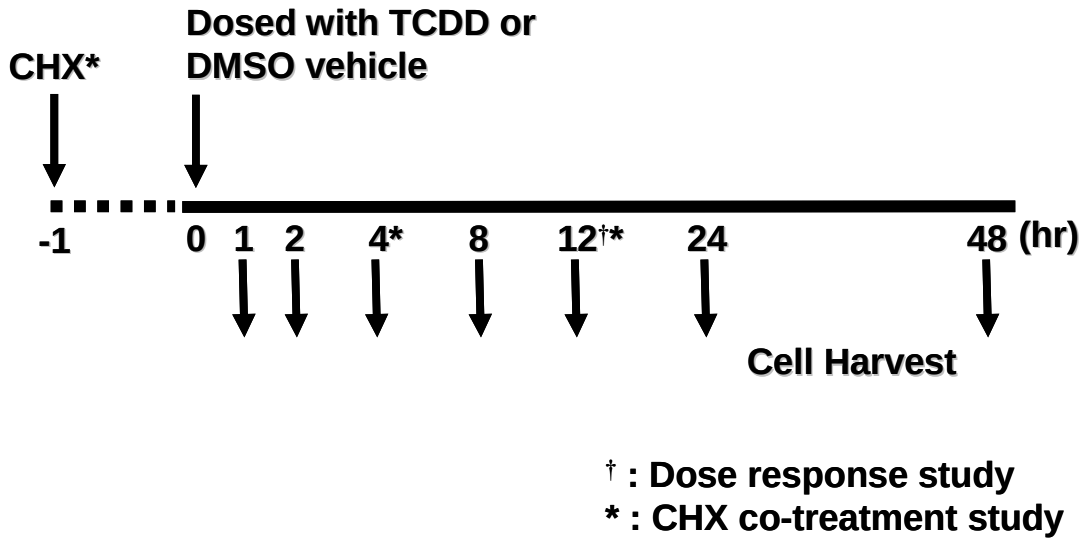

Figure 11. HL1-1 TCDD time course, dose response and cycloheximide (CHX) study designs.
For the time course study, HL1-1 cells were treated with either 10 nM TCDD or 0.1% DMSO and harvested at 1, 2, 4, 8, 12, 24, or 48 hrs post-treatment. For the dose response study, HL1-1 cells were treated with 0.001, 0.01, 0.1, 1, 10, 100 nM TCDD or 0.1 % DMSO vehicle and harvested 12 hrs post-treatment (as indicated †). For the CHX study, 10 μg/mL CHX was treated 1 hr prior to 10 nM TCDD or 0.1% DMSO treatment. Treatment groups were harvested at 4 and 12 hrs post-treatment (as indicated *). Three replicates were conducted in all studies.

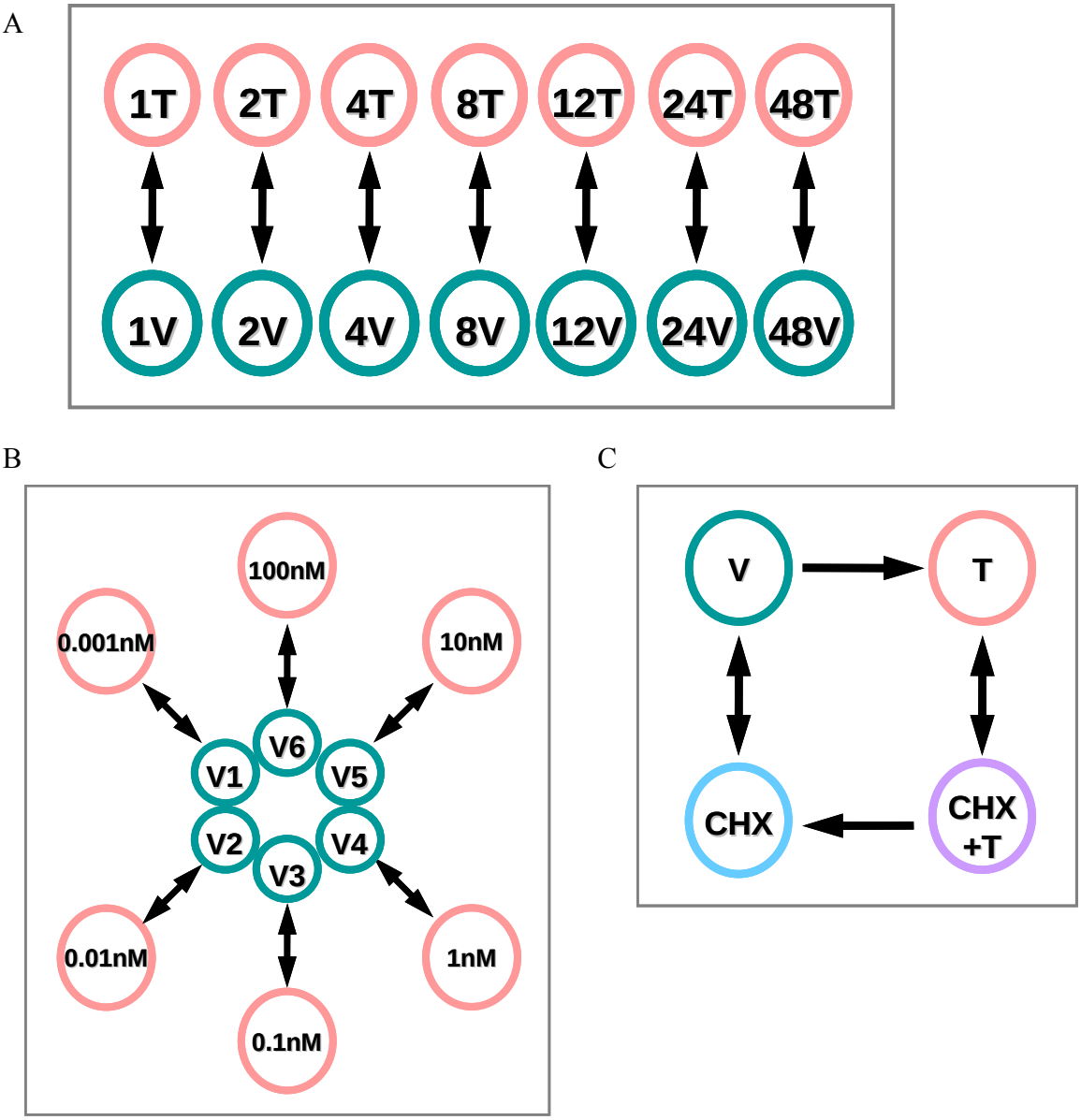

Figure 12. Microarray experimental designs.
Microarray experimental designs for (A) HL1-1 TCDD time course, (B) dose response and (C) CHX study. (A) Temporal gene expression changes were analyzed using an independent reference design that results in two independent labeling of each sample. Numbers indicate time of cell harvesting (hours), T indicate TCDD treatment and V indicate DMSO vehicle treatment. (B) Dose response gene expression changes were analyzed using a spoke design. Each dose treatment sample was compared with independent vehicle control. (C) CHX gene expression changes were analyzed using a 2x2 factorial design. This design allows for multiple comparisons to identify significant changes in gene expression between treatments. Each arrow represents a single microarray where arrow heads represent Cy5-labeled samples and arrow tails represent Cy3-labeled samples and double headed arrows indicate dye swap labeled on different arrays.

Genetics and Van Andel Research Institute. Detailed protocols for processing of microarrays including the labeling of the cDNA probe are available at http://dbzach.fst.msu.edu/interfaces/microarray.html.

Briefly, the Genisphere 900 3DNA Array Detection (Genisphere Inc., Hatfield, PA) indirect incorporation kit was used to generate cDNA samples for hybridization according to manufacturer's protocol. After 20 hrs of cDNA hybridization, slides were washed and re-hybridized with a Cy3:Cy5 (1:1) dendrimer mixture to indirectly incorporate dyes at the Cy3- and Cy5-dendrimer-tagged cDNA for 16 hrs. Slides were then scanned at 635 nm (Cy3) and 532 nm (Cy5) using a GenePix 4000B Array Scanner (Molecular Devices, Union City, CA). Images were analyzed for feature and background intensities using GenePix Pro 6.1 (Molecular Devices).

MICROARRAY DATA NORMALIZATION AND ANALYSIS

Data were normalized using a semi-parametric approach [20]. Empirical Bayes analysis was used to calculate posterior probabilities (P1(*t*) value) of expression change on a per gene and time point or dose group basis using the model-based *t*-value [21]. The data were filtered using a P1(*t*) and fold change to obtain the most reproducible differentially expressed genes for initial analysis and interpretation. All raw and normalized data were stored in the toxicogenomic information management system (TIMS) dbZach which supports microarray data management, mining, visualization and knowledge management [22, 23]. Expression changes that passed the criteria were analyzed by hierarchical clustering (GeneSpring 6.0, Agilent Technologies Inc., Santa Clara, CA and Multiexperiment Viewer (MeV) in TM4 software [24]) using uncentered Pearson correlation with average linkage. Normalization and empirical Bayes analysis were performed using SAS 9.1 (SAS Institute, Cary, NC) and R 2.0.1 (http://www.r-project.org).

Dose response analysis was performed using Graph Pad Prism 4.0 (GraphPad Software, San Diego, CA). Functional categorization of genes was performed using Database for Annotation, Visualization and Integrated Discovery (DAVID) analysis as a gene ontology tool [25].

QUANTITATIVE REAL-TIME PCR (QRT-PCR) ANALYSIS

QRT-PCR was performed for a selected number of genes to verify microarray data. Total RNA (1.5 μg) was reverse transcribed by SuperScript II according to the manufacturer's protocol (Invitrogen). cDNA products were then amplified with gene specific primers designed using Primer3 [26] and SYBR Green PCR reaction mixture (Applied Biosystems, Foster City, CA) on an Applied Biosystems PRISM 7500 Sequence Detection System. Input copy number was quantified using a standard curve of log copy number versus threshold cycle (Ct). The copy number of each sample was standardized to the geometric mean of β-actin (ACTB) and glyceraldehyde-3-phosphate dehydrogenase (GAPDH) to control for differences in RNA loading, quality, and cDNA synthesis. For graphing purposes, the relative gene expression levels were scaled such that the expression level of the time-matched vehicle treated control group was equal to 1. Official names and abbreviations, forward and reverse primer sequences, and product length are listed in Table 3.

IDENTIFICATION OF DRES

Intergenic regions 10kb upstream of RefSeq annotated transcription start sites (TSS) were obtained from the University of California Santa Cruz (UCSC) Genome Browser and deposited into dbZach [23]. Core DRE sequences (5'-GCGTG-3') were computationally identified, extended by the flanking 7 base pairs and scored using a position weight matrix (PWM) application [27]. The PWM was developed using experimentally verified dioxin response

elements (DREs); DRE sequences are from genome sequence. Putative DREs are those with a matrix similarity score greater than 0.80 [28-30].

RESULTS

EXPRESSION AND FUNCTIONALITY OF AHR IN HL1-1 CELLS

AhR mRNA was detected in HL1-1 cells, C57BL/6 hepatic tissue, human HepG2 and mouse Hepa1c1c7 cells (Figure 13A). AhR protein expression was confirmed by Western blot (Figure 13B). Treatment of HL1-1 cells with TCDD resulted in the dose-dependent induction (>600-fold) of CYP1A1 mRNA with an EC_{50} of 8.30 nM (Figure 14), which is less sensitive compared to other human *in vitro* models (HepG2: 0.68 nM [31], HepG2: 0.2 nM and fresh hepatocytes: 0.14 nM [32]). There was no indication of TCDD treatment mediated differences with respect to growth or physical appearance. Collectively, these results confirm the functionality and responsiveness of HL1-1 AhR to TCDD.

MICROARRAY ANALYSIS OF TCDD INDUCIBLE DOSE AND TEMPORAL GENE EXPRESSION PROFILES

Temporal and dose-dependent changes in gene expression were determined using custom human cDNA microarrays consisting of 9,684 features representing 6,995 unique genes. Differentially expressed genes were identified using P1(t) values greater than 0.9999 and |fold change| > 1.5 as the criteria. 113 unique genes (72 induced; 41 repressed) exhibited dose dependent regulation with a majority exhibiting differential expression between 1 - 100 nM TCDD (Figure 15A). EC_{50}s ranged from 0.18 nM for ACSL3 to 37.3 nM for MOBP, while induction and repression ranged from 40- to -2-fold for genes CYP1B1 and GALNT1, respectively.

Table 3. Gene names and primer sequences for QRT-PCR

RefSeq	Gene name	Gene symbol	Entrez Gene ID	Forward Primer	Reverse Primer	Product Size (bp)
Human						
NM_001101	actin, beta	ACTB	60	CATCCCCCAAAGTTCACAAT	AGTGGGGTGGCTTTTAGGAT	125
NM_002046	glyceraldehyde-3-phosphate dehydrogenase	GAPDH	2597	GGCCTCCAAGGAGTAAGACC	AGGGGTCTACATGGCAACTG	147
NM_001621	aryl hydrocarbon receptor	AHR	157873	TGTTGGACGTCAGCAAGTTC	TGGTGCCCAGAATAATGTGA	197
NM_009992	cytochrome P450, family 1, subfamily A, polypeptide 1	CYP1A1	13076	AAGTGCAGATGCGGTCTTCT	AAAGTAGGAGGCAGGCACAA	140
NM_000104	cytochrome P450, family 1, subfamily B, polypeptide 1	CYP1B1	1545	CACCAAGGCTGAGACAGTGA	GATGACGACTGGGCCTACAT	164
NM_000693	aldehyde dehydrogenase 1 family, member A3	ALDH1A3	220	GGTGGACCTGCTTACAGAGC	TCCACGGTATGCACTAACCA	165
NM_003486	solute carrier family 7 (cationic amino acid transporter, y+ system), member 5	SLC7A5	8140	AGGAGCCTTCCTTTCTCCTG	CTGCAAACCCTAAGGCAGAG	181
Mouse						
NM_007393	actin, beta, cytoplasmic	Actb	11461	GCTACAGCTTCACCACCACA	TCTCCAGGGAGGAAGAGGAT	123
NM_008084	glyceraldehyde-3-phosphate dehydrogenase	Gapdh	14433	GTGGACCTCATGGCCTACAT	TGTGAGGGAGATGCTCAGTG	125
NM_013464	aryl-hydrocarbon receptor	Ahr	11622	ACCAGAACTGTGAGGGTTGG	TCTGAGGTGCCTGAACTCCT	155

A

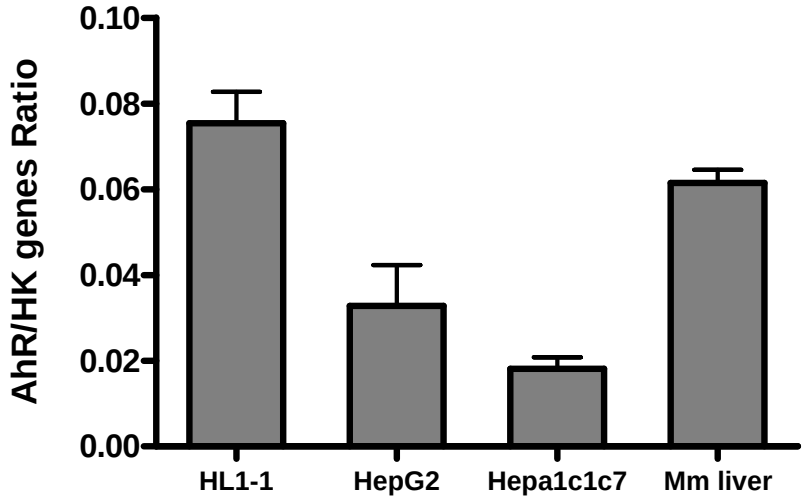

B

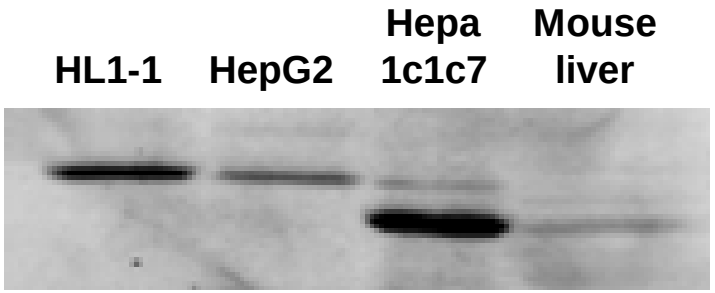

Figure 13. Basal AhR mRNA and protein expression in HL1-1 cells.
(A) AhR mRNA levels were measured by QRT-PCR and normalized to several housekeeping (HK) genes. HL1-1: human liver stem cell, HepG2: human hepatoma cell, Hepa1c1c7: mouse hepatoma cell, and Mm liver: C57BL/6 mouse liver. Error bars represent the SEM for the average. (B) AhR protein expression in HL1-1 cells, HepG2 cells, Hepa1c1c7 cells and C57BL/6 mouse liver detected by Western analysis. The mw is estimated to be 112 and 95 kDa for human and rodent AhR, respectively.

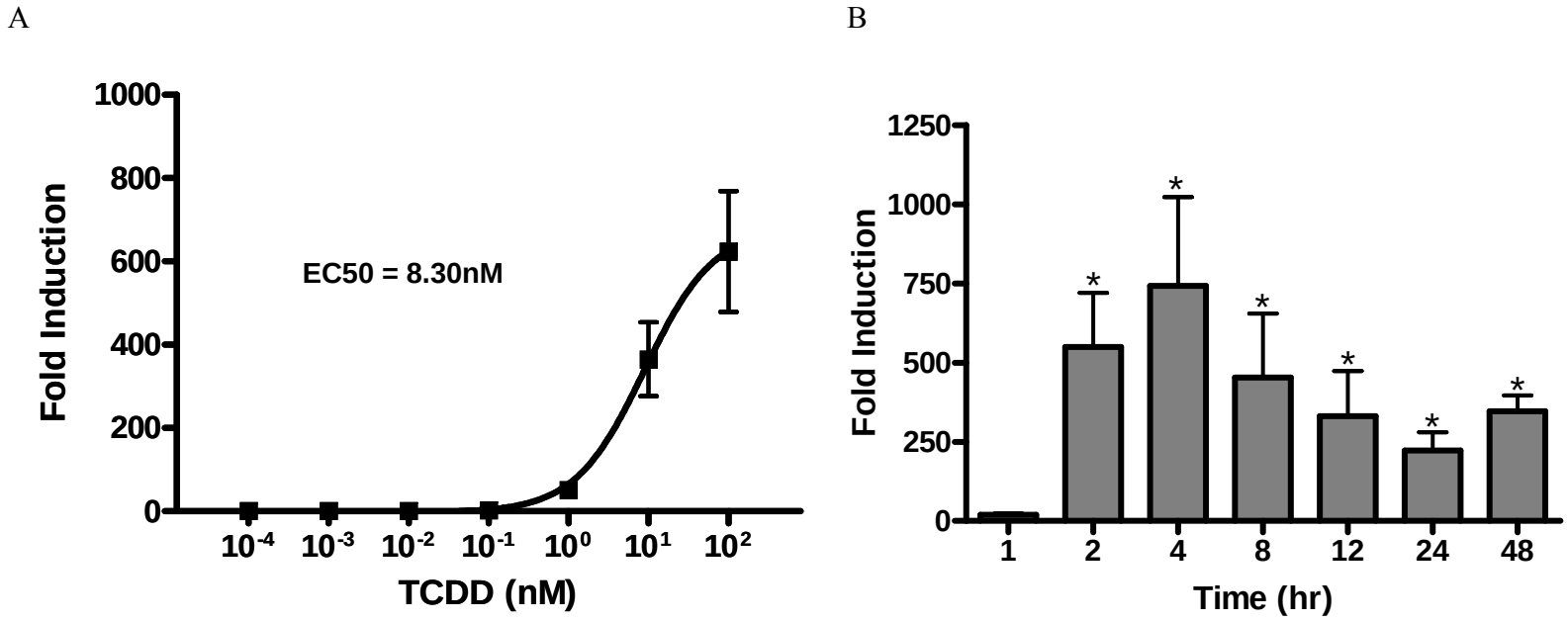

Figure 14. CYP1A1 expression induction by TCDD in HL1-1 cells.
QRT-PCR verification of CYP1A1 mRNA levels from the dose response (12 hr) (A) and time course (10 nM TCDD) (B) studies in HL1-1 cells treated with TCDD. The EC_{50} value for CYP1A1 expression was 8.3 nM. Error bars represent the SEM for the average fold change. The asterisk (*) indicates $p < 0.05$.

In the time course study, 144 unique genes were differentially regulated by TCDD at one or more time points (Figure 15B). Hierarchical clustering identified induced and repressed expression with three distinct, temporal clusters of early (2-4 hrs), mid (8-12 hrs), and late (24-48 hrs) responses (Figure 16). Early and mid time point groups showed vast differences in their expression profiles, illustrating a temporal cascade of responses.

A subset of responsive genes including CYP1B1, ALDH1A3 and SLC7A5 was verified by QRT-PCR (Figure 17). There was good agreement between the microarray and QRT-PCR data for the temporal expression profiles with comparable EC_{50} values.

IDENTIFICATION OF PUTATIVE TCDD PRIMARY RESPONSE GENES FROM CHX STUDIES

HL1-1 cells were pretreated with CHX to inhibit *de novo* protein synthesis in order to identify putative primary gene expression responses mediated by the AhR. Following treatment 78 and 203 differentially expressed genes ($P1(t) > 0.9999$ and $|\text{fold change}| > 1.5$) were identified at 4 and 12 hrs, respectively (Figure 18). These genes were classified into putative primary, secondary or unclassified groups. 47 genes at 4 hrs and 53 genes at 12 hrs were putatively determined to be primary responses. A total of 78 unique genes were identified as putative primary responses with 22 genes in common at both time points.

Putative primary responses were associated with xenobiotic and lipid metabolism, cell cycle regulation, transcription regulation, transport and signal transduction (Table 4). This included the prototypical xenobiotic metabolism related genes such as cytochrome P450s and aldehyde dehydrogenases which were highly induced. Other primary responses included genes associated with lipid metabolism (APOM, PLD3, ST8SIA1, ACSL3), cell cycle regulation (CDCA5, KANK1, FHIT, CTGF), and transcriptional regulation (MXD3, DEAF1,SERTAD2). The regulation of transcription factors and subsequent changes in gene expression is a hallmark

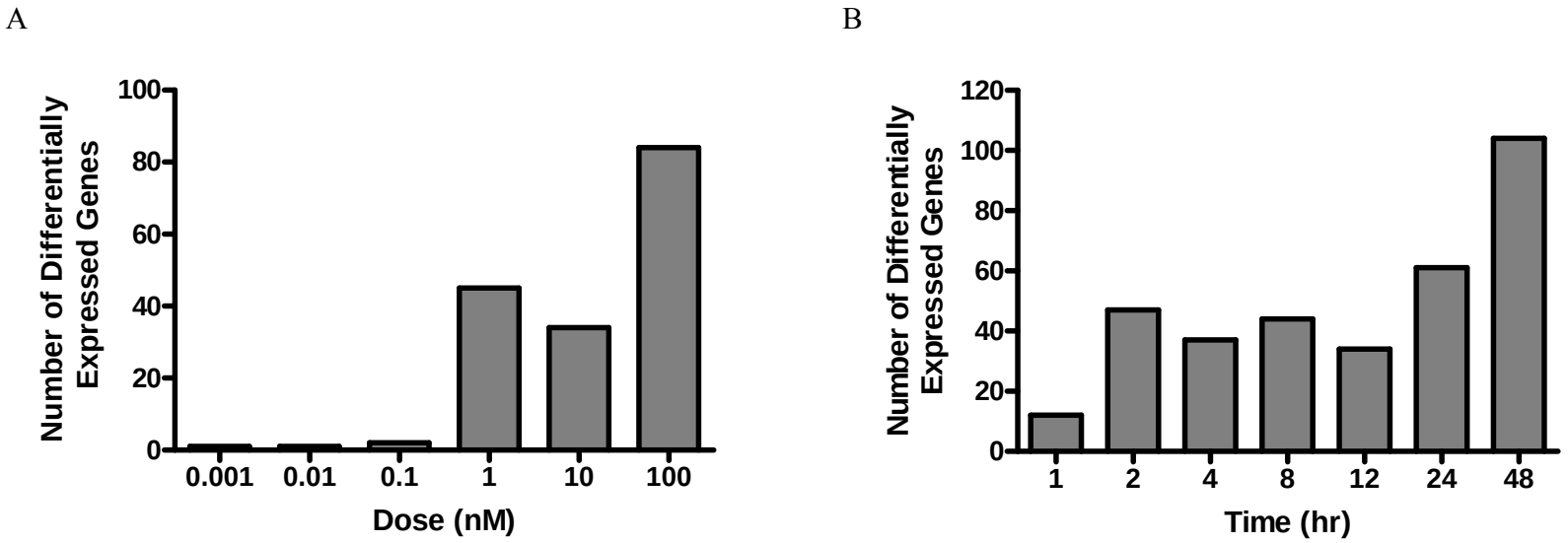

Figure 15. Number of genes exhibiting differential expression changes in the TCDD (A) dose-response (12 hr) and (B) time course study (10 nM TCDD).
The number of differentially expressed genes exhibited dose-dependent induction and steady increase between 1 and 8 hr, followed by a decrease at 12 hr but further increases at 24 and 48 hr.

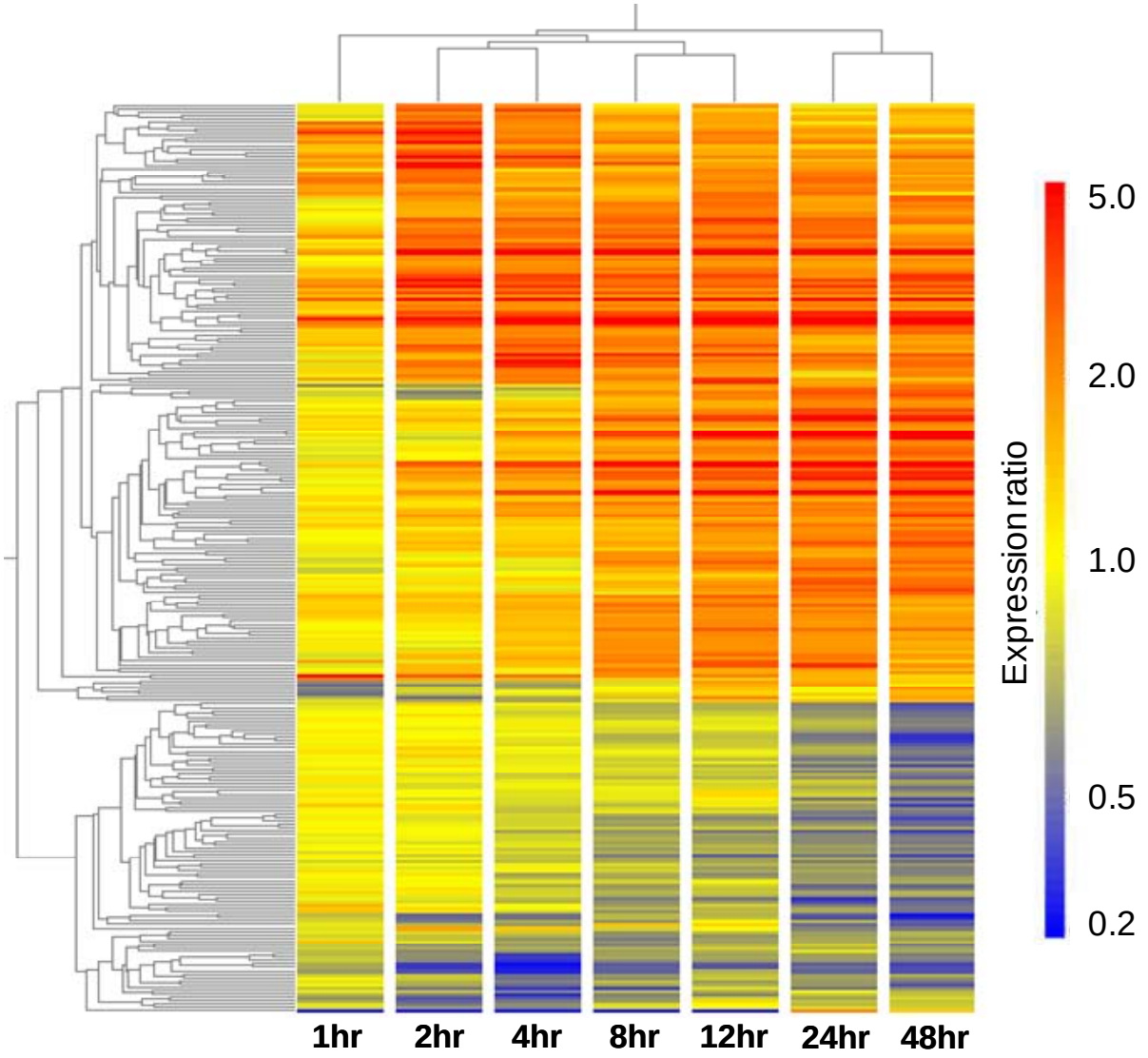

Figure 16. HL1-1 TCDD time course hierarchical clustering.
Hierarchical clustering illustrates the induction and repression of 273 differentially expressed features representing 155 unique genes. Differentially expressed genes clustered according to early (2-4 hr), mid (8-12 hr), and late (24-48 hr) time points.

Figure 17. QRT-PCR verification of CYP1B1, ALDH1A3 and SLC7A5 microarray results in the time course (10 nM TCDD) and dose response (12 h) studies.
Fold changes were calculated relative to time-matched vehicle controls. Bar (left axis) and lines (right axis) represent QRT-PCR and cDNA microarray data, respectively. EC_{50} values were calculated from QRT-PCR and cDNA microarray (parenthesized value) data, respectively. Results are represented as the average of three biological replicates. QRT-PCR data error bars represent the SEM for the average fold change. The asterisk (*) indicates $p < 0.05$ for QRT-PCR.

Figure 17 (Cont'd)

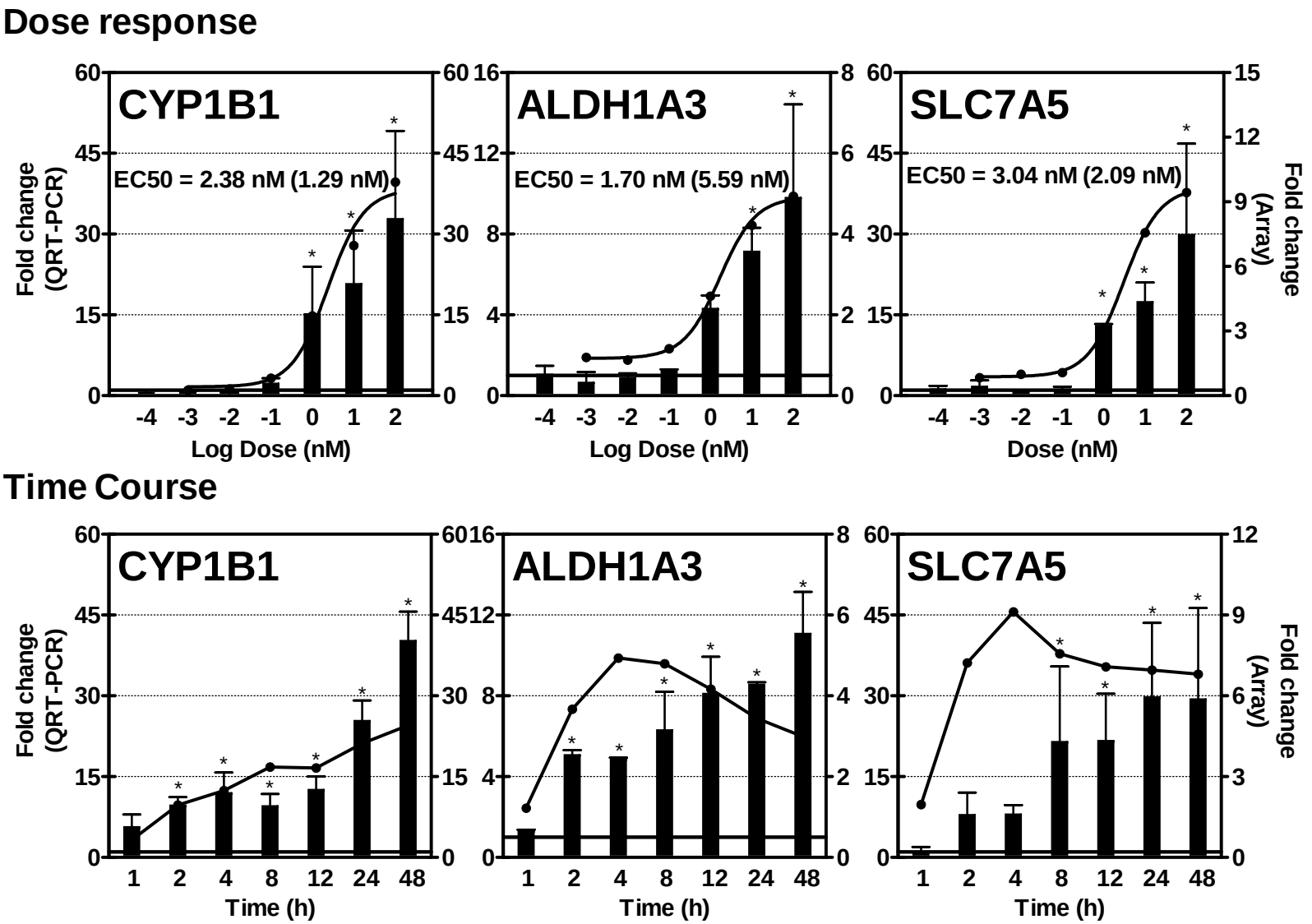

of TCDD action [33]. Immune response genes (IL1A, IL1B, CD8A), signal transduction related genes (MAPK7, PRKCB) and transporters (SLC2A1, SLC7A5, MTCH2) were also identified as putative primary responses. Computational analysis of the regulatory region of these putative primary responses revealed that 71 of the 78 genes had one or more putative DREs with a matrix similarity score greater than > 0.8 (Table 4).

COMPARISON OF HL1-1 GENE EXPRESSION WITH HUMAN HEPATOMA HEPG2 CELLS

Temporal changes in gene expression elicited by TCDD in HL1-1 cells were compared to intra-laboratory time course studies conducted in other model systems. 251 HL1-1 genes were identified as differentially expressed in the time course study using relaxed filtering criteria ($P1(t) > 0.999$ and $|\text{fold change}| > 1.3$) to include responses on the margins. Using the same relaxed criteria and the same study design, cDNA microarray, and data analysis strategy, 1,057 HepG2 genes were identified as differentially expressed at one or more time points following treatment with 10 nM TCDD (Dere et al., manuscript in preparation). Only 74 common genes were differentially regulated in HL1-1 and HepG2 cells by TCDD (Table 5, Figure 19A). Of these, 55 exhibited similar temporal expression patterns (38 induced; 17 repressed (Table 5, Figure 19B)), and 12 were classified as putative primary responses. Of the 19 genes exhibiting divergent regulation (7 induced in HL1-1 but repressed in HepG2; 12 repressed in HL1-1 but induced in HepG2 (Table 5, Figure 19C)), none were putative primary responses in the HL1-1 based on the CHX study.

HL1-1 specific responses were associated with immune and lipid/xenobiotic metabolic processes (Figure 19D), while HepG2 specific responses were involved in the cytoskeleton, calcium signaling and lipid metabolism. Other functional associations included transport, cell cycle, signal transduction and transcriptional regulation.

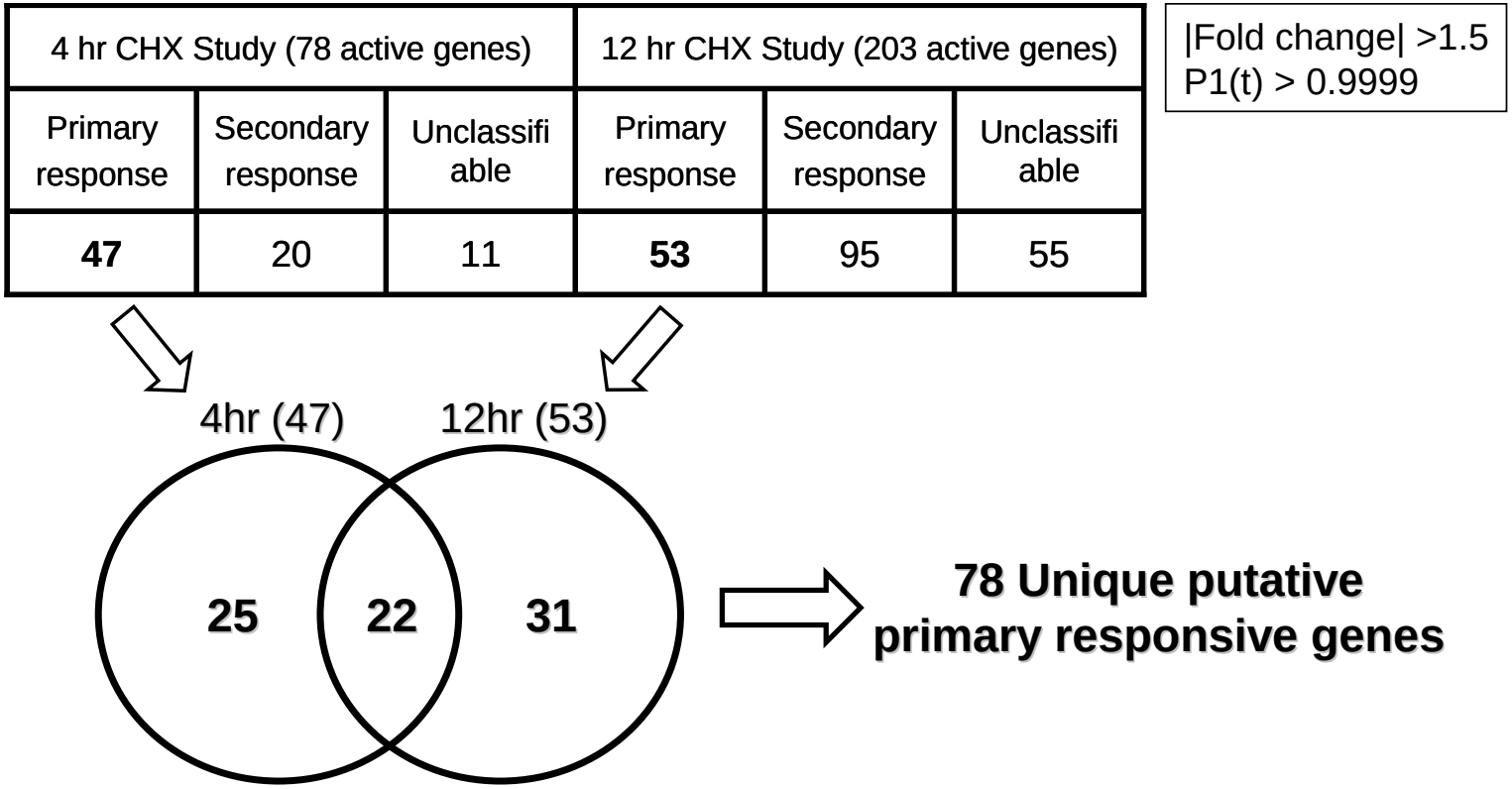

Figure 18. Putative primary TCDD responsive genes from CHX study.
Microarray analysis identified 78 and 203 TCDD-responsive genes at 4 and 12 hr, respectively. CHX co-treatment identified 47 and 53 genes classified as putative primary responsive genes at 4 and 12 hr, respectively. 78 unique putative primary responses were identified at both time points.

Table 4. Functional categorization of putative primary response genes elicited by TCDD

Functional Category[a]	Entrez GeneId	Gene Symbol	Gene Name	DRE Count[b]	4 hr FC[c]			12 hr FC[c]		
					T/V	TC/V	C/V	T/V	TC/V	C/V
Drug metabolism	1543	CYP1A1[d]	cytochrome P450, family 1, subfamily A, polypeptide 1	13	**507**	**4136**	**28**	**222**	**26794**	**513**
	1545	CYP1B1	cytochrome P450, family 1, subfamily B, polypeptide 1	7	**9.0**	**9.0**	1.3	**11.1**	**14.9**	**2.9**
	224	ALDH3A2	aldehyde dehydrogenase 3 family, member A2	6	**10.0**	**8.3**	-1.2	**5.5**	**15.1**	-1.4
	220	ALDH1A3	aldehyde dehydrogenase 1 family, member A3	3	**8.6**	**7.5**	-1.1	**5.3**	**12.0**	-1.3
Lipid metabolism	8733	GPAA1	glycosylphosphatidylinositol anchor attachment protein 1 homolog (yeast)	9	**1.8**	**2.8**	1.5	1.5	**3.7**	**1.9**
	5919	RARRES2	retinoic acid receptor responder 2	8	**2.4**	**1.8**	1.2	**3.0**	**3.9**	**1.6**
	55937	APOM	apolipoprotein M	8	1.2	1.2	1.0	**2.0**	1.1	-1.2
	51084	CRYL1	crystallin, lambda 1	7	**2.4**	**2.7**	1.0	**2.2**	**10.1**	1.0
	23646	PLD3	phospholipase D family, member 3	6	**1.6**	**2.9**	**1.6**	1.1	**2.7**	-1.1
	9108	MTMR7	myotubularin related protein 7	6	**3.1**	**4.9**	1.3	**1.7**	**6.9**	**1.5**
	6489	ST8SIA1	ST8 alpha-N-acetyl-neuraminide alpha-2,8-sialyltransferase 1	4	**1.7**	**2.2**	**1.5**	**2.2**	**5.4**	**2.4**
	2181	ACSL3	acyl-CoA synthetase long-chain family member 3	7	**-2.0**	**-1.8**	1.0	1.2	**2.7**	-1.2
	2896	GRN	granulin	6	**-2.2**	**-3.1**	-1.1	-1.2	**-3.2**	1.2

Table 4 (cont'd)

Functional Category[a]	Entrez GeneId	Gene Symbol	Gene Name	DRE Count[b]	4 hr FC[c]			12 hr FC[c]		
					T/V	TC/V	C/V	T/V	TC/V	C/V
Regulation of cell cycle	23189	KANK1	KN motif and ankyrin repeat domains 1	6	**2.2**	**2.1**	1.0	**1.6**	**1.7**	-1.3
	5069	PAPPA	pregnancy-associated plasma protein A, pappalysin 1	3	**2.5**	**2.4**	**1.6**	**1.7**	**5.8**	**1.7**
	113130	CDCA5	cell division cycle associated 5	2	**8.6**	**14.8**	1.4	**2.8**	**33.3**	**2.1**
	2272	FHIT	fragile histidine triad gene	1	1.2	1.2	1.4	**1.8**	**2.4**	1.4
	5270	SERPINE 2	serpin peptidase inhibitor, clade E, member 2	0	**2.9**	**2.6**	**1.6**	**2.0**	**7.1**	**1.9**
	5764	PTN	pleiotrophin	0	**1.8**	**2.6**	**1.9**	**1.6**	**5.8**	**1.8**
	1490	CTGF	connective tissue growth factor	2	**-2.3**	**-2.2**	1.0	**-1.7**	**-1.9**	**1.7**
Regulation of transcription	83463	MXD3	MAX dimerization protein 3	13	**2.4**	**2.8**	-1.1	**2.1**	**9.2**	1.0
	10522	DEAF1	deformed epidermal autoregulatory factor 1	13	1.2	1.1	1.0	**1.7**	**1.9**	1.3
	22938	SNW1	SNW domain containing 1	8	**2.0**	**1.6**	1.1	**2.6**	**2.8**	1.4
	10062	NR1H3	nuclear receptor subfamily 1, group H, member 3	8	**2.4**	**1.8**	1.2	**3.3**	**3.7**	**1.8**
	2002	ELK1	ELK1, member of ETS oncogene family	7	**2.5**	**4.9**	**2.0**	**2.4**	**9.5**	**2.8**
	84759	PCGF1	polycomb group ring finger 1	6	**1.6**	**1.7**	-1.1	**1.7**	**3.0**	1.1
	22936	ELL2	elongation factor, RNA polymerase II, 2	4	1.4	-1.1	-1.4	**2.1**	1.5	-1.3
	9792	SERTAD2	SERTA domain containing 2	1	**1.6**	**6.7**	**2.8**	**2.0**	**8.7**	**4.4**
	10370	CITED2	Cbp/p300-interacting transactivator, with Glu/Asp-rich carboxy-terminal domain, 2	3	**-1.9**	**-1.7**	-1.1	1.4	**2.3**	1.0

Table 4 (cont'd)

Functional Category[a]	Entrez GeneId	Gene Symbol	Gene Name	DRE Count[b]	4 hr FC[c]			12 hr FC[c]		
					T/V	TC/V	C/V	T/V	TC/V	C/V
Signal transduction	2889	RAPGEF1	Rap guanine nucleotide exchange factor (GEF) 1	12	**1.7**	1.4	1.2	**2.2**	**2.3**	1.1
	11156	PTP4A3	protein tyrosine phosphatase type IVA, member 3	10	**1.8**	**1.7**	1.1	1.4	**2.7**	1.2
	29990	PILRB	paired immunoglobin-like type 2 receptor beta	10	1.3	1.4	1.1	**1.6**	**1.9**	1.1
	51768	TM7SF3	transmembrane 7 superfamily member 3	9	1.2	1.1	-1.1	**1.6**	**3.0**	1.2
	136	ADORA2B	adenosine A2b receptor	9	**1.9**	**2.5**	1.2	**1.9**	**6.4**	1.5
	3553	IL1B	interleukin 1, beta	6	**7.6**	**19.3**	**6.7**	**4.1**	**76.1**	**17.2**
	3552	IL1A	interleukin 1, alpha	2	**3.6**	**14.2**	**9.2**	**2.6**	**51.1**	**13.6**
	5598	MAPK7	mitogen-activated protein kinase 7	2	**1.6**	**6.4**	**2.7**	**1.7**	**5.7**	**2.4**
	5579	PRKCB	protein kinase C, beta	1	**2.2**	**3.1**	1.0	1.3	**3.2**	**-1.7**
	4322	MMP13	matrix metallopeptidase 13 (collagenase 3)	0	**2.5**	**3.6**	**1.5**	1.4	**4.6**	1.3
	56990	CDC42SE2	CDC42 small effector 2	0	**2.0**	**2.5**	1.0	**-1.7**	**-1.5**	**1.5**
	4986	OPRK1	opioid receptor, kappa 1	0	1.4	1.5	1.3	**1.9**	**4.8**	**2.1**
	925	CD8A	CD8a molecule	2	-1.1	1.0	1.1	**1.5**	**1.8**	1.3
	4982	TNFRSF11B	tumor necrosis factor receptor superfamily, member 11b	1	**-1.7**	**-1.8**	1.0	-1.1	**-3.0**	1.0

Table 4 (cont'd)

Functional Category[a]	Entrez GeneId	Gene Symbol	Gene Name	DRE Count[b]	4 hr FC[c]			12 hr FC[c]		
					T/V	TC/V	C/V	T/V	TC/V	C/V
Transport	29066	CLCN3	zinc finger CCCH-type containing 7A	13	**1.6**	**1.6**	1.0	1.3	**1.7**	-1.1
	6583	SLC22A4	solute carrier family 22 (organic cation transporter), member 4	13	**2.2**	**4.1**	**1.9**	**2.2**	**7.5**	**3.2**
	6566	SLC16A1	solute carrier family 16 (monocarboxylic acid transporters), member 1	11	**2.4**	**2.2**	1.1	**2.0**	**4.5**	1.5
	6513	SLC2A1	solute carrier family 2 (facilitated glucose transporter), member 1	9	**3.3**	**6.5**	1.4	**1.7**	**8.2**	1.0
	8140	SLC7A5	solute carrier family 7 (cationic amino acid transporter, y+ system), member 5	7	**9.6**	**12.2**	1.0	**5.1**	**26.6**	1.3
	23788	MTCH2	mitochondrial carrier homolog 2 (C. elegans)	4	**2.9**	**5.0**	1.0	**1.6**	**5.8**	-1.1
RNA processing	56342	PPAN	peter pan homolog (Drosophila)	10	**2.4**	**3.8**	1.5	**1.5**	**4.9**	1.5
	2091	FBL	fibrillarin	7	**1.7**	**2.8**	1.3	**1.6**	**4.4**	1.3
	2332	FMR1	fragile X mental retardation 1	6	**1.8**	**2.7**	1.1	**1.6**	**4.4**	1.2
Regulation of translation	1965	EIF2S1	eukaryotic translation initiation factor 2, subunit 1 alpha, 35kDa	5	**1.6**	**3.3**	**2.6**	**1.8**	**9.4**	**5.3**
	1983	EIF5	eukaryotic translation initiation factor 5	9	**-1.6**	-1.3	1.0	**-1.8**	**-2.0**	-1.4
Protein biosynthesis	51665	ASB1	ankyrin repeat and SOCS box-containing 1	6	1.1	1.1	1.0	**1.6**	**1.9**	1.3
	51065	RPS27L	ribosomal protein S27-like	5	**1.7**	**1.6**	1.0	**1.6**	1.4	1.1
	51081	MRPS7	mitochondrial ribosomal protein S7	7	**-2.2**	**-2.0**	1.0	1.0	**2.6**	**-1.6**

Table 4 (cont'd)

Functional Category[a]	Entrez GeneId	Gene Symbol	Gene Name	DRE Count[b]	4 hr FC[c]			12 hr FC[c]		
					T/V	TC/V	C/V	T/V	TC/V	C/V
Apoptosis	10059	DNM1L	dynamin 1-like	12	**1.6**	**1.7**	1.1	-1.4	1.0	**2.1**
	79370	BCL2L14	BCL2-like 14 (apoptosis facilitator)	9	**2.1**	**2.5**	1.2	**1.8**	**5.0**	1.3
	317	APAF1	apoptotic peptidase activating factor	1	-1.2	-1.2	-1.1	**-1.7**	**-2.2**	**-1.7**
Protein modification	200185	KRTCAP2	keratinocyte associated protein 2	15	**2.5**	**4.0**	1.3	1.4	**3.9**	1.3
	10413	YAP1	Yes-associated protein 1, 65kDa	4	**1.9**	**1.8**	-1.2	**2.1**	**3.4**	1.3
	64710	NUCKS1	nuclear casein kinase and cyclin-dependent kinase substrate 1	1	**1.9**	**1.9**	-1.1	1.4	**1.8**	-1.2
	90701	SEC11L3	SEC11-like 3 (S. cerevisiae)	1	**1.9**	**2.5**	1.2	**-1.6**	**-2.2**	1.3
	8507	ENC1	ectodermal-neural cortex (with BTB-like domain)	4	**-2.1**	**-2.0**	1.0	**-1.6**	**-2.2**	1.4
	2589	GALNT1	UDP-N-acetyl-alpha-D-galactosamine:polypeptide N-acetylgalactosaminyltransferase 1 (GalNAc-T1)	0	**-5.9**	**-5.8**	-1.3	**-2.4**	**-7.1**	1.1
DNA metabolic process	10951	CBX1	chromobox homolog 1 (HP1 beta homolog Drosophila)	15	1.1	1.3	1.3	**1.6**	**1.9**	1.5
	10606	PAICS	phosphoribosylaminoimidazole carboxylase, phosphoribosylaminoimidazole succinocarboxamide synthetase	8	1.2	1.2	1.0	**1.6**	1.3	-1.1
	6742	SSBP1	single-stranded DNA binding protein 1	2	1.4	**2.0**	**1.8**	**1.5**	**4.4**	**2.5**

Table 4 (cont'd)

Functional Category[a]	Entrez GeneId	Gene Symbol	Gene Name	DRE Count[b]	4 hr FC[c]			12 hr FC[c]		
					T/V	TC/V	C/V	T/V	TC/V	C/V
Etc	90488	C12orf23	chromosome 12 open reading frame 23	10	1.2	1.1	1.1	**1.8**	**3.2**	**1.8**
	84079	ANKRD27	ankyrin repeat domain 27 (VPS9 domain)	9	**2.2**	**3.6**	-1.2			
	79798	ARMC5	armadillo repeat containing 5	7	**1.6**	**2.8**	1.1	**1.7**	**2.4**	1.1
	23313	C22orf9	chromosome 22 open reading frame 9	7	1.5	**1.5**	1.1	**1.8**	**2.4**	1.2
	11346	SYNPO	synaptopodin	5	**2.4**	**7.5**	**2.5**	**1.7**	**9.8**	**3.2**
	57223	SMEK2	SMEK homolog 2, suppressor of mek1 (Dictyostelium)	3	**2.5**	**2.0**	1.2	**2.0**	**2.5**	-1.2
	4077	NBR1	neighbor of BRCA1 gene 1	0	1.4	**3.1**	1.5	**1.9**	**4.6**	**2.7**
	22948	CCT5	chaperonin containing TCP1, subunit 5 (epsilon)	6	**-2.2**	**-1.7**	1.3	**-1.5**	**-1.7**	1.5
	3188	HNRPH2	heterogeneous nuclear ribonucleoprotein H2 (H')	6	**-1.7**	-1.4	1.0	-1.3	1.3	**2.1**

a. Funtional categories was performed using an in-house Gene Ontology tool

b. DRE identified in -10kb to transcriptional start site (TSS) and 5' UTR

c. Expression fold changes (FC) determined by microarray analysis and numbers in bold font indicate |FC| > 1.5
T/V: TCDD treatment vs vehicle, T+C/V: TCDD & CHX co-treatment vs vehicle, C/V: CHX treatment vs vehicle

d. Gene expressiion data was measured by QRT-PCR

GENE EXPRESSION PROFILE COMPARISON TO OTHER MODEL SYSTEMS

Comparison of HL1-1 differential gene expression to mouse Hepa1c1c7 cell [34] and C57BL/6 hepatic tissue [35] were also examined using relaxed filtering criteria (P1(t) > 0.999 and |fold change| > 1.3) to include those responses approaching the initial criteria (P1(t) > 0.9999, |fold change| > 1.5). All of these studies used comparable study designs, cDNA microarray platforms and data analysis strategies.

5505 orthologous genes, defined by HomoloGene (http://www.ncbi.nlm.nih.gov/HomoloGene/), were represented across the human and mouse cDNA arrays (Figure 20A). Comparison of HL1-1 to C57BL/6 liver tissue, and Hepa1c1c7 cells identified only 32 and 18 common differentially expressed genes, respectively (Figure 20B, Table 6). However, not all common differentially expressed genes exhibited the same expression pattern. For example, of the 18 genes differentially expressed in both HL1-1 cells and Hepa1c1c7 cells, 10 exhibited the same pattern (6 induced and 4 repressed genes), while 8 were divergently regulated (6 genes induced in HL1-1 cells were repressed in Hepa1c1c7; 2 genes repressed in HL1-1 were induced in Hepa1c1c7). Similar analyses were conducted between HL1-1 and C57BL/6 hepatic tissue differential gene expression data sets (Figure 20B, Table 7). Across all four models, only three genes (IRF1, SLC12A7 and ID3) were differentially expressed with only one gene (IRF1) exhibiting the same expression pattern.

Functional annotations of the common TCDD regulated genes were associated with cell cycle regulation, and development. Several collagenases were differentially expressed in HL1-1 and mouse Hepa1c1c7 hepatoma cells, although some responses (e.g., CDC25B) were divergently regulated suggesting species-specific effects (Table 7) [27, 30, Sun, 2004 #172]. Comparison of the functional annotation of differentially expressed genes in HL1-1 cell and

Table 5. HL1-1 vs. HepG2 Overlapping Genes: Functional Categories

Entrez GeneId	Gene Name	Gene Symbol	HL1-1		HepG2		Functions
			FC	Time Points	FC	Time Points	
Co-induced (38)							
7545	Zic family member 1 (odd-paired homolog, Drosophila)	ZIC1	2.6	2,4,8,12,24,48	9.1	2,4,8,12,24,48	transcription regulator activity
9792	SERTA domain containing 2	SERTAD2*	2.2	1,2,4,12,24,48	3.6	1,2,4,8,12,24,48	transcription regulator activity
10025	thyroid hormone receptor associated protein 5	THRAP5	1.7	2,4,8	1.7	8,12,24,48	transcription regulator activity
3659	interferon regulatory factor 1	IRF1	1.6	4,8,12	1.3	12	transcription regulator activity
10265	iroquois homeobox protein 5	IRX5	1.6	2,4	1.7	2,4,8,12,24	transcription regulator activity
58508	myeloid/lymphoid or mixed-lineage leukemia 3	MLL3	1.6	1,2,12,24,48	1.3	24	transcription regulator activity
7799	PR domain containing 2, with ZNF domain	PRDM2	1.5	2,4,12,24,48	1.4	8,12,24	transcription regulator activity
6256	retinoid X receptor, alpha	RXRA	1.4	2,4,8,12	1.8	4,8,12,24,48	transcription regulator activity
5463	POU domain, class 6, transcription factor 1	POU6F1	1.4	8,12,24,48	2.2	8,12,24,48	transcription regulator activity
56342	peter pan homolog (Drosophila)	PPAN*	2.1	2,4,8,12,48	2.2	2,4,8,12,24,48	RNA splicing
8140	solute carrier family 7 (cationic amino acid transporter, y+ system), member 5	SLC7A5*	9.1	1,2,4,8,12,24,48	1.4	24	transport

Table 5 (cont'd)

Entrez GeneId	Gene Name	Gene Symbol	HL1-1		HepG2		Functions
			FC	Time Points	FC	Time Points	
7529	tyrosine 3-monooxygenase/tryptophan 5-monooxygenase activation protein, beta polypeptide	YWHAB	3.0	1,2,4,8,12	2.7	1,2,4,8,12,24	transport
6513	solute carrier family 2 (facilitated glucose transporter), member 1	SLC2A1*	2.2	1,2,4,8,12,24, 48	1.3	8,24	transport
10723	solute carrier family 12 (potassium/chloride transporters), member 7	SLC12A7	1.5	2,4,8	2.0	8,12,24,48	transport
9962	solute carrier family 23 (nucleobase transporters), member 2	SLC23A2	1.5	2,3,12,48	2.1	4,8,12,24,48	transport
5579	protein kinase C, beta 1	PRKCB1*	2.1	1,2,4,8,12,24, 48	1.6	12,24	signal transduction
54978	chromosome 2 open reading frame 18	C2orf18	1.4	8,12,24	3.4	4,8,12,24,48	signal transduction
196883	adenylate cyclase 4	ADCY4	1.4	8,12,24	1.3	12	signal transduction
83604	transmembrane protein 47	TMEM47	1.4	8,12,24	2.1	8,12,24,48	transmembrane
118672	chromosome 10 open reading frame 89	C10orf89	1.4	8,12,24	1.8	8,12,24,48	regulation of translation
22934	ribose 5-phosphate isomerase A (ribose 5-phosphate epimerase)	RPIA	2.5	2,4,8,12,24,4 8	25.7	1,2,4,8,12,24, 48	carbohydrate metabolism
51102	mitochondrial trans-2-enoyl-CoA reductase	MECR	1.4	8,12,24	1.7	12,24	lipid metabolic process

Table 5 (cont'd)

Entrez GeneId	Gene Name	Gene Symbol	HL1-1		HepG2		Functions
			FC	Time Points	FC	Time Points	
10	N-acetyltransferase 2 (arylamine N-acetyltransferase)	NAT2	1.7	12,24,48	1.6	24,48	Caffeine metabolism
6303	spermidine/spermine N1-acetyltransferase	SAT	1.4	2,4,8,24	1.4	12,24	amino groups metabolism
5682	proteasome (prosome, macropain) subunit, alpha type, 1	PSMA1	1.6	2,4,8,12,24, 48	22.6	1,2,4,8,12,24, 48	protein metabolism
7298	thymidylate synthetase	TYMS	1.7	2,4,8,12,48	1.7	8,12,24	DNA metabolic process
706	benzodiazapine receptor (peripheral)	BZRP	2.3	2,4,8,12,24, 48	22.4	1,2,4,8,12,24, 48	cell proliferation
8453	cullin 2	CUL2	1.5	48	1.5	12	cell proliferation
1848	dual specificity phosphatase 6	DUSP6	1.4	12,24,48	1.9	1,2,4,8,12,24	regulation of cell cycle
92335	protein kinase LYK5	LYK5	1.4	24,48	2.8	8,12,24,48	cell cycle
2683	UDP-Gal:betaGlcNAc beta 1,4- galactosyltransferase, polypeptide 1	B4GALT1	1.4	12,24	1.9	8,12,24,48	regulation of apoptosis
928	CD9 molecule	CD9	1.5	48	1.6	24,48	developmental process
1080	cystic fibrosis transmembrane conductance regulator, ATP-binding cassette	CFTR	1.3	24,48	3.9	4,8,12,24,48	developmental process
2821	glucose phosphate isomerase	GPI	2.4	2,4,8,12,24, 48	1.7	24,48	immune system process

Table 5 (cont'd)

Entrez GeneId	Gene Name	Gene Symbol	HL1-1		HepG2		Functions
			FC	Time Points	FC	Time Points	
2152	coagulation factor III (thromboplastin, tissue factor)	F3	1.7	2,4,8,12,24	1.5	8,12,24	immune system process
3108	major histocompatibility complex, class II, DM alpha	HLA-DMA	1.5	1	1.5	1,4,8	immune system process
83699	SH3 domain binding glutamic acid-rich protein like 2	SH3BGRL2	1.4	8,12,24	2.1	8,12,24,48	SH3 domain binding
220004	chromosome 11 open reading frame 66	C11orf66	1.7	2,4,8,12,24	1.5	12	
Co-repressed (17)							
2181	acyl-CoA synthetase long-chain family member 3	ACSL3*	-2.2	2,4,8,12,24,48	-1.7	2,12,24,48	Lipid metabolism
1490	connective tissue growth factor	CTGF*	-2.3	2,4,8,12,24,48	-2.0	2,12,24,48	cell differentiation
22948	chaperonin containing TCP1, subunit 5 (epsilon)	CCT5*	-2.1	2,4,8,12,24,48	-2.3	2,4,12,24,48	protein folding
80273	GrpE-like 1, mitochondrial (E. coli)	GRPEL1	-1.3	24	-1.3	24,48	protein folding
2589	UDP-N-acetyl-alpha-D-galactosamine:polypeptide N-acetylgalactosaminyltransferase 1 (GalNAc-T1)	GALNT1*	-3.1	2,4,8,12,24,48	-1.6	4,8,12,24	protein modification process
23788	mitochondrial carrier homolog 2 (C. elegans)	MTCH2*	-1.5	4	-1.5	24,48	transport
7376	nuclear receptor subfamily 1, group H, member 2	NR1H2	-2.4	2,4,8,12	-1.7	24,48	transcription regulator activity

Table 5 (cont'd)

Entrez GeneId	Gene Name	Gene Symbol	HL1-1		HepG2		Functions
			FC	Time Points	FC	Time Points	
8896	BUD31 homolog (yeast)	BUD31	-1.8	24,48	-1.7	12,24,48	transcription regulator activity
8507	ectodermal-neural cortex (with BTB-like domain)	ENC1*	-1.6	4,8,12,24,48	-1.4	48	developmental process
317	apoptotic peptidase activating factor	APAF1*	-1.5	12,24,48	-1.7	24,48	regulation of apoptosis
1902	endothelial differentiation, lysophosphatidic acid G-protein-coupled receptor, 2	EDG2	-1.6	8,12,24,48	-1.7	24,48	signal transduction
4074	mannose-6-phosphate receptor (cation dependent)	M6PR	-1.6	24,48	-1.7	12,24	signal transduction
3925	stathmin 1/oncoprotein 18	STMN1	-1.4	24,48	-1.5	24	signal transduction
231	aldo-keto reductase family 1, member B1 (aldose reductase)	AKR1B1	-2.3	24,48	-1.4	24	carbohydrate metabolism
4913	nth endonuclease III-like 1 (E. coli)	NTHL1	-2.3	24,48	-1.4	24	DNA repair
5420	podocalyxin-like	PODXL	-1.4	48	-1.4	24	immune system process
9768	KIAA0101	KIAA0101	-1.5	12,24,48	-1.7	24,48	intracellular
HL1_Up/HepG2_Down (7)							
23204	ADP-ribosylation factor-like 6 interacting protein	ARL6IP	1.9	12,24,48	-1.3	48	endomembrane system
54606	DEAD (Asp-Glu-Ala-Asp) box polypeptide 56	DDX56	1.7	4,8,12,24,48	-1.4	4	rRNA processing

Table 5 (cont'd)

Entrez GeneId	Gene Name	Gene Symbol	HL1-1		HepG2		Functions
			FC	Time Points	FC	Time Points	
5786	protein tyrosine phosphatase, receptor type, A	PTPRA	1.6	2,4,8,12,24,48	-1.5	24,48	signal transduction
4851	Notch homolog 1, translocation-associated (Drosophila)	NOTCH1	1.6	8,12,24	-1.5	24,48	transcription regulator activity
5578	protein kinase C, alpha	PRKCA	1.4	24,48	-1.5	12,24,48	regulation of apoptosis
11332	acyl-CoA thioesterase 7	ACOT7	1.3	48	-1.4	24	lipid metabolic process
57608	KIAA1462	KIAA1462	1.6	8,12,24,48	-1.3	48	
HL1_Down/HepG2_Up (12)							
199	allograft inflammatory factor 1	AIF1	-3.2	2,4,24,48	1.8	4,8,12,24,48	regulation of cell cycle
652	bone morphogenetic protein 4	BMP4	-1.9	1,2,4,8,24	1.9	8,12,24,48	regulation of cell cycle
10293	TRAF interacting protein	TRAIP	-1.8	2,4,8	1.6	8,12,24,48	regulation of apoptosis
834	caspase 1, apoptosis-related cysteine peptidase (interleukin 1, beta, convertase)	CASP1	-1.3	2,48	1.4	24	regulation of apoptosis
3399	inhibitor of DNA binding 3, dominant negative helix-loop-helix protein	ID3	-2.5	2,4,24,48	1.9	4,8,12,24,48	regulation of transcription
7077	TIMP metallopeptidase inhibitor 2	TIMP2	-1.3	48	1.6	24,48	cell proliferation

Table 5 (cont'd)

Entrez GeneId	Gene Name	Gene Symbol	HL1-1		HepG2		Functions
			FC	Time Points	FC	Time Points	
85440	dedicator of cytokinesis 7	DOCK7	-1.5	48	1.4	24	cell differentiation
9200	protein tyrosine phosphatase-like (proline instead of catalytic arginine), member A	PTPLA	-1.4	8,24	1.3	12	developmental process
22937	sterol regulatory element binding proteins (SREBF) chaperone	SCAP	-1.8	4,24,48	2.6	4,8,12,24,48	lipid metabolic process
214	activated leukocyte cell adhesion molecule	ALCAM	-1.6	24,48	1.5	12,24,48	immune response
2745	glutaredoxin (thioltransferase)	GLRX	-1.5	48	2.0	12,24,48	transport
2806	glutamic-oxaloacetic transaminase 2, mitochondrial (aspartate aminotransferase 2)	GOT2	-1.3	48	1.5	12,24	amino acid metabolism

* Putative primary responses based on the CHX co-treatment study

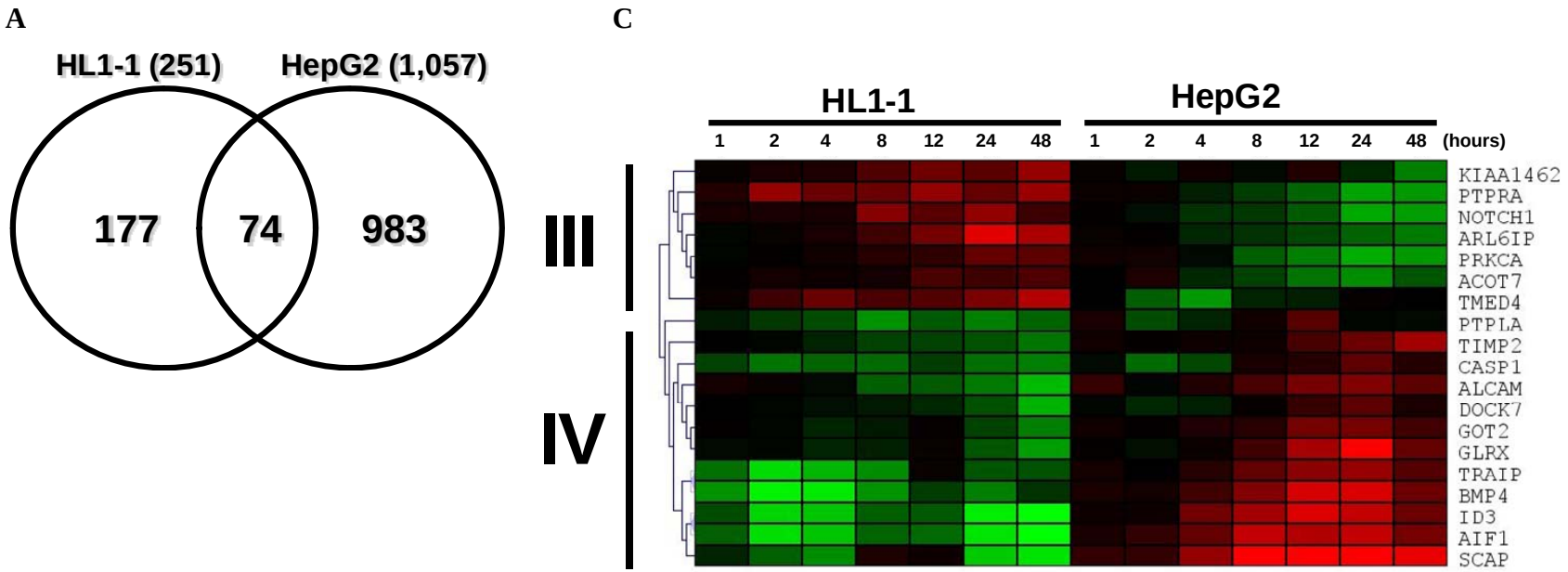

Figure 19. Cluster analysis of HL1-1 and HepG2 differentially expressed genes.
(A) 74 differentially expressed genes were identified in both HL1-1 and HepG2 cells following TCDD treatment. (B) Cluster analysis of the 55 genes that exhibited the same regulation in both HL1-1 and HepG2 cells. I: Gene set induced in both cell lines. II: Gene set repressed in both cell lines. The asterisk (*) indicates putative primary responses based on the CHX study. (C) Cluster analysis was performed on the 19 divergently regulated genes. III: Gene set induced in HL1-1, but repressed in HepG2. IV: Gene set repressed in HL1-1, but induced in HepG2. (D) Examples of specific HL1-1 and HepG2 gene expression responses grouped by functional annotation.

Figure 19 (cont'd)
C

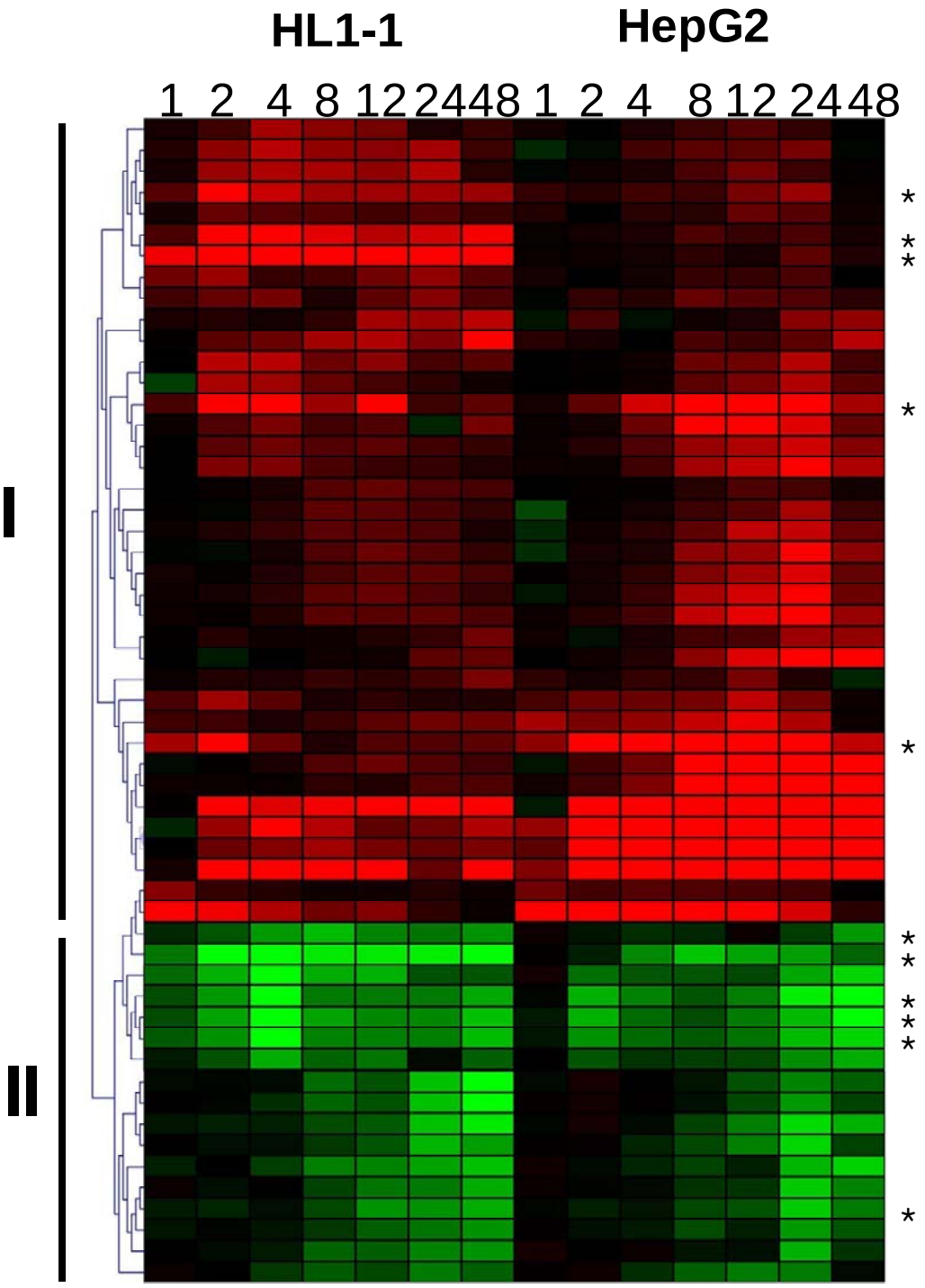

Figure 19 (cont'd)
D

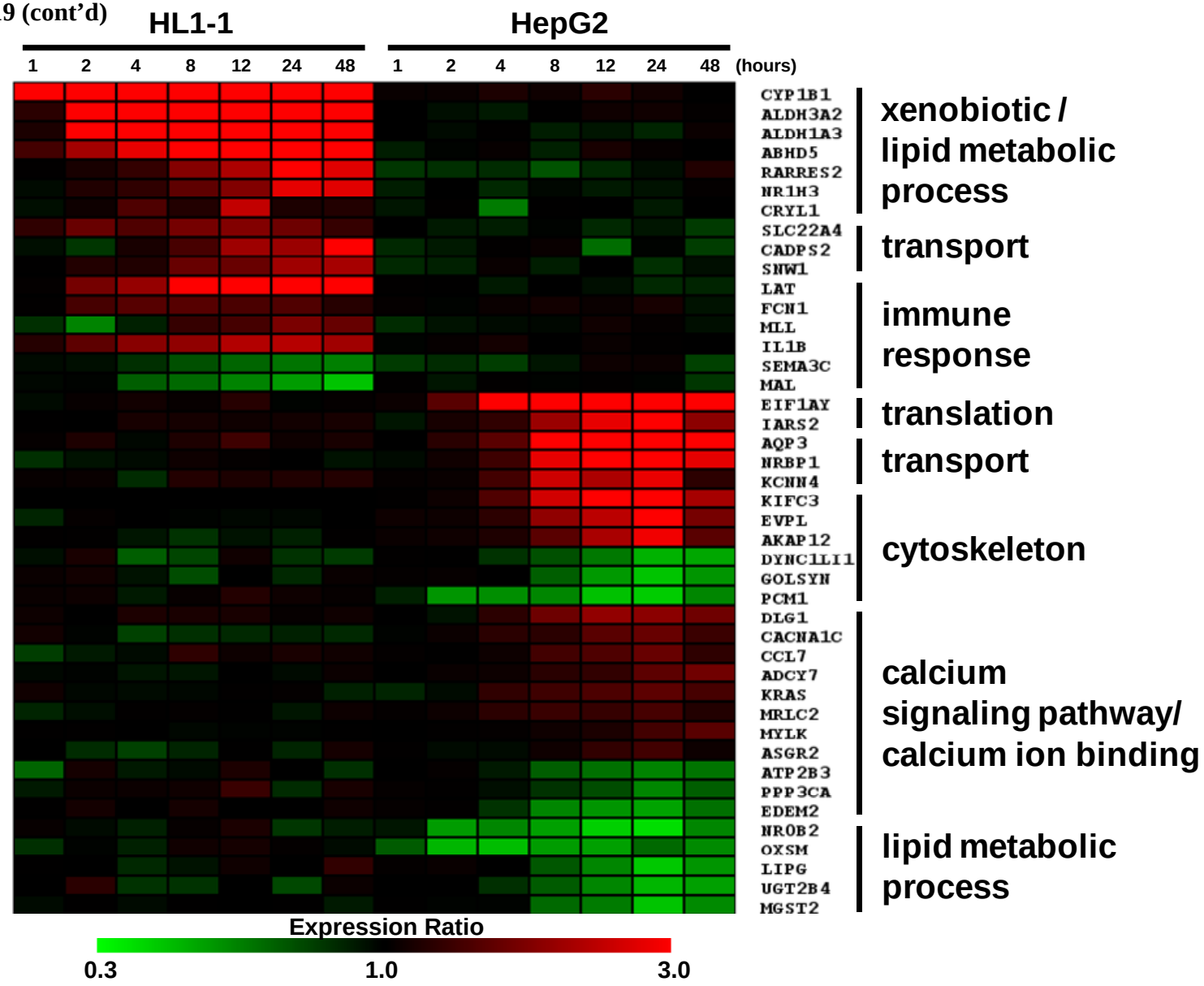

hepatic mouse tissue identified transcriptional regulation, signal transduction, metabolism, apoptosis and transport as being commonly regulated by TCDD (Table 7). *In vitro* and *in vivo* comparisons have previously reported that some genes were divergently regulated [34]. For example, the transcription regulation-related genes CEBPZ and ID3, and the signal transduction-related genes DUSP6, ERBB3 and MTMR7 were divergently regulated in HL1-1 cell compared to hepatic mouse tissue.

DISCUSSION

In this study, AhR-mediated gene expression in HL1-1 human liver stem cells was compared to other *in vitro* and *in vivo* TCDD data sets. The normalcy and self-renewal properties of HL1-1 cells provide a unique, *in vitro* system that may more accurately reflect *in vivo* human responses to TCDD. As with other models, HL1-1 cells express a functional AhR, as evident by western analysis and the induction of several AhR gene battery members, including CYP1A1 and aldehyde dehydrogenases. Although comparable functional pathways are affected in each model, further examination indicates that different genes within common functions were differentially regulated. Furthermore, there were several examples of orthologs exhibiting divergent regulation (e.g., induced in one model but repressed in another). Interestingly, functional categorization of TCDD elicited differential gene expression is consistent with reported species-specific responses [30, 36] suggesting that HL1-1 cells may more accurately reflect *in vivo* human responses to TCDD.

Human HepG2 cells are a popular model for investigating hepatotoxicity. Comparison of HepG2 and HL1-1 gene expression profiles revealed the co-regulation of several putative primary responses including CYP1A1, PRKCB, PPAN, SERTAD2, SLC2A1 and SLC7A5. In contrast, several divergently regulated genes not classified as primary responses were expressed

Figure 20. Comparative analysis of HL1-1, HepG2, Hepa1c1c7 and C57BL/6 hepatic tissue gene expression profiles.
(A) The number of genes represented on the human and mouse cDNA arrays. In total 5,505 orthologs were represented on both platforms. (B) Comparative analysis of the TCDD elicited temporal gene expression of HL1-1, HepG2, Hepa1c1c7 and C57BL/6 mice hepatic tissue (Mm liver) studies. Collectively, 251, 1057, 770 and 1465 differentially expressed genes were identified from HL1-1, HepG2, Hepa1c1c7 and mouse liver TCDD time course study, respectively, using relaxed filtering criteria ($P1(t) > 0.999$ and $|\text{fold change}| > 1.3$) to include responses on the margins. 74, 18 and 32 differentially expressed genes were identified when comparing HL1-1 cells to HepG2 cells, Hepa1c1c7 cells, and C57BL/5 hepatic tissue, respectively. Further analysis identified 13 conserved genes between HL1-1, HepG2 and mouse liver, 3 conserved genes between HL1-1, HepG2 and Hepa1c1c7, and 8 conserved genes between HL1-1, Hepa1c1c7 and mouse liver.

Figure 20 (Cont'd)

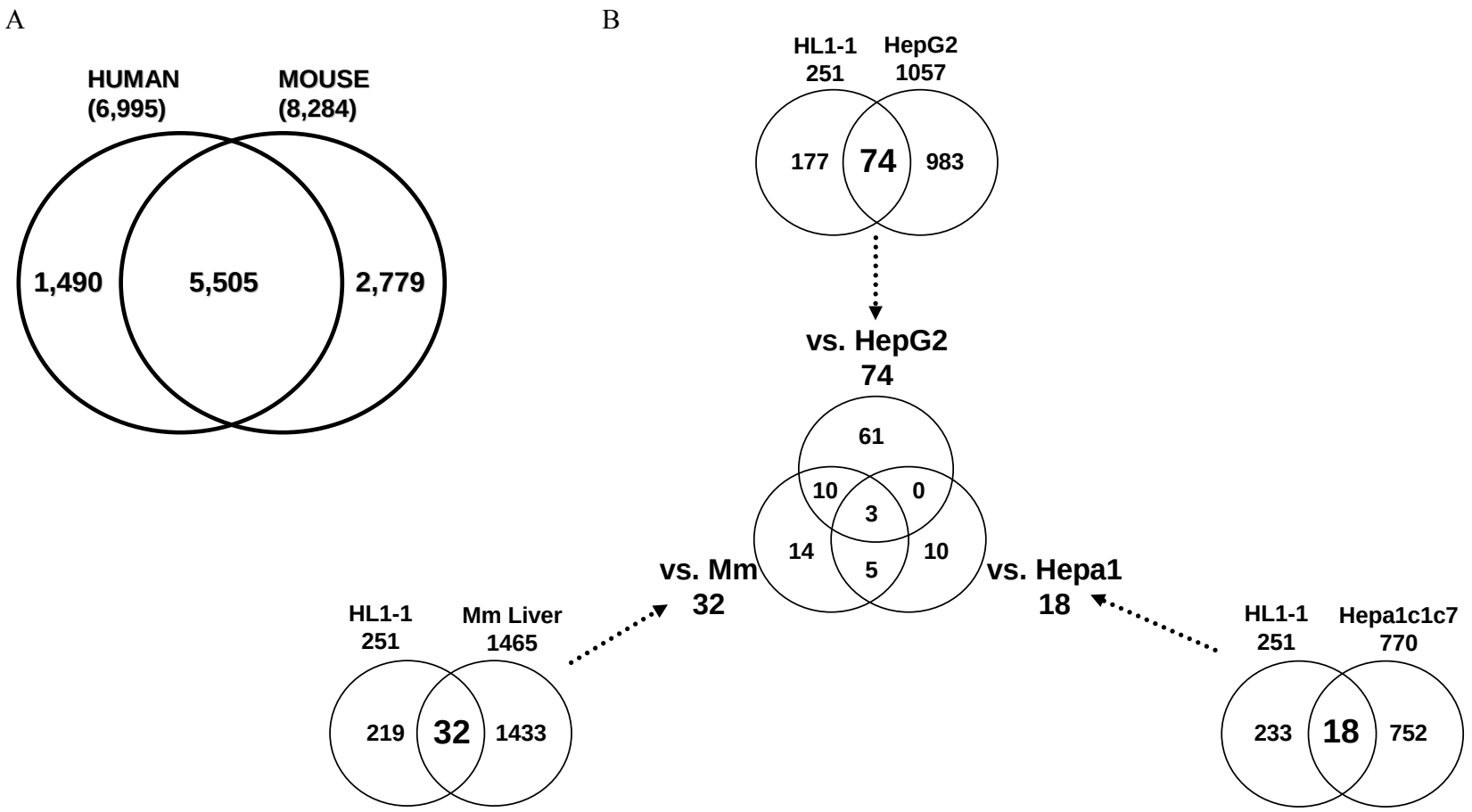

Table 6. HL1-1 vs. Hepa1c1c7 Overlapping Genes: Functional Categories

Homolo -gene ID	Entrez GeneId	Gene name	Gene Symbol	Functions
Co-induced (6)				
1658	3659	interferon regulatory factor 1	IRF1	regulation of transcription
50009	84658	integrin, beta 1	ITGB1	cell adhesion / migration
49860	113130	cell division cycle associated 5	CDCA5	cell cycle progression
20548	4322	matrix metallopeptidase 13 (collagenase 3)	MMP13	collagen catabolism
36176	4826	neuronatin	NNAT	development
9070	23299	bicaudal D homolog 2 (Drosophila)	BICD2	cytoskeleton
Co-repressed (4)				
2902	8888	MCM3 minichromosome maintenance deficient 3 (S. cerevisiae) associated protein	MCM3AP	cell cycle arrest
58	1028	cyclin-dependent kinase inhibitor 1C (p57, Kip2)	CDKN1C	cell cycle arrest
1633	3399	inhibitor of DNA binding 3, dominant negative helix-loop-helix protein	ID3	negative regulation of transcription
7776	8692	hyaluronoglucosaminidase 2	HYAL2	carbohydrate metabolism
HL1-1 up/ Hepa1c1c7 down (6)				
21312	10723	solute carrier family 12 (potassium/chloride transporters), member 7	SLC12A7	ion transport
2225	6279	S100 calcium binding protein A8 (calgranulin A)	S100A8	inflammatory response
48120	5329	plasminogen activator, urokinase receptor	PLAUR	signal transduction
41451	994	cell division cycle 25B	CDC25B	regulation of cell cycle
9866	54940	OCIA domain containing 1	OCIAD1	cell adhesion
2492	7288	tubby like protein 2	TULP2	visual perception
HL1-1 down/ Hepa1c1c7 up (2)				
36201	10512	sema domain, immunoglobulin domain (Ig), short basic domain, secreted, (semaphorin) 3C	SEMA3C	immune response
26151	23304	ubiquitin protein ligase E3 component n-recognin 2	UBR2	ubiquitin cycle

Table 7. HL1-1 vs. Mouse Hepatic Tissue Overlapping Genes: Functional Categories

Homolo -gene ID	Entrez GeneId	Gene name	Gene Symbol	Functions
Co-up (14)				
68035	1545	cytochrome P450, family 1, subfamily B, polypeptide 1	CYP1B1	xenobiotic metabolizing enzyme
1658	3659	interferon regulatory factor 1	IRF1	regulation of transcription
3832	2002	ELK1, member of ETS oncogene family	ELK1	regulation of transcription
32049	4851	Notch homolog 1, translocation-associated (Drosophila)	NOTCH1	regulation of transcription
55621	1848	dual specificity phosphatase 6	DUSP6	signal transduction
20457	2065	v-erb-b2 erythroblastic leukemia viral oncogene homolog 3 (avian)	ERBB3	signal transduction
99732	9108	myotubularin related protein 7	MTMR7	signal transduction
15780	11332	acyl-CoA thioesterase 7	ACOT7	lipid metabolism
49860	113130	cell division cycle associated 5	CDCA5	cell cycle
50009	84658	integrin, beta 1	ITGB1	cell adhesion / migration
68520	6513	solute carrier family 2 (facilitated glucose transporter), member 1	SLC2A1	carbohydrate transport
41088	51099	abhydrolase domain containing 5	ABHD5	aromatic compound metabolism
2080	5682	proteasome (prosome, macropain) subunit, alpha type, 1	PSMA1	ubiquitin-dependent protein degradation
10683	57099	apoptosis, caspase activation inhibitor	AVEN	apoptosis
Co-down (5)				
1577	2896	granulin	GRN	cell-cell signaling
3278	2181	acyl-CoA synthetase long-chain family member 3	ACSL3	lipid metabolism
26151	23304	ubiquitin protein ligase E3 component n-recognin 2	UBR2	ubiquitin cycle
10859	57704	glucosidase, beta (bile acid) 2	GBA2	bile acid metabolism
10966	83698	calneuron 1	CALN1	calcium ion binding

Table 7 (cont'd)

Homolo -gene ID	Entrez GeneId	Gene name	Gene Symbol	Functions
HL1-1 up/ Mouse liver down (9)				
3045	2791	guanine nucleotide binding protein (G protein), gamma 11	GNG11	signal transduction
20621	5786	protein tyrosine phosphatase, receptor type, A	PTPRA	signal transduction
199	3990	lipase, hepatic	LIPC	lipid catabolism
13090	84759	polycomb group ring finger 1	PCGF1	regulation of transcription
20420	928	CD9 molecule	CD9	cell adhesion
21312	10723	solute carrier family 12 (potassium/chloride transporters), member 7	SLC12A7	ion transport
48120	5329	plasminogen activator, urokinase receptor	PLAUR	chemotaxis
11174	53838	chromosome 11 open reading frame 24	C11orf24	oxidoreductase
12876	83699	SH3 domain binding glutamic acid-rich protein like 2	SH3BGRL2	unknown
HL1-1 down/ Mouse liver up (4)				
1229	214	activated leukocyte cell adhesion molecule	ALCAM	antimicrobial humoral response
4210	10153	CCAAT/enhancer binding protein zeta	CEBPZ	regulation of transcription
1633	3399	inhibitor of DNA binding 3, dominant negative helix-loop-helix protein	ID3	transcription corepressor activity
2902	8888	MCM3 minichromosome maintenance deficient 3 associated protein	MCM3AP	DNA replication

at later time points suggesting that they may be secondary effects of TCDD. In addition, a number of cell specific responses were observed. For example, HL1-1 specific responses included xenobiotic and lipid metabolism and immune responses that correlated with *in vivo* mice effects [35], while HepG2 exhibited cytoskeleton and calcium signaling responses related to cell-adhesion, tumor cell motility and tumor promotion [37-39]. This may be due to differences in basal expression levels or other unique cell characteristics [40]. For example, primary rat hepatocytes cultured on standard collagen had basal gene expression levels more comparable to whole liver rather than rat hepatoma cells [41].

Comparisons of HL1-1 cells to other *in vitro* (i.e., Hepa1c1c7 cells) and *in vivo* (i.e., hepatic tissue from C57BL/6 mice) models identified several common TCDD responses, as well model specific differential gene expression. Although the structure, function, and mechanism of action of the AhR is highly conserved [42], comparative toxicogenomic and computational DRE search studies suggest that TCDD elicited gene expression profiles may be species-specific. Computational analysis of the regulatory regions of orthologs using a position weight matrix suggests that DREs are not conserved between humans, mice and rats [27]. Moreover, *in vivo* rat vs. mouse [30], and *in vitro* (HepG2 vs. Hepa1c1c7 vs. H4IIE) (Dere *et al.*, manuscript in preparation) studies indicate that the hepatic gene expression profiles are species specific, despite the conserved induction of xenobiotic metabolizing genes. Moreover, identified putative primary responses differ between species (Dere *et al.*, manuscript in preparation). Nevertheless, TCDD does affect common pathways across species and models, but appears to do so by regulating the expression of non-orthologous genes within those pathways.

Collectively, these studies not only demonstrate the utility of HL1-1 cells but also the limitations of extrapolating from *in vitro* models to *in vivo* effects. Although *in vitro* models

have the advantage of reducing the complexity of a tissue response to allow a more focused analysis of the effects of TCDD on a specific cell type, it does not replicate other interactions that may be important in eliciting the toxic responses observed *in vivo* [34]. However, in addition to being a normal human cell which may more accurately reflect human responses relative to rodent models, HL1-1 cells are also stem-like which may be novel targets of toxicity [12].

REFERENCES

REFERENCES

1. Denison, M.S. and S. Heath-Pagliuso, *The Ah receptor: a regulator of the biochemical and toxicological actions of structurally diverse chemicals.* Bull Environ Contam Toxicol, 1998. **61**(5): p. 557-68.

2. Knerr, S. and D. Schrenk, *Carcinogenicity of 2,3,7,8-tetrachlorodibenzo-p-dioxin in experimental models.* Mol Nutr Food Res, 2006. **50**(10): p. 897-907.

3. IARC, *IARC Working Group on the Evaluation of Carcinogenic Risks to Humans: Polychlorinated Dibenzo-Para-Dioxins and Polychlorinated Dibenzofurans. Lyon, France, 4-11 February 1997.* IARC Monogr Eval Carcinog Risks Hum, 1997. **69**: p. 1-631.

4. Okey, A.B., *An aryl hydrocarbon receptor odyssey to the shores of toxicology: the Deichmann Lecture, International Congress of Toxicology-XI.* Toxicol Sci, 2007. **98**(1): p. 5-38.

5. Olson, H., et al., *Concordance of the toxicity of pharmaceuticals in humans and in animals.* Regul Toxicol Pharmacol, 2000. **32**(1): p. 56-67.

6. Abbott, A., *Cell culture: biology's new dimension.* Nature, 2003. **424**(6951): p. 870-2.

7. MacGregor, J.T., et al., *In vitro human tissue models in risk assessment: report of a consensus-building workshop.* Toxicol Sci, 2001. **59**(1): p. 17-36.

8. Pritchard, J.F., et al., *Making better drugs: Decision gates in non-clinical drug development.* Nat Rev Drug Discov, 2003. **2**(7): p. 542-53.

9. MacGregor, J.T., *SNPs and chips: genomic data in safety evaluation and risk assessment.* Toxicol Sci, 2003. **73**(2): p. 207-8.

10. Li, A.P., *Screening for human ADME/Tox drug properties in drug discovery.* Drug Discov Today, 2001. **6**(7): p. 357-366.

11. Rohwedel, J., et al., *Embryonic stem cells as an in vitro model for mutagenicity, cytotoxicity and embryotoxicity studies: present state and future prospects.* Toxicol In Vitro, 2001. **15**(6): p. 741-53.

12. Davila, J.C., et al., *Use and application of stem cells in toxicology.* Toxicol Sci, 2004. **79**(2): p. 214-23.

13. Rolletschek, A., P. Blyszczuk, and A.M. Wobus, *Embryonic stem cell-derived cardiac, neuronal and pancreatic cells as model systems to study toxicological effects.* Toxicol Lett, 2004. **149**(1-3): p. 361-9.

14. Carere, A., A. Stammati, and F. Zucco, *In vitro toxicology methods: impact on regulation from technical and scientific advancements.* Toxicol Lett, 2002. **127**(1-3): p. 153-60.

15. Ahuja, Y.R., V. Vijayalakshmi, and K. Polasa, *Stem cell test: a practical tool in toxicogenomics.* Toxicology, 2007. **231**(1): p. 1-10.

16. Ek, M., et al., *Expression of drug metabolizing enzymes in hepatocyte-like cells derived from human embryonic stem cells.* Biochem Pharmacol, 2007. **74**(3): p. 496-503.

17. Chang, C.C., Tsai,J.L., Kuo,K.K., Wang,K.H., Chiang,C.H., Kao,A.P., Tai,M.H. and Trosko,J.E., *Expression of Oct-4, alpha fetoprotein and vimentin and lack of gap-junctional intercellular communication (GJIC) as common phenotypes for human adult liver stem cells and hepatoma cells.* Proc. Am. Assoc. Cancer Res., 2004. **45**: p. 642.

18. Tai, M.H., et al., *Oct4 expression in adult human stem cells: evidence in support of the stem cell theory of carcinogenesis.* Carcinogenesis, 2005. **26**(2): p. 495-502.

19. Yang, Y.H. and T. Speed, *Design issues for cDNA microarray experiments.* Nat Rev Genet, 2002. **3**(8): p. 579-88.

20. Eckel, J.E., et al., *Normalization of two-channel microarray experiments: a semiparametric approach.* Bioinformatics, 2005. **21**(7): p. 1078-83.

21. Eckel, J.E., et al., *Empirical bayes gene screening tool for time-course or dose-response microarray data.* J Biopharm Stat, 2004. **14**(3): p. 647-70.

22. Burgoon, L.D., et al., *dbZach: A MIAME-compliant toxicogenomic supportive relational database.* Toxicol Sci, 2006. **90**(2): p. 558-68.

23. Burgoon, L.D. and T.R. Zacharewski, *dbZach toxicogenomic information management system.* Pharmacogenomics, 2007. **8**(3): p. 287-91.

24. Saeed, A.I., et al., *TM4: a free, open-source system for microarray data management and analysis.* Biotechniques, 2003. **34**(2): p. 374-8.

25. Dennis, G., Jr., et al., *DAVID: Database for Annotation, Visualization, and Integrated Discovery.* Genome Biol, 2003. **4**(5): p. P3.

26. Rozen, S. and H. Skaletsky, *Primer3 on the WWW for general users and for biologist programmers.* Methods Mol Biol, 2000. **132**: p. 365-86.

27. Sun, Y.V., et al., *Comparative analysis of dioxin response elements in human, mouse and rat genomic sequences.* Nucleic Acids Res, 2004. **32**(15): p. 4512-23.

28. N'Jai, A., et al., *Comparative temporal toxicogenomic analysis of TCDD- and TCDF-mediated hepatic effects in immature female C57BL/6 mice.* Toxicol Sci, 2008. **103**(2): p. 285-97.

29. Kopec, A.K., et al., *Comparative toxicogenomic examination of the hepatic effects of PCB126 and TCDD in immature, ovariectomized C57BL/6 mice.* Toxicol Sci, 2008. **102**(1): p. 61-75.

30. Boverhof, D.R., et al., *Comparative toxicogenomic analysis of the hepatotoxic effects of TCDD in Sprague Dawley rats and C57BL/6 mice.* Toxicol Sci, 2006. **94**(2): p. 398-416.

31. Zeiger, M., et al., *Inducing effects of dioxin-like polychlorinated biphenyls on CYP1A in the human hepatoblastoma cell line HepG2, the rat hepatoma cell line H4IIE, and rat primary hepatocytes: comparison of relative potencies.* Toxicol Sci, 2001. **63**(1): p. 65-73.

32. Silkworth, J.B., et al., *Comparison of TCDD and PCB CYP1A induction sensitivities in fresh hepatocytes from human donors, sprague-dawley rats, and rhesus monkeys and HepG2 cells.* Toxicol Sci, 2005. **87**(2): p. 508-19.

33. Reymann, S. and J. Borlak, *Transcriptome profiling of human hepatocytes treated with Aroclor 1254 reveals transcription factor regulatory networks and clusters of regulated genes.* BMC Genomics, 2006. **7**: p. 217.

34. Dere, E., et al., *In vivo-in vitro toxicogenomic comparison of TCDD-elicited gene expression in Hepa1c1c7 mouse hepatoma cells and C57BL/6 hepatic tissue.* BMC Genomics, 2006. **7**: p. 80.

35. Boverhof, D.R., et al., *Temporal and dose-dependent hepatic gene expression patterns in mice provide new insights into TCDD-Mediated hepatotoxicity.* Toxicol Sci, 2005. **85**(2): p. 1048-63.

36. Boutros, P.C., et al., *Dioxin-responsive AHRE-II gene battery: identification by phylogenetic footprinting.* Biochem Biophys Res Commun, 2004. **321**(3): p. 707-15.

37. Puga, A., A. Maier, and M. Medvedovic, *The transcriptional signature of dioxin in human hepatoma HepG2 cells.* Biochem Pharmacol, 2000. **60**(8): p. 1129-42.

38. Monteiro, P., et al., *Dioxin-mediated up-regulation of aryl hydrocarbon receptor target genes is dependent on the calcium/calmodulin/CaMKIalpha pathway.* Mol Pharmacol, 2008. **73**(3): p. 769-77.

39. Tannheimer, S.L., et al., *Carcinogenic polycyclic aromatic hydrocarbons increase intracellular Ca2+ and cell proliferation in primary human mammary epithelial cells.* Carcinogenesis, 1997. **18**(6): p. 1177-82.

40. Harris, A.J., S.L. Dial, and D.A. Casciano, *Comparison of basal gene expression profiles and effects of hepatocarcinogens on gene expression in cultured primary human hepatocytes and HepG2 cells.* Mutat Res, 2004. **549**(1-2): p. 79-99.

41. Boess, F., et al., *Gene expression in two hepatic cell lines, cultured primary hepatocytes, and liver slices compared to the in vivo liver gene expression in rats: possible*

implications for toxicogenomics use of in vitro systems. Toxicol Sci, 2003. **73**(2): p. 386-402.

42. McGregor, D.B., et al., *An IARC evaluation of polychlorinated dibenzo-p-dioxins and polychlorinated dibenzofurans as risk factors in human carcinogenesis.* Environ Health Perspect, 1998. **106 Suppl 2**: p. 755-60.

CHAPTER 5

Kim S, Kiyosawa N, Burgoon LD, Chang CC, and Zacharewski TR: **PPARα-mediated responses in human adult liver stem cells: comparative in vivo/in vitro cross-species studies**. *Toxicol Sci* (Submitted August 19, 2011)

CHAPTER 5

PPARα-MEDIATED RESPONSES IN HUMAN ADULT LIVER STEM CELLS: *IN VIVO*/*IN VITRO* AND CROSS-SPECIES COMPARISONS

ABSTRACT

The peroxisome proliferator-activated receptor α (PPARα) is a ligand activated transcription factor that regulates a variety of biological processes including lipid metabolism and energy homeostasis. Peroxisome proliferators (PPs) are non-genotoxic carcinogens in rodents, but humans are resistant to peroxisome proliferation and carcinogenesis. In this study, we examined differential gene expression elicited by clofibrate (CLO) and Wy-14,643 (WY) in C57BL/6 mouse liver compared to responses in human HepG2 hepatoma and HL1-1 adult stem cells. Mice were gavaged with sesame oil, 300 mg/kg CLO or WY for 2, 4, 8, 12, 18 or 24 h, or every 24 h and sacrificed after 1, 4 or 14 days. Although no significant changes in body weight gain were observed, WY induced relative liver weight at 4 and 14 days. Genome-wide hepatic gene expression analysis identified 719 and 1,443 unique genes that were differentially expressed by CLO and WY, respectively (|fold change|>1.5, P1(t)>0.99). Functional analysis associated the differentially expressed genes with lipid metabolism, transport, cell cycle and immune response. Using relaxed statistical criteria, ~90% of CLO and ~75% of the WY differentially expressed genes were in common between both treatments. Hierarchical clustering revealed only early time points (2-8h) clustered together. Complementary QRTPCR studies in human HL1-1 and HepG2 cells treated with 50 μM WY or DMSO for 1, 2, 4, 8, 12, 24 or 48 h identified a minimal number of conserved orthologous responses (e.g., Pdk4, Adfp and Angptl4)

while some genes (i.e., Bmf, a tumor suppressor) exhibited induction in human cells but repression in mice. These data suggest that PPs elicit species-specific PPAR-mediated gene expression.

INTRODUCTION

Peroxisome proliferators (PPs) are a diverse class of compounds that include industrial chemicals, drugs and endogenous steroids and lipids [1, 2]. While synthetic PPs, such as fibrates, are commonly used to treat dyslipidemia, other including pesticides, plasticizers and solvents are inadvertently introduced into the environment. They elicit a broad spectrum of biochemical and physiological responses such as liver hyperplasia and hypertrophy, peroxisome proliferation and increases in mitochondrial, peroxisomal, and microsomal fatty acid oxidation [3] mediated by peroxisome proliferator-activated receptors (PPAR), a family of ligand-activated transcription factors (TFs) [4]. PPARs exert their effects following ligand binding and dimerization with the retinoid X receptor (RXR). The heterodimer complex interacts with peroxisome proliferator response elements (PPRE) in the regulatory regions of target genes to modulate gene expression. Given their role in lipid metabolism and regulation by exogenous ligands, PPARs are active drug development targets for the treatment of hyperlipidemia, diabetes and obesity [5, 6].

PPARα and -γ are the most widely studied of the three isoforms (PPARα, -β/δ and -γ). PPARα and β/δ regulate catabolic energy metabolism, while PPARγ regulates anabolic lipid metabolism [2]. Studies with PPARα agonists, such as fibrates, suggest PPARα activation induces fatty acid oxidation in hepatic peroxisomes [7]. Fibrates were introduced as treatments for metabolic disorders in the early 1960s with the release of clofibrate with the subsequent development of other fibrates, including fenofibrate, gemfibrozil, bezafibrate and ciprofibrate [6, 8]. However, results from rodent carcinogenesis studies suggested fibrates and other

hypolipidemic drugs (i.e. Wy-14,643 and tibric acid) induce hepatic carcinogenesis curtailing their clinical use [9]. Gene knockout studies confirmed that PP-induced pleiotropic responses, including peroxisome proliferation and the development of non-genotoxic hepatocarcinomas, are PPARα-mediated [10, 11].

The human risk of PP-induced hepatocarcinomas is uncertain. Clinical studies suggest humans are resistant to PP-induced peroxisome proliferation and hepatic carcinogenesis [12-14]. PP-treated of PPARα humanized mice exhibit diminished peroxisome prolifereration and hepatocarcinoma incidence, suggesting that structural differences between human and mouse PPARα may lead to differential susceptibility [15, 16]. There are also significant differences between species in the levels of expression, structure and function of PPARα, as well as co-regulator proteins and PPRE distribution [17-20]. In order to further elucidate the molecular basis for PPARα-mediated species-specific responses, comparative cross-species studies are required.

There are many models, such as humanized mice [21] to human hepatoma cell line and primary hepatocyte [22] were implemented to study cross-species comparison to human. Human adult stem cells isolated from liver tissue are an attractive *in vitro* alternative with many advantages including the fact that they are a non-transformed intact cell from human tissue with proliferating and differentiation ability. They will provide an unlimited source of intact human cells and may be more predictive of human responses. It could also be a potential target for certain toxic end points, such as tumor development [23-25].

In this study, we examined CLO- and WY-elicited gene expression in C57BL/6 mouse liver and compared with WY-elicited gene expression in adult HL1-1 human stem cells and HepG2 human hepatoma cells to further investigate species-specific responses to PPs.

MATERIALS & METHODS

HUSBANDRY

Female C57BL/6 mice, ovariectomized by the supplier on postnatal day (PND) 20, were obtained from Charles River Laboratories (Raleigh, NC) on PND 25. The immature ovariectomized mouse was used to negate potential interactions with estrogens produced by the developing ovaries [26], and to facilitate comparisons with other data sets obtained using the same model, study design and analysis methods [27-30]. Mice were housed in polycarbonate cages containing cellulose fiber chip bedding (Aspen Chip Laboratory Bedding, Northeastern Products, Warrensberg, NY) maintained at 40-60% humidity and 23°C with a 12 h dark/light cycle (7 am - 7 pm). Animals were allowed free access to de-ionized water and Harlan Teklad 22/5 Rodent Diet 8640 (Madison, WI). Mice were acclimatized for 4 days prior to dosing.

TREATMENTS AND NECROPSY

Mice (n = 5) were orally gavaged once for the acute study or daily for sub-chronic studies with 300 mg/kg body weight CLO (Sigma-Aldrich, St Louis, MO) or WY (Sigma-Aldrich) in 0.1 ml of sesame oil (Sigma-Aldrich) vehicle. Time-matched vehicle controls (n = 5) were similarly gavaged with sesame seed oil vehicle. In acute studies, mice were sacrificed 2, 4, 8, 12, 18, and 24 h post-dose by cervical dislocation (Figure 21A) while sub-chronic animals were sacrificed 24 h after the last dose (1, 4 and 14 days) (Figure 21B). Body and liver weights were recorded and sections of the left lateral liver lobe (approximately 0.1 g) were snap-frozen in liquid nitrogen and stored at -80°C. The right lateral lobe was fixed in 10% neutral buffered formalin (NBF, VWR International, West Chester, PA) for histological analysis. All procedures were performed with the approval of the Michigan State University All-University Committee on Animal Use and Care.

CULTURE AND TREATMENT OF CELL LINES

HL1-1 cells [31] were maintained in a modified MCDB 153 media (Keratinocyte-SFM, Invitrogen Corporation, Carlsbad, CA) supplemented with N-acetyl-L-cysteine (2 mM), L-ascorbic acid 2-phosphate (0.2 mM) (referred to as K-NAC medium) and 50 μg/mL gentamycin (Invitrogen). Added growth factors/hormones included rEGF (5 ng/mL), bovine pituitary extract (50 mg/mL) and 10% fetal bovine serum (FBS) (Hyclone, Logan, UT). HepG2 cells were maintained in phenol-red free DMEM/F12 media (Invitrogen) supplemented with 5% FBS (Hyclone), 50 μg/mL gentamycin (Invitrogen), 100 U/mL penicillin and 100 μg/mL streptomycin (Invitrogen). 1×10^6 cells were seeded into a 25 cm^2 cell culture flask (#430639, vent cap) (Corning Inc., Corning, NY) and incubated under standard conditions (5% CO_2, 37°C). For the time course studies, cells were treated with 50 uM WY (Sigma-Aldrich) or 0.1% (v/v) DMSO (Sigma-Aldrich) vehicle and harvested at 1, 2, 4, 8, 12, 24 or 48 h post-treatment (Figure 21C).

MTT ASSAY

Cell viability was assessed at 0, 3, 10, 30, 50, 100, 200, 300, 500, 1000, 1500 and 2000 μM clofibrate, fenofibrate and Wy-14,643 at 24 h using the 3-(4,5-dimethyl-2-thiazolyl)-2,5-diphenyl-2H tetrazorium bromide (MTT) assay (Sigma-Aldrich). Briefly, MTT (5mg/mL) was added following 24 h incubation and incubated for an additional 3 h with MTT. DMSO was then added to solubilize the MTT formazan, and absorbance was measured at 595 and 650 nm. Corrected absorbance was determined by subtracting the 650 nm value from the 595 nm background value. Relative cell viability was calculated as a percentage of control. Cell viability relative to dose was plotted to delineate PP concentrations that depressed MTT-

formazan production by 50% (LC_{50}; Yoshii, 1997). LC_{50} values are expressed as the mean ± SEM from three separate experiments.

PROTEIN PREPARATION AND WESTERN BLOT

Cell and tissue lysates for Western blot analysis were prepared in RIPA buffer (1x PBS, 0.1% SDS, 1% IGEPAL CA-630 and 0.5% Na-Deoxycholate) with protease inhibitor cocktail tablet (Roche Diagnostics, Mannheim, Germany) and quantified using the modified Lowry assay (Bio-Rad, DC Protein Assay, Hercules, CA). Cell and tissue lysates were electrophoretically separated on a denaturing 12% SDS-polyacrylamide gel and transferred onto nitrocellulose membrane (Amersham Biosciences Inc., Piscataway, NJ). Membranes were probed with anti-human rabbit PPARα (H-98) polyclonal antibody followed by horseradish peroxidase-conjugated secondary antibodies (Santa Cruz Biotechnology Inc., Santa Cruz, CA). Immunochemical staining and fluorescence detection on X-ray film was performed using the SuperSignal West Dura substrate (Thermo Fisher Scientific, Inc., Waltham, MA).

RNA ISOLATION

Total RNA was isolated from left lateral liver sections using Trizol Reagent (Invitrogen, Carlsbad, CA). Samples were removed from -80°C storage and homogenized in 1 ml Trizol Reagent using a Mixer Mill 300 tissue homogenizer (Retsch, Germany). Cells were harvested in TRIzol® Reagent (Invitrogen) and stored at -80^{o}C. Total RNA was isolated according to the manufacturer's protocol and resuspended in RNA Storage Solution (Ambion Inc., Austin, TX). RNA samples were quantified spectrophotometrically (A_{260}) and assessed for purity by A_{260}/A_{280} ratio and by visual inspection on a denaturing agarose gel.

MICROARRAY ANALYSIS OF DIFFERENTIAL GENE EXPRESSION

Treated and time-matched vehicle control samples were hybridized to independent arrays on the same array slide using one-color labeling (Cy3) of Whole Mouse Genome 4 × 44 K Oligo Microarray Kit (Agilent Technologies, Inc, Santa Clara, CA) with three biological replicates performed at each time point (Figure 21D). Microarray analysis was performed according to the manufacturer's protocol (Agilent Manual: G4140-90040 v. 5.7). The microarrays were scanned at 532 nm (Cy3) using a GenePix 4000B microarray scanner (Molecular Devices, Union City, CA). Images were analyzed using GenePix Pro 6.0 (Molecular Devices).

MICROARRAY DATA NORMALIZATION AND STATISTICAL ANALYSIS

Data were normalized using a semi-parametric approach. Model-based t-values were calculated from normalized data, comparing treated and vehicle responses per time-point. Empirical Bayes analysis was used to calculate posterior probabilities (P1(*t*) value) of activity on a per gene and time point basis using the model-based *t*-value [32]. Normalization and empirical Bayes analysis were performed using SAS 9.2 (SAS Institute, Cary, NC) and R 2.11.0 (http://www.r-project.org). The data were filtered using a P1(*t*) and fold change cutoff to identify differentially regulated genes for subsequent analysis and interpretation. All raw and normalized data were stored in dbZach, which supports microarray data management, mining, visualization and knowledge management [33]. Differentially expressed genes were analyzed by hierarchical clustering (Multiexperiment Viewer (MeV) in TM4 software [34]) using Pearson correlation with average linkage. Dose response analysis of cytotoxicity was performed using Graph Pad Prism 5.0 (GraphPad Software, San Diego, CA). Annotation and functional categorization of differentially regulated genes was performed using Database for Annotation, Visualization and Integrated Discovery (DAVID) [35]. Unless stated otherwise, all data were

analyzed by analysis of variance (ANOVA) followed by Tukey's *post hoc* tests. Differences between treatment groups were considered significant when $p < 0.05$.

QUANTITATIVE REAL-TIME PCR (QRT-PCR) ANALYSIS

QRT-PCR was performed as verification of microarray data for selected genes. For each sample, 1.5 μg of total RNA was reverse transcribed by SuperScript II reverse transcriptase using an anchored oligo-dT primer as described by the manufacturer's instructions (Invitrogen). 1.5 μL of cDNA template was used in a 30 μL PCR reaction containing 0.1 μM of forward and reverse gene-specific primers designed using Primer3[36] and SYBR Green PCR reaction mixture (Applied Biosystems, Foster City, CA). PCR amplification was conducted in MicroAmp Optical 96-well reaction plates (Applied Biosystems) on an Applied Biosystems PRISM 7500 Sequence Detection System under 10 min initial denaturation and enzyme activation at 95°C, followed by 40 cycles of 95°C for 15 s and 60°C for 1 min. A dissociation protocol was performed to assess the specificity of the primers and the uniformity of the PCR products. Target gene cDNAs were quantified using a standard curve of log copy number versus threshold cycle (Ct). The copy number of each sample was standardized to the geometric mean of two house-keeping genes, β-actin (ACTB) and glyceraldehyde-3-phosphate dehydrogenase (GAPDH), to control for differences in RNA loading, quality, and cDNA synthesis [37]. For graphing purposes, the relative gene expression levels were scaled such that the expression level of the time-matched vehicle treated control group was equal to 1. Official gene names and abbreviations, forward and reverse primer sequences, and product length for the genes verified by QRT-PCR are listed in Table 8.

Table 8. Gene names and primer sequences for QRT-PCR

RefSeq	Gene name	Gene symbol	Entrez Gene ID	Forward Primer	Reverse Primer	Product Size (bp)
Mouse						
NM_007393	actin, beta, cytoplasmic	Actb	11461	GCTACAGCTT CACCACCACA	TCTCCAGGGA GGAAGAGGAT	123
NM_008084	glyceraldehyde-3-phosphate dehydrogenase	Gapdh	14433	GTGGACCTCA TGGCCTACAT	TGTGAGGGAG ATGCTCAGTG	125
NM_011144	peroxisome proliferator activated receptor alpha	Ppara	19013	TCTGTGGGCT CACTGTTCTG	AACTACCTGC TCAGGGCTCA	177
NM_015729	acyl-Coenzyme A oxidase 1, palmitoyl	Acox1	11430	CTCCCACTCT GGTCTTCCTG	AGCCACCATG ATTGAAGTCC	124
NM_013743	pyruvate dehydrogenase kinase, isoenzyme 4	Pdk4	27273	GGCCATCCAT GTAGGAGAGA	GCCTGTGGGA AATAGGATGA	107
NM_010011	cytochrome P450, family 4, subfamily a, polypeptide 10	Cyp4a10	13117	ACCTACGTGC TGAGGTGGAC	CTGTTGGTGA TCAGGGTGTG	107
NM_177406	cytochrome P450, family 4, subfamily a, polypeptide 12a	Cyp4a12a	277753	TTCCAGTCTC CTTGCCTGTC	GGTGCAGGTT AGGGAGATCA	127
NM_013464	aryl-hydrocarbon receptor	Ahr	11622	ACCAGAACTG TGAGGGTTGG	TCTGAGGTGC CTGAACTCCT	155
NM_007408	adipose differentiation related protein	Adfp	11520	ACTGGCTGGT AGGTCCCTTT	CCTCAGACTG CTGGACCTTC	75
NM_020581	angiopoietin-like 4	Angptl4	57875	GGAAAAGATG CACCCTTCAA	TGCTGGATCT TGCTGTTTTG	113
NM_138313	BCL2 modifying factor	Bmf	171543	CCTTTGCTGG AGCCAAGTAG	TGCAGACAGA TCCAGTCCAG	112

Table 8 (cont'd)

RefSeq	Gene name	Gene symbol	Entrez Gene ID	Forward Primer	Reverse Primer	Product Size (bp)
Human						
NM_001101	actin, beta	ACTB	60	CATCCCCCAA AGTTCACAAT	AGTGGGGTGG CTTTTAGGAT	125
NM_002046	glyceraldehyde-3-phosphate dehydrogenase	GAPDH	2597	GGCCTCCAAG GAGTAAGACC	AGGGGTCTAC ATGGCAACTG	147
NM_005036	peroxisome proliferative activated receptor, alpha	PPARA	65260	GCAGAAACCC AGAACTCAGC	ATGGCCCAGT GTAAGAAACG	141
NM_004035	acyl-Coenzyme A oxidase 1, palmitoyl	ACOX1	51	TTTCTTCACTG CAGGGCTTT	GGAAAGGAGG GATTTTGAGC	115
NM_002612	pyruvate dehydrogenase kinase, isozyme 4	PDK4	5166	TCTGAGGCTG ATGACTGGTG	CAAACATTCA GGAAGCAGCA	137
NM_000778	cytochrome P450, family 4, subfamily A, polypeptide 11	CYP4A11	1579	GAGGAATGCC TTTCACCAGA	GTTGAGCCTT CCTCAGTTGG	125
NM_001122	adipose differentiation-related protein	ADFP	123	ACACCCTCCT GTCCAACATC	GCATTGCGGA ACACTGAGTA	103
NM_139314	angiopoietinlike protein 4	ANGPTL4	51129	TCCGTACCCT TCTCCACTTG	AGTACTGGCC GTTGAGGTTG	124
NM_001003940	Bcl2 modifying factor	BMF	90427	CCTGAGAACT GAGCCCAGAC	GAGTGAGTTC CTGGCTTTGC	112
NM_001001547	CD36 molecule	CD36	948	AGATGCAGCC TCATTTCCAC	GCCTTGGATG GAAGAACAAA	150

Table 8 (cont'd)

RefSeq	Gene name	Gene symbol	Entrez Gene ID	Forward Primer	Reverse Primer	Product Size (bp)
NM_002810	proteasome (prosome, macropain) 26S subunit, non-ATPase, 4	PSMD4	5710	AGCCATTCGA AATGCTATGG	GCTACCCTTTC CCTCCAGTC	105
NM_004159	proteasome (prosome, macropain) subunit, beta type, 8 (large multifunctional peptidase 7)	PSMB8	5696	CACGGGTAGT GGGAACACTT	GACAACGCCT CCAGAATAGC	142
NM_001540	heat shock 27kDa protein 1	HSPB1	3315	ACGAGATCAC CATCCCAGTC	CTTTACTTGGC GGCAGTCTC	91
NM_000128	coagulation factor XI	F11	2160	AAGCAGTGTG AATGGGTTCC	TACAAACACCA AGCCCCTTC	133
NM_000063	complement component 2	C2	717	GCGTTGCCAT TATCACCTTT	AGGCTGCTGAT CACCTCAGT	94

Figure 21. Time course study designs.
The *in vivo* time course studies consisted of a single dose. Animals were sacrificed 2-24 hrs after exposure **(A)** or received a daily dose and sacrificed 1-14 days after exposure **(B)** with either 300 mg/kg body weight clofibrate, Wy-14,643 or sesame seed oil vehicle, n = 5. **(C)** For the *in vitro* time course study, HL1-1 or HepG2 cells were treated with either 50 uM Wy-14,643 or 0.1% DMSO and harvested 1-48 hrs post treatment, n = 3. **(D)** Microarray experimental design for the mouse *in vivo* time course study. Temporal gene expression changes were analyzed using an independent reference design. PP treated samples and time-matched vehicle controls were hybridized on independent arrays using one-color labeling (Cy3), n = 3. Mouse 4 × 44 K Oligo Microarrays (Agilent Technologies, Inc, Santa Clara, CA) were used for global gene expression analysis. T: PP treatment and V: sesame oil vehicle treatment.

Figure 21 (Cont'd)

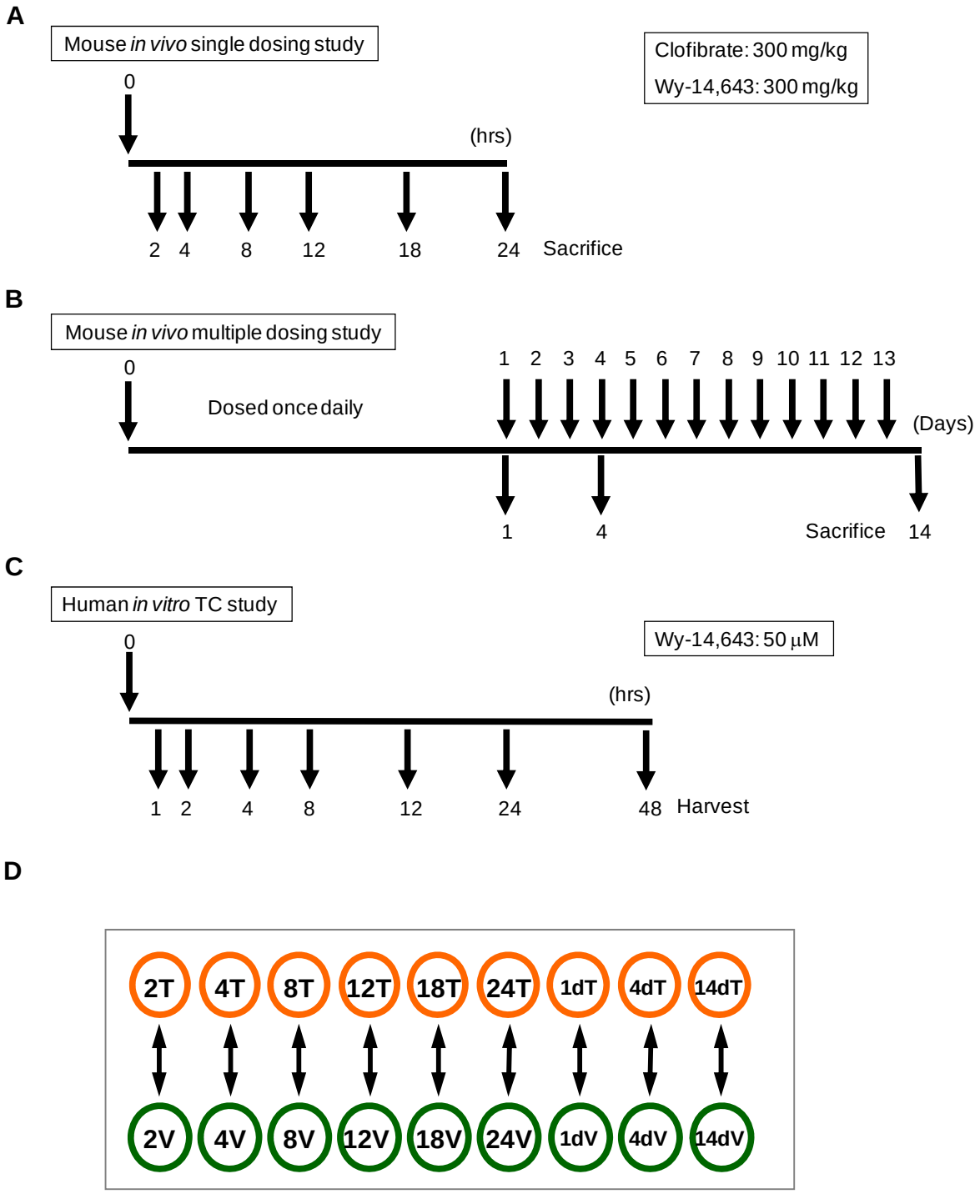

RESULTS

BODY WEIGHT, RELATIVE LIVER WEIGHT (RLW) AND HISTOPATHOLOGY

PPs did not elicit significant changes in body weight or RLWs following acute exposure in mice (Figure 22). However, RLWs were induced ($p < 0.05$) by 300 mg/kg WY at 4 and 14 days, and by 300 mg/kg CLO at 14 days compared to time- and vehicle-matched controls. Although there were no significant histological findings following acute exposure (>24 h), sub-chronic treatments (4-14 days) induced hyperplastic and hypertrophic hepatocyte growth and hepatomegaly, with no signs of irreversible hepatocellular injury (Figure 23).

TEMPORAL GENE EXPRESSION CHANGES

Gene expression was assessed using Agilent microarrays containing ~44,000 oligonucleotide probes representing ~34,200 annotated genes of which 21,000 are unique. Genes were identified as differentially regulated if the P1(t) > 0.99 and |fold change| > 1.5 compared to time-matched vehicle controls. In total, 719 and 1,443 genes were differentially expressed by clofibrate and Wy-14,643, respectively, at one or more time points. The number of differentially expressed genes steadily increased between 2 and 8 h following both treatments, with additional increases elicited by Wy-14,643 after 24 h and fewer changes elicited by clofibrate after 12 h (Figure 24A). Hierarchical clustering revealed early treatments (2-8 hrs) cluster by time, whereas later doses (12-24 hrs) cluster by treatment (Figure 25).

In total, 321 genes were induced while 398 genes were repressed by clofibrate with changes ranging from 81.3-fold induction for Pdk4 (pyruvate dehydrogenase kinase, isoenzyme 4) to 7.9-fold repression for Bmf (Bcl2 modifying factor). Wy-14,643 induced 1,060 genes, while 383 genes were repressed, with fold changes ranging from +123-fold induction for Pdk4 to -177-fold repression for Fmo3 (flavin containing monooxygenase 3). The greatest overlap in the

A

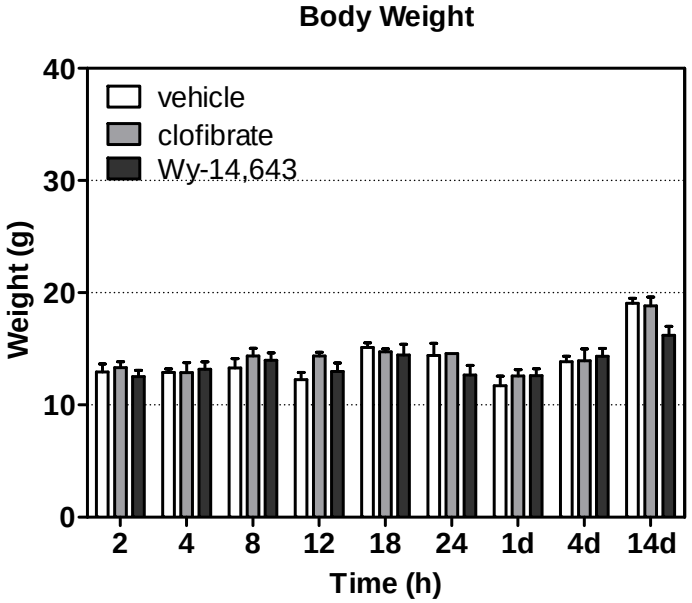

B

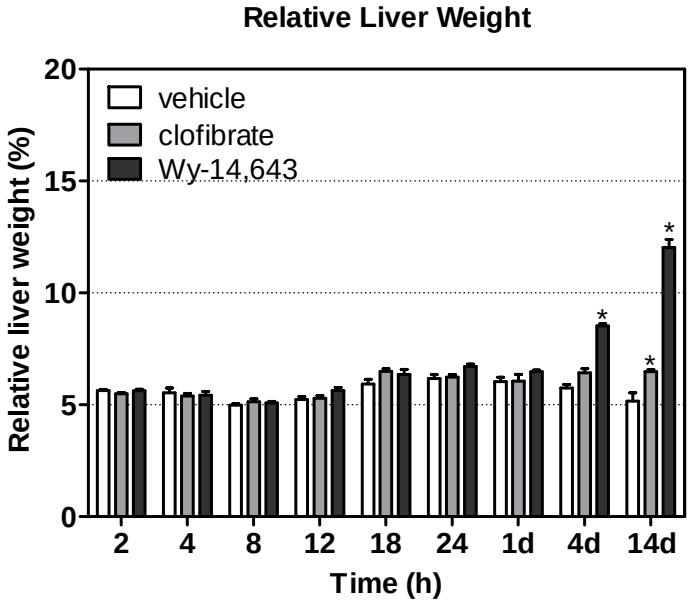

Figure 22. Clofibrate and Wy-14,643 effects on (A) **body weight and** (B) **relative liver weight (RLW).**
Immature ovariectomized C57BL/6 mice were orally gavaged with 300 mg/kg clofibrate, Wy-14,643 or sesame oil vehicle at time 0 and every 24 hrs thereafter. Mice were sacrificed 2, 4, 8, 12, 18 or 24 hrs after the initial dose for the acute study and 1, 4 or 14 days for the sub-chronic study. Bars are mean ± standard error (SE). *$p < 0.05$ compared to vehicle controls within a time-point, N = 5.

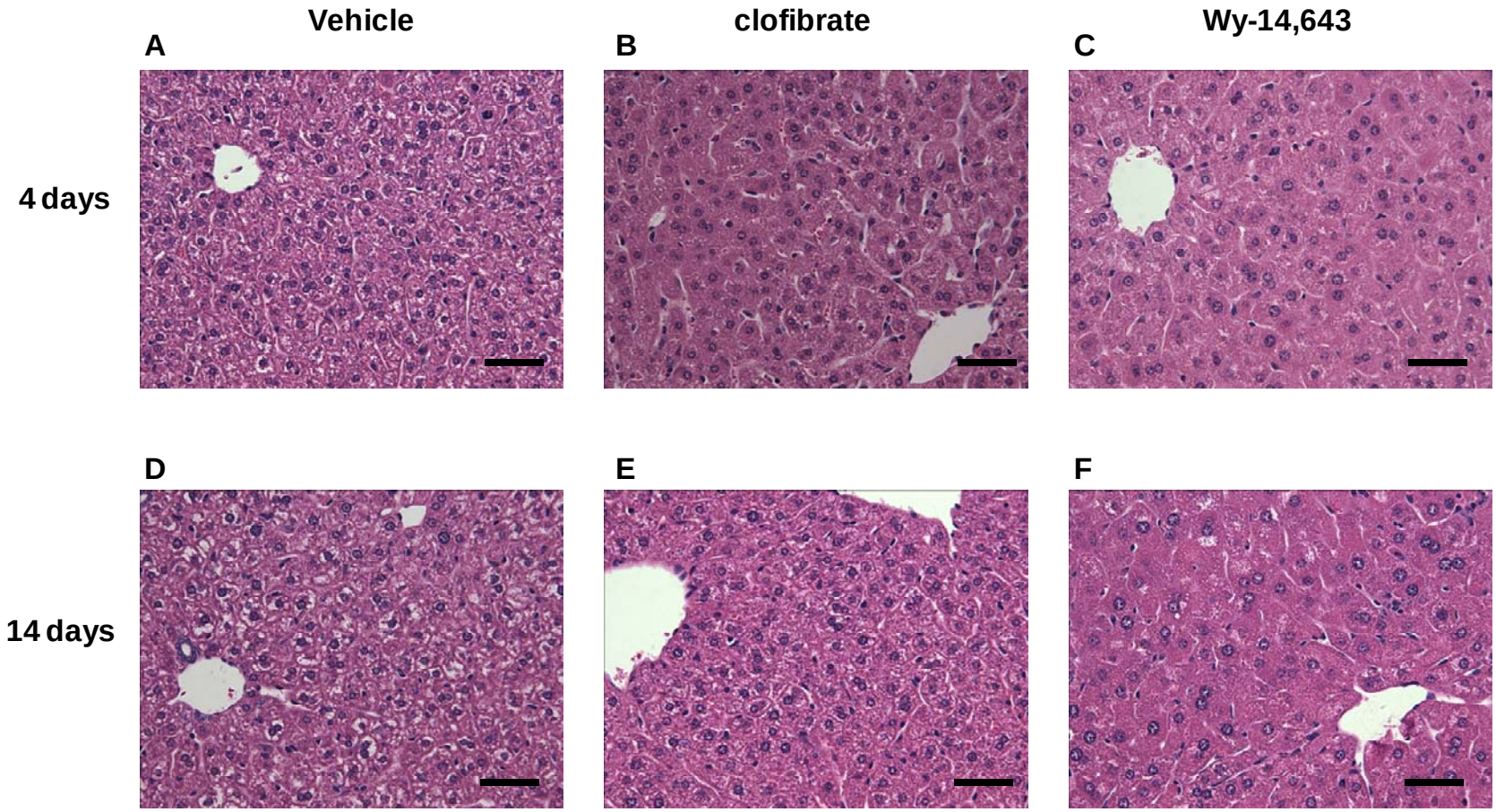

Figure 23. Representative histopathology results from vehicle-, clofibrate-, and Wy-14,643-treated mice at 4 and 14 days. Sub-chronic Wy-14,643 treatments (C, F) induced hyperplastic and hypertrophic hepatocyte growth and hepatomegaly without any signs of irreversible hepatocellular injury. Bars=50um.

number of differentially expressed genes between clofibrate and Wy-14,643 occurred 8 h post-dose (Figure 24A).

To include marginal responses, relaxed filtering criteria (P1(t) > 0.9 and |fold change| > 1.3) were applied. The number of differentially regulated genes increased to 3,600 and 6,639 for clofibrate and Wy-14,643, respectively (Figure 24B), with an overlap of 90% for clofibrate and 65% for Wy-14,643. Correlation analysis of the 1,221 overlapping differentially expressed genes revealed a high correlation between clofibrate and Wy-14,643 gene expression profiles indicating similarities in significance and expression profiles (Figure 24C).

A subset of prototypical mouse PPARα responsive genes (Acox1, Pdk4, Cyp4a10 and Cyp4a12) was verified by QRT-PCR. Overall, there was good agreement between microarray and QRT-PCR data for temporal gene expression profiles and induction levels (Figure 26). There was some evidence of data compression for Pdk4 and Cyp4a12 when microarray data was compared to QRT-PCR due to the limited dynamic fluorescence intensity range (0 ~ 65,535) [27].

FUNCTIONAL ANNOTATION OF CONSERVED RESPONSIVE GENES

Fifty common differentially expressed genes with the highest induction at 8 h which is the most overlapping time point between clofibrate and Wy-14,643 treatments were functionally annotated with the Database for Annotation, Visualization and Integrated Discovery (DAVID) (Figure 27). Over-represented functions were associated with lipid or carbohydrate metabolism, transport, cell cycle and immune response. For example, over-represented lipid or carbohydrate metabolism genes included prototypical PPARα responsive genes such as Acot2 and 4 (acyl-CoAs hydrolyze), Cd36 (fatty acid transport), Cpt1 (mitochondrial β-oxidation), Pdk4 (glucose metabolism) and Cyp4s (medium- & long-chain fatty acid metabolism). However, there were

Figure 24. Mouse hepatic temporal response comparison between clofibrate and Wy-14643 treatment.
(**A**) Number of genes exhibiting differential expression (P1(t) > 0.99 and |fold change| >1.5) in response to clofibrate (CLO) or Wy-14,643 (Wy). **(B)** Comparison of genes differentially expressed following clofibrate and Wy-14,643 treatments. Venn analysis using stringent filtering criteria (P1(t) > 0.99 and |fold change| > 1.5) and relaxed criteria (P1(t) > 0.9 and |fold change| > 1.3) are shown. Shaded areas represent number of marginal differentially expressed genes which are included by relaxed criteria. The numbers represent unique genes. **(C)** Correlation plot of genes differentially expressed by clofibrate and Wy-14,643 using the relaxed filtering criteria. Correlation analysis was used to compare significance and expression profile to identify similarities and differences between clofibrate and Wy-14,643 temporal data sets. A majority of genes (80.5%) were found within the upper right-hand quadrant indicating clofibrate and Wy-14,643 elicit similar gene expression and significance profiles.

Figure 24 (Cont'd)

A

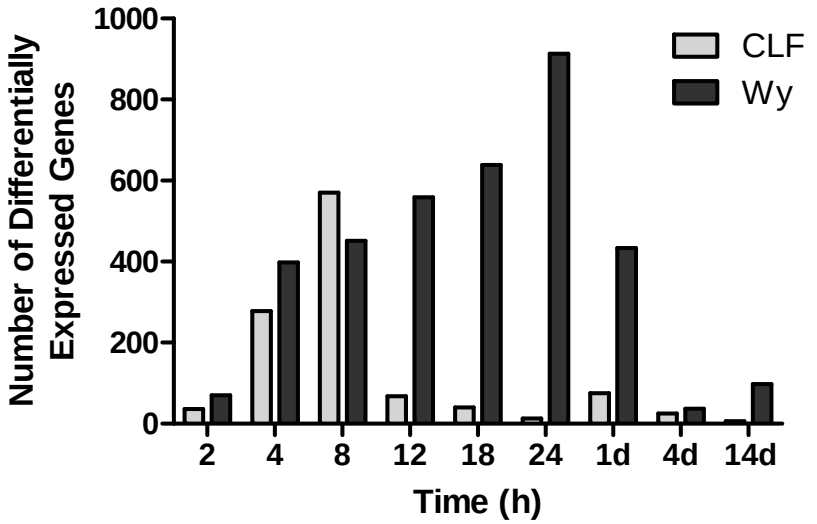

B

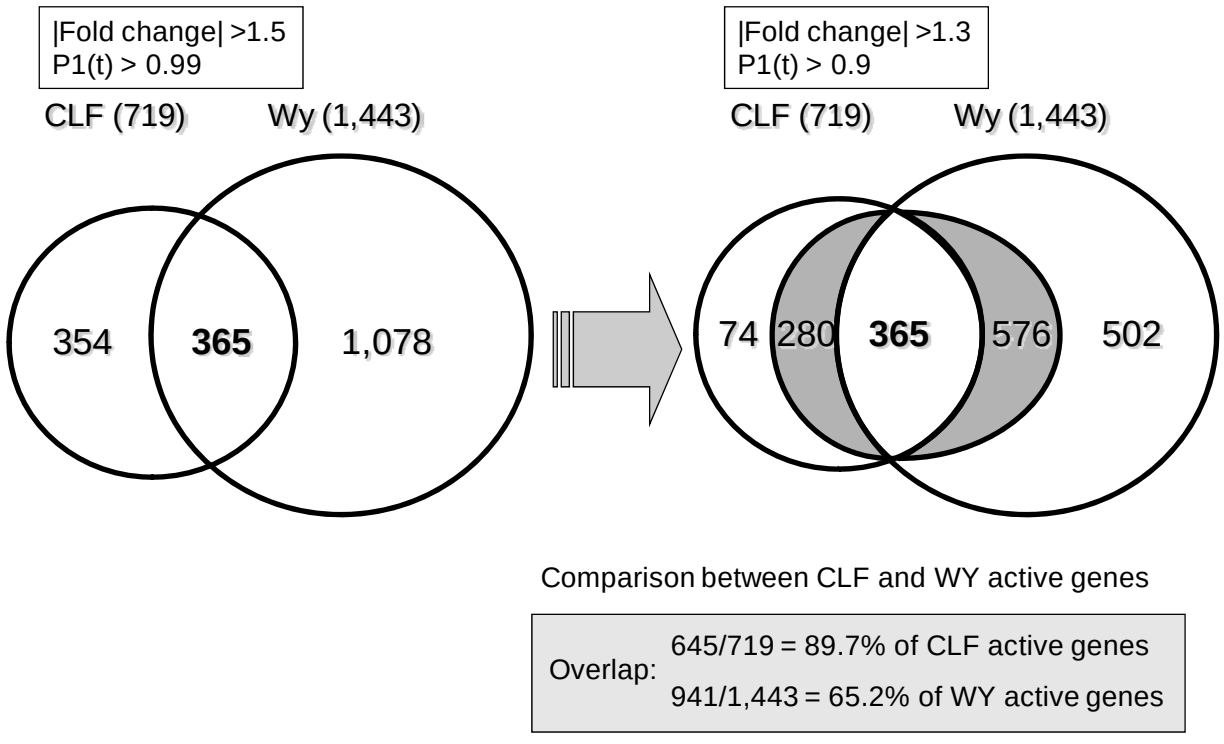

Comparison between CLF and WY active genes

Overlap:	645/719 = 89.7% of CLF active genes
	941/1,443 = 65.2% of WY active genes

Figure 24 (Cont'd)

C

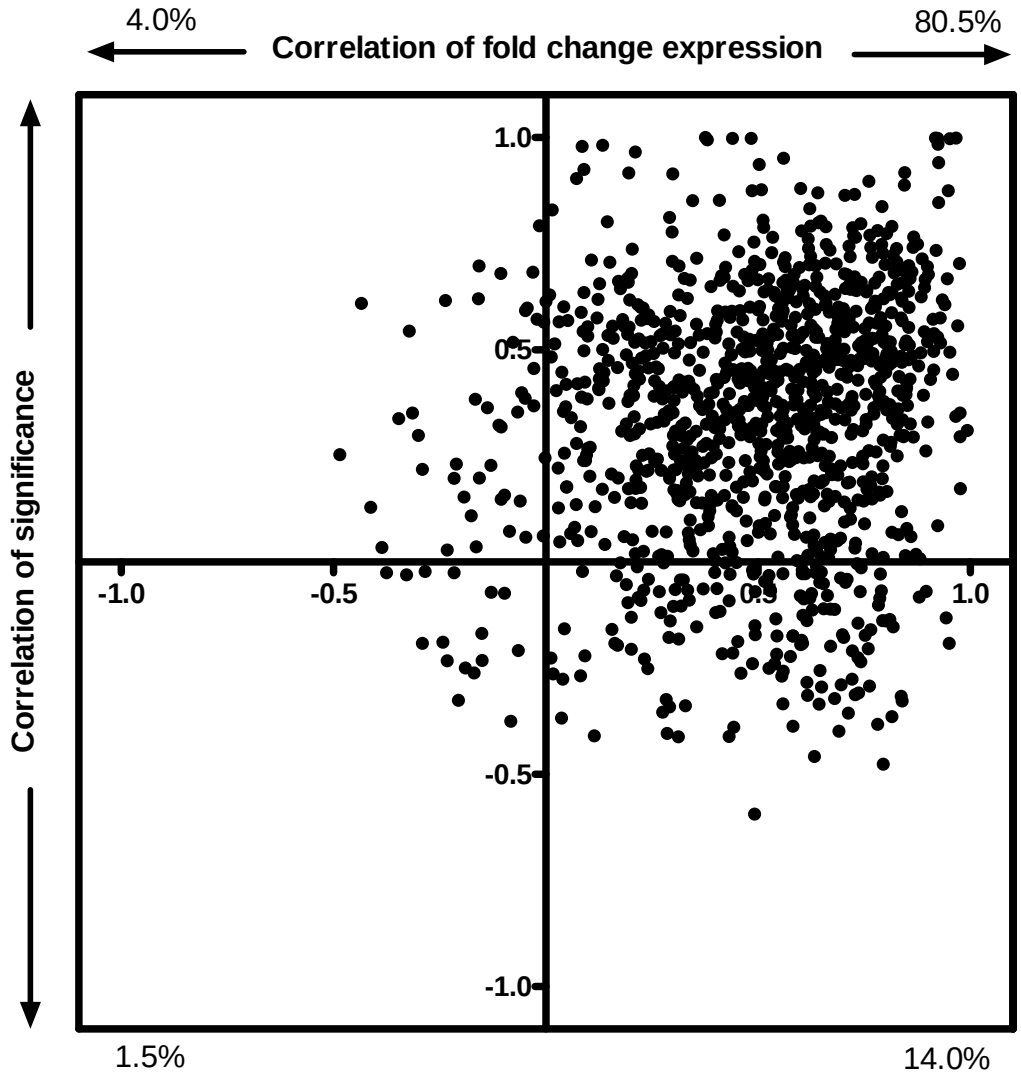

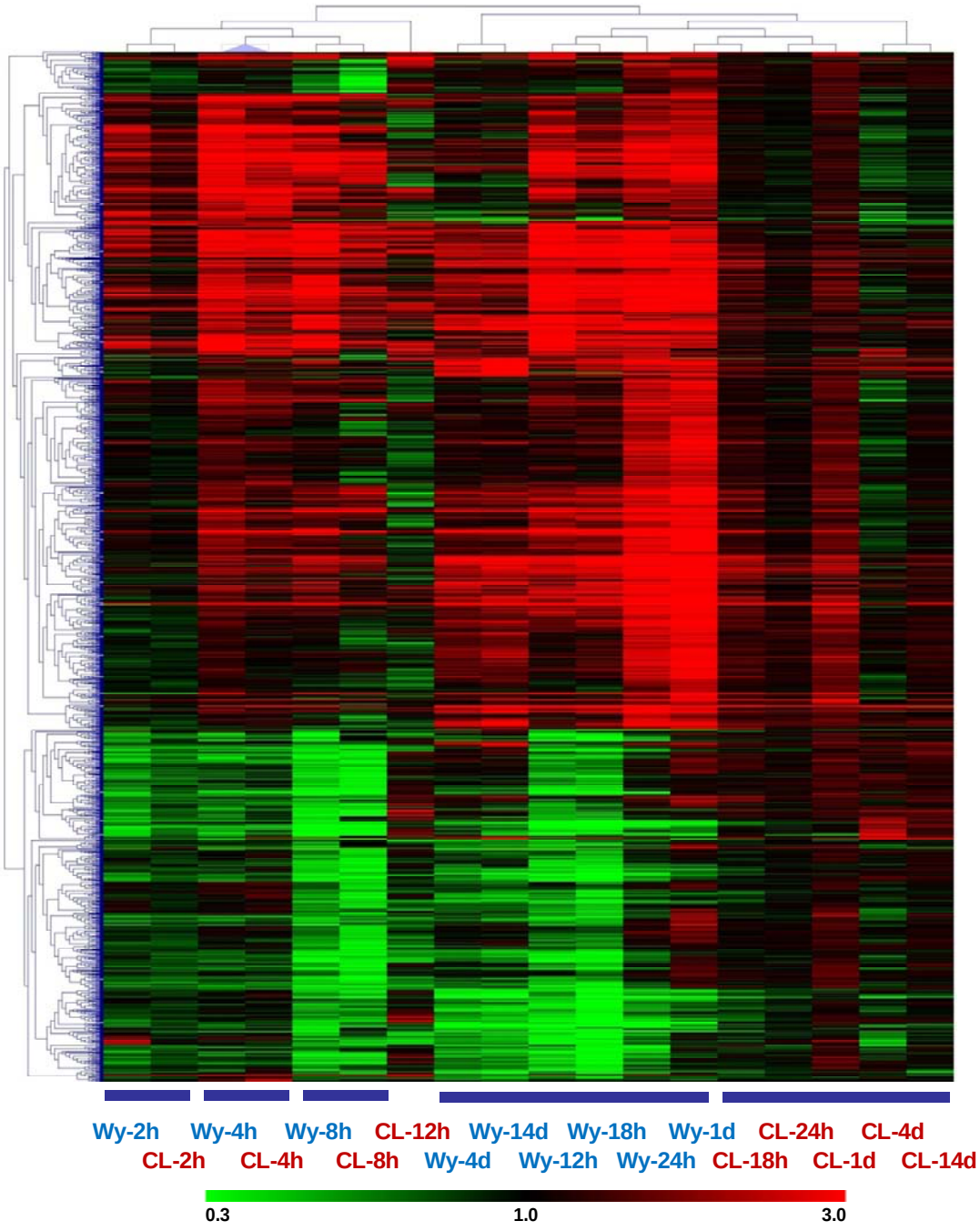

Figure 25. Hierarchical clustering of 410 differentially expressed genes by gene and time. Both Wy-14,643 and clofibrate treatment clustered together at early time points (2 ~ 8 h). At later time points (12 h+) the clustering is separated according to chemical treatment. Each bar represents fold change of gene expression compared with time-matched vehicle control. Purple bars indicate clustered groups. Wy: Wy-14,643, CL: clofibrate.

temporal differences between clofibrate and Wy-14,643 elicited differential gene expression. For example, Wy-14,643 induced gene expression at all time points, while induction by clofibrate diminished after 8 h.

Among the 1,797 unique genes differentially expressed by clofibrate or Wy-14,643, 1,110 were induced and 653 were repressed, while 34 showed a mixed response. Overrepresented induced genes were involved in the proteasome complex, PPAR signaling, fatty acid metabolism, peroxisome organization, and mitochondrial transport (Table 9). All of these over-represented functions are consistent with the role of PPARα in lipid metabolism. Moreover, the differential expression of DNA repair and cell cycle related genes is consistent with reports of PPARα induced DNA damage and cell proliferation, related to tumor induction [38, 39].

For repressed genes, over-represented functions were associated with amino and nucleotide sugar metabolism, complement and coagulation cascades, and glycosphingolipid biosynthesis, oxidation reduction, and immune response (Table 10). The insulin signaling, lipid process and storage, and high-density lipoprotein particle related pathways were also enriched as well as apoptosis and ErbB signaling.

PATHWAY MAPPING ANALYSIS

Over-represented functions, such as lipid metabolism, were mapped onto KEGG pathways (Table 11, Figure 28A). Several fatty acid transport & oxidation, VLDL receptor and lipoprotein lipase-related genes were induced at all time points. However, other lipogenesis and HDL component-related genes were down regulated at late time points. Proteasome subunit components as well as heat shock proteins (HSPs) were also induced (Table 11, Figure 28B). The 26S proteasome and HSPs play key roles in protein maintenance and endoplasmic reticulum (ER) stress protection. In contrast, genes associated with complement and coagulation cascades

Figure 26. QRT-PCR verification of selected microarray time course results.
Proto-typical PPARα responsive genes are indicated by the official gene symbol. The same RNA used for microarray analysis was examined by QRT-PCR. Bars (left axis) and lines (right axis) represent QRT-PCR and microarray data, respectively. Bars are mean ± SE for the average fold change, *$p < 0.05$ for QRT-PCR, $N = 3$.

Figure 26 (Cont'd)

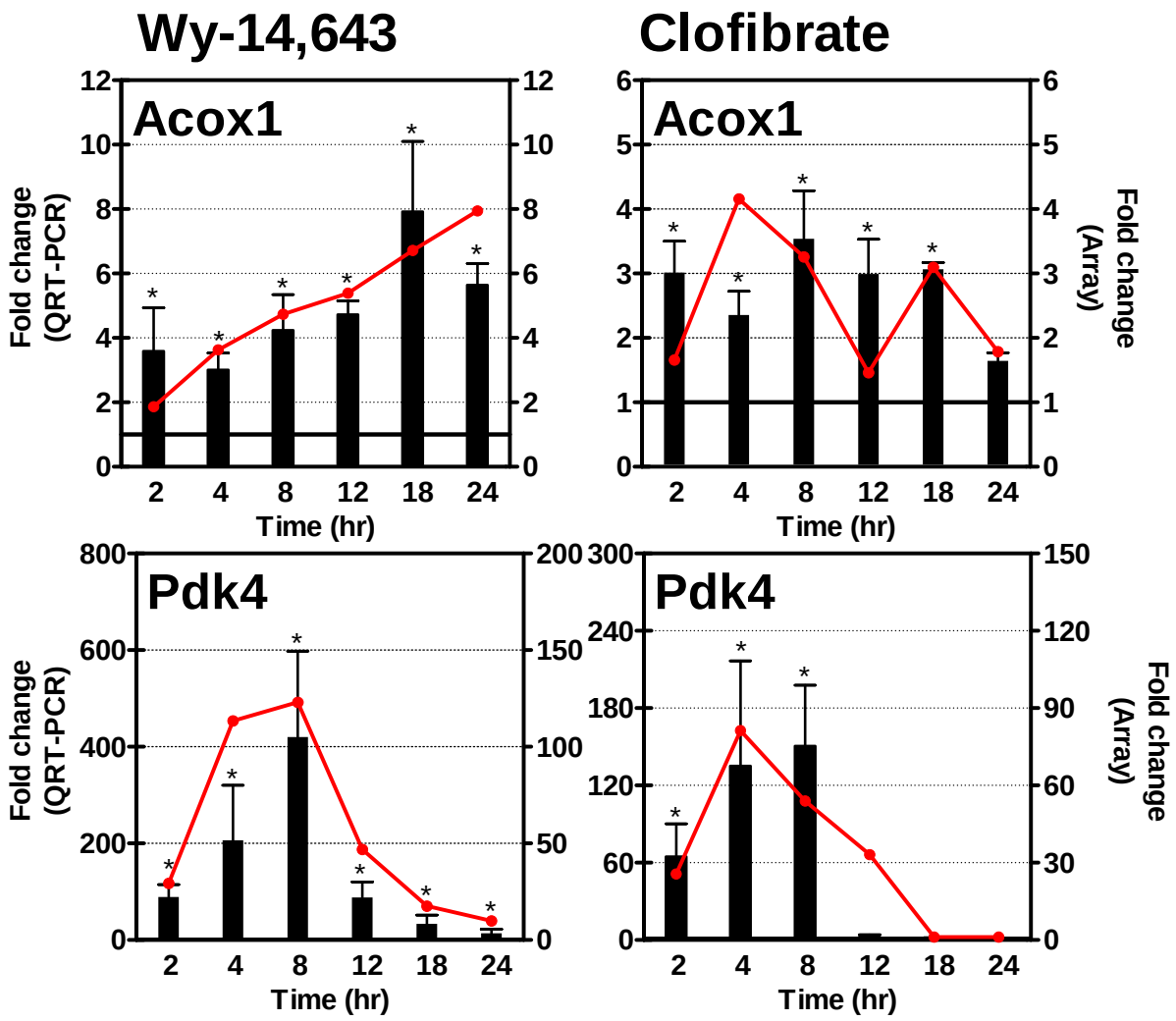

Figure 26 (Cont'd)

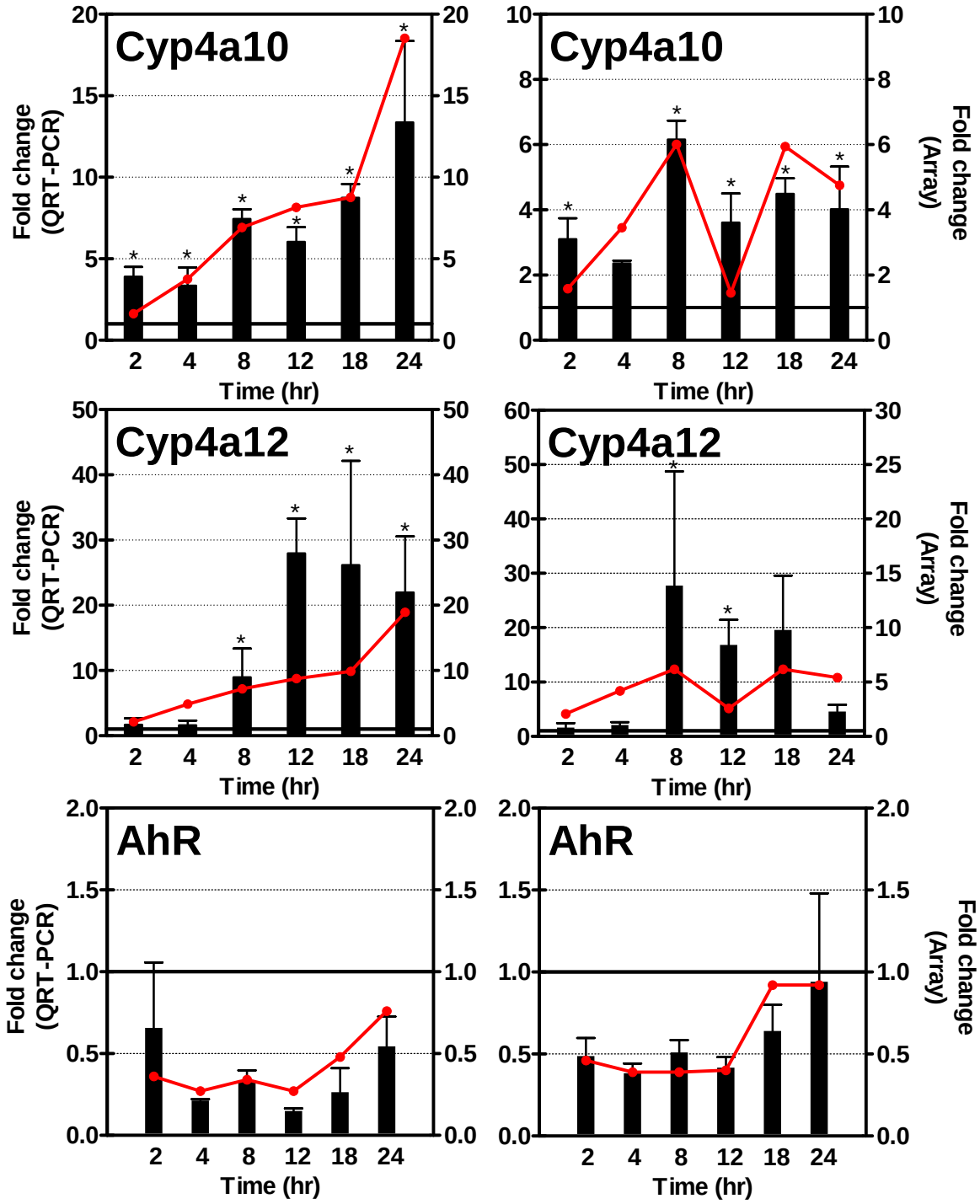

Figure 27. Functional categorization of the top 50 genes differentially expressed by Wy-14,643 and clofibrate treatment.
Genes were ranked by induction ratio and functionally annotated using the Database for Annotation, Visualization and Integrated Discovery (DAVID). Each bar represents the average fold change in gene expression compared with time-matched vehicle control.

Figure 27 (Cont'd)

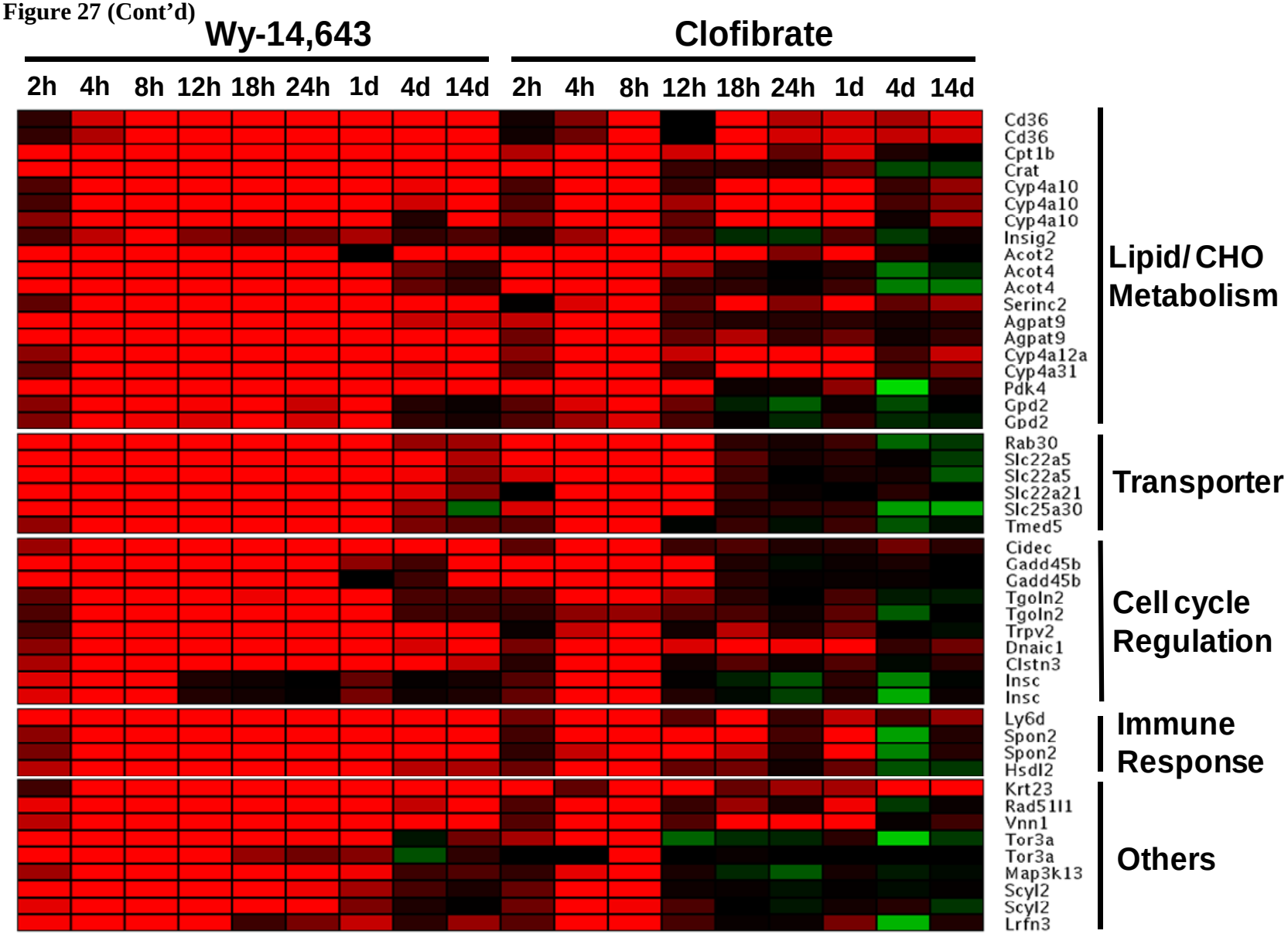

Table 9. Over-represented gene ontology groups induced following PP treatment. BP: biological process, CC: Cellular component

Category	Term	Count	P Value	Benjamini
KEGG_PATHWAY				
mmu03050	Proteasome	22	5.04E-14	8.87E-12
mmu03320	PPAR signaling pathway	25	1.68E-11	1.48E-09
mmu00071	Fatty acid metabolism	17	3.33E-09	1.95E-07
mmu01040	Biosynthesis of unsaturated fatty acids	11	2.08E-06	9.15E-05
mmu00280	Valine, leucine and isoleucine degradation	11	3.54E-04	1.03E-02
mmu04115	p53 signaling pathway	11	8.46E-03	1.17E-01
mmu00020	Citrate cycle (TCA cycle)	6	3.76E-02	2.86E-01
mmu02010	ABC transporters	7	5.38E-02	3.71E-01
GOTERM_BP				
GO:0006631	fatty acid metabolic process	38	2.18E-12	4.72E-09
GO:0007031	peroxisome organization	12	2.15E-09	1.55E-06
GO:0006839	mitochondrial transport	14	1.67E-07	5.17E-05
GO:0030163	protein catabolic process	60	3.80E-07	8.23E-05
GO:0070585	protein localization in mitochondrion	10	9.38E-07	1.85E-04
GO:0006412	translation	40	1.29E-06	2.33E-04
GO:0006511	ubiquitin-dependent protein catabolic process	21	6.39E-05	5.31E-03
GO:0008610	lipid biosynthetic process	32	1.47E-04	1.02E-02
GO:0006457	protein folding	19	1.48E-04	9.96E-03
GO:0016042	lipid catabolic process	19	2.93E-04	1.70E-02
GO:0007006	mitochondrial membrane organization	8	3.36E-04	1.90E-02
GO:0006637	acyl-CoA metabolic process	7	4.77E-04	2.61E-02
GO:0006413	translational initiation	9	7.76E-04	4.11E-02
GO:0051004	regulation of lipoprotein lipase activity	3	8.34E-03	2.54E-01
GO:0043574	peroxisomal transport	3	2.59E-02	5.35E-01
GO:0015908	fatty acid transport	4	2.95E-02	5.78E-01
GO:0006281	DNA repair	20	3.04E-02	5.85E-01
GO:0010883	regulation of lipid storage	3	5.06E-02	7.01E-01
GO:0007049	cell cycle	42	8.40E-02	8.11E-01
GOTERM_CC				
GO:0005739	mitochondrion	199	1.89E-41	8.03E-39
GO:0005777	peroxisome	35	8.86E-18	4.17E-16
GO:0000502	proteasome complex	25	1.42E-15	5.56E-14

Table 10. Over-represented gene ontology groups repressed following PP treatment. BP: biological process, CC: Cellular component

Category	Term	Count	P Value	Benjamini
KEGG_PATHWAY				
mmu00520	Amino sugar and nucleotide sugar metabolism	8	4.97E-04	7.78E-02
mmu04610	Complement and coagulation cascades	10	6.96E-04	5.52E-02
mmu00604	Glycosphingolipid biosynthesis	5	1.15E-03	6.05E-02
mmu00330	Arginine and proline metabolism	8	1.56E-03	4.96E-02
mmu04910	Insulin signaling pathway	12	5.34E-03	1.35E-01
mmu00983	Drug metabolism	6	1.96E-02	3.01E-01
mmu04210	Apoptosis	8	2.33E-02	2.95E-01
mmu04142	Lysosome	9	4.08E-02	3.64E-01
mmu05214	Glioma	6	5.76E-02	4.54E-01
mmu02010	ABC transporters	5	5.86E-02	4.40E-01
mmu04012	ErbB signaling pathway	7	6.49E-02	4.38E-01
GOTERM_BP				
GO:0009063	cellular amino acid catabolic process	9	1.82E-04	1.56E-01
GO:0055114	oxidation reduction	35	1.80E-03	3.81E-01
GO:0007264	small GTPase mediated signal transduction	18	1.91E-03	3.59E-01
GO:0006955	immune response	26	3.86E-03	5.14E-01
GO:0007010	cytoskeleton organization	20	4.23E-03	4.83E-01
GO:0016042	lipid catabolic process	11	6.80E-03	5.07E-01
GO:0008202	steroid metabolic process	12	8.86E-03	5.15E-01
GO:0008652	cellular amino acid biosynthetic process	6	9.59E-03	5.13E-01
GO:0002526	acute inflammatory response	8	1.04E-02	5.28E-01
GO:0010876	lipid localization	9	3.77E-02	7.90E-01
GO:0032869	cellular response to insulin stimulus	5	3.85E-02	7.90E-01
GO:0008610	lipid biosynthetic process	15	4.69E-02	8.22E-01
GO:0019915	lipid storage	3	5.56E-02	8.52E-01
GOTERM_CC				
GO:0005764	lysosome	18	2.79E-05	8.28E-03
GO:0005783	endoplasmic reticulum	46	1.19E-04	8.83E-03
GO:0005739	mitochondrion	52	4.13E-02	4.84E-01
GO:0034364	high-density lipoprotein particle	3	8.28E-02	6.01E-01

pathway, which are related to immune and inflammatory responses, were down regulated (Table 11, Figure 28C).

IN VITRO PPAR EXPRESSION AND CELL CYTOTOXICITY

Basal PPARα mRNA expression levels were comparable in HL1-1 human liver stem cells, HepG2 human hepatoma cells and Hepa1c1c7 mouse hepatoma cells and mouse liver based on RT-PCR (Figure 29A). Protein expression was also confirmed by western blot in each model (Figure 29B).

The cytotoxic effects of Wy-14,643, clofibrate and fenofibrate were examined in HL1-1 and HepG2 cells. Overall, HL1-1 cells were more resistance than HepG2 to PP treatment (Table 12 and Figure 30). Wy-14,643 elicited the greatest cytotoxicity with an LC_{50} value of 740 and 459 uM in HL1-1 and HepG2 cells, respectively. In HL1-1 cells, fenofibrate elicited minimal cytotoxicity (LC_{50} 2,600 uM) followed by clofibrate (1,300 uM). In HepG2 cells, clofibrate was the least toxic (1,470 uM) followed by fenofibrate (767 uM). Neither cell line exhibited cytotoxicity below 100 uM.

COMPARISON OF MOUSE IN VIVO GENE EXPRESSION WITH HUMAN IN VITRO MODELS

HL1-1 and HepG2 temporal gene expression responses elicited by 50 uM Wy-14,643 were compared for selected genes by QRT-PCR (Figure 21C). Orthologous lipid/cholesterol metabolism genes including PDK4, ADFP and ANGPTL4, showed comparable responses across species although there were temporal and magnitude differences (Figure 31). However, several species-specific responses were identified. For example, BMF (Bcl2 modifying factor), a gene associated with apoptosis signaling and tumor suppression was repressed in mouse liver but induced in HL1-1 and HepG2 cells. Other PPARα responsive genes, including ACOX1, CD36 and CPT1A, were induced in mouse liver but not differentially expressed in HL1-1 cells (Figure

32). Furthermore, proteasome component (PSMD4 and PSMB8), heat shock protein (HSPB1) and coagulation factor (F11) genes were differentially expressed in mice treated with PP, but were not changed in HL1-1 cells.

DISCUSSION

Temporal gene expression differences between Wy-14,643 and clofibrate that can be partially explained by their different plasma half-lives (clofibrate ~2 hrs [40]; Wy-14,643 ~1 h [41]) and pharmacodynamic properties. In addition, Wy-14,643 exhibits non-linear absorption and elimination behavior when compared to clofibrate [41]. Cell-based transactivation assays, with limited metabolic capabilities, also indicate Wy-14,643 (EC50 = 0.63uM compared to 50uM for clofibrate) is more potent and has greater (30-150-fold) relative binding affinity for PPARα [42, 43]. Although PPARα typically has a short half-life due to proteasome degradation, ligand binding protects it from ubiquitination, resulting in prolonged ligand-induced differential gene expression [44]. Collectively, these differences are consistent with the larger number of differentially expressed genes and prolonged expression elicited by Wy-14,643 when compared to clofibrate.

Analysis of differentially expressed genes identified over-represented functions associated with fatty acid metabolism. Several fatty acid oxidation related genes, including mitochondrial β-oxidation (Cpt1, Acad, Hadha, and Ucp2), peroxisomal β-oxidation (Acox1) and microsomal ω-hydroxylation (Cyp4As), were strongly induced at all time points. Fatty acid transport (Cd36), lipoprotein lipase (Lpl), and hormone sensitive lipase (Hsl) were also induced, while lipid catabolism, HDL particle and insulin signaling related genes were repressed. These changes are consistent with increases in fatty acid-metabolism and transport, and the repression of lipogenesis resulting in the clearance of hepatic and plasma lipids.

Table 11. PP elicited differentially expressed genes used for pathway mapping analysis

GeneID	Symbol	Wy	Time points	Clo	Time points	Functional Description
Lipid metabolism related genes						
De novo synthesis						
20787	Srebf1			**Down**	8h	activate lipogenesis
14104	Fasn	**Down**	12h	**Down**	12h	malonyl CoA -> palmitate (C16:0)
FA transport						
11520	Adfp	**Up**	2,8,12h	**Up**		FA transport related
12491	Cd36	**Up**	4,8,12,18,24h,4, 14d	**Up**	4,8,12,18,24h, 4,14d	FA translocalase (FAT)
19299	Abcd3	**Up**	4,8,12,18,24h,4, 14d	**Up**	4,8,12h	FA peroxisomal import
Fatty acid metabolism (oxidation)						
12894	Cpt1a	**Up**	4,12,18,24h	**Up**	4,12h	mitochondrial β-oxidation rate limiting enzyme
12895	Cpt1b	**Up**	2,4,8,12,18,24h, 4,14d	**Up**	2,4,8,12,18h	
11363	Acadl	**Up**	4,8,12,18,24h,4, 14d	**Up**	4,8,12,18h	mitochondrial β-oxidation
11364	Acadm	**Up**	24h			
11409	Acads	**Up**	24h,14d			
97212	Hadha	**Up**	4,8,12,18,24h,4, 14d	**Up**	2,4,8,12,18,24 h	
11430	Acox1	**Up**	4,8,12,18,24h,4, 14d	**Up**	4,8,12,18h	peroxisomal β-oxidation
93732	Acox2	**Up**	24h			
13117	Cyp4a10	**Up**	4,8,12,18,24h,4, 14d	**Up**	4,8,12,18,24h, 14d	microsomal ω-oxidation
277753	Cyp4a12a	**Up**	2,4,8,12,18,24h, 4,14d	**Up**	2,4,8,12,18,24 h,4,14d	
666168	Cyp4a31	**Up**	4,8,12,18,24h,4, 14d	**Up**	4,8,12,18,24h	
Esterification						
13350	Dgat1	**Up**	24h			esterification
67800	Dgat2	**Down**	8,12,18h,14d	**Down**	8h	
Lipid secretion						
17777	Mttp	**Up**	4,8,12,18,24 h	**Up**	4h	make VLDL. Lipid secretion

Table 11 (cont'd)

GeneID	Symbol	Wy	Time points	Clo	Time points	Functional Description
Lipoprotein related genes						
HDL related						
11808	Apoa4	**Down**	18h,4,14d	**Down**	18h,14d	HDL component, LCAT activator
20778	Scarb1	**Down**	8,18h,4d	**Down**	18h	receptor for HDL (detect ApoA)
11307	Abcg1	**Up**	14d			cholesterol transfer to ApoA1 to make pre b-HDL
26357	Abcg2	**Up**	8,12,18,24h,4,14d	**Up**	8,12h	
18830	Pltp	**Up**	24h,4,14d			CE & TG transfer between lipoproteins
VLDL related						
17777	Mttp	**Up**	4,8,12,18,24 h	**Up**	4h	make VLDL. Lipid secretion
22359	Vldlr	**Up**	8,12,18,24 h,4,14d	**Up**	4,8h	receptor for VLDL
Chylomicron related						
228357	Lrp4	**Up**	24h			receptor for Chylomicron remenant
Lipase related						
11814	Apoc3	**Down**	4,14d			inhibit LPL
16956	Lpl	**Up**	8,12,18,24h,4,14d	**Up**	14d	lipoprotein lipase
16890	Lipe	**Up**	4,12,24h	**Up**	4h	hormone sensitive lipase

Table 11 (cont'd)

GeneID	Symbol	Wy	Time points	Clo	Time points	Functional Description
Proteasome pathway						
alpha subunit						
26440	Psma1	**Up**	18,24h,14d			20S Core particles alpha subunits
19166	Psma2	**Up**	18,24h			
19167	Psma3	**Up**	24h,14d			
26441	Psma4	**Up**	24h			
26442	Psma5	**Up**	4,8,12,18,24 h			
26443	Psma6	**Up**	18,24h,14d			
26444	Psma7	**Up**	24h			
73677	Psma8	**Up**	4,14d			
beta subunit						
19170	Psmb1	**Up**	24h,14d			20S Core particles beta subunits
26445	Psmb2	**Up**	18,24h			
26446	Psmb3	**Up**	24h			
19173	Psmb5	**Up**	18,24 h,4,14d			
19175	Psmb6	**Up**	24h			
19177	Psmb7	**Up**	24h,14d			
16913	Psmb8	**Down**	8,18,24 h,4,14d	**Down**	8,12h,4d	Immunoproteasome subunits
16912	Psmb9	**Down**	8,12,18h	**Down**	8,12h	
19171	Psmb10	**Down**	12,18h			
26S subunit						
19182	Psmc3	**Up**	24h			Regulatory particles PA700 (Base)
23996	Psmc4	**Up**	24h			
67089	Psmc6	**Up**	18,24h	**Up**	8h	
70247	Psmd1	**Up**	24h			
21762	Psmd2	**Up**	12,24h			
19185	Psmd4	**Up**	4,8,12,18,24 h,4,14d	**Up**	4,12h	Regulatory particles PA700 (Lid)
66998	Psmd5	**Up**	24h			
66413	Psmd6	**Up**	4,12,18,24 h			
17463	Psmd7	**Up**	4,24h			
57296	Psmd8	**Up**	24h			
67151	Psmd9	**Up**	24h	**Up**	4d	
69077	Psmd11	**Up**	12,24h			
66997	Psmd12	**Up**	4,12,24h	**Up**	8h	
23997	Psmd13	**Up**	24h			
59029	Psmd14	**Up**	18,24h,14d	**Up**	8h	

Table 11 (cont'd)

GeneID	Symbol	Wy	Time points	Clo	Time points	Functional Description
other subunit						
107047	Psmg2	**Up**	24h			Assembly chaperone
103554	Psme4	**Up**				PA200
228769	Psmf1	**Up**		**Up**	4h	PI31
Chaperone (Hsp)						
193740	Hspa1a	**Up**	2,4,8,12,24h	**Up**	2,4,12h	Hsp70
15519	Hsp90aa1	**Up**	2,4,8,24h,4,14d	**Up**	2,4,8h (4d down)	Hsp86/90
15516	Hsp90ab1	**Up**	24h			
15525	Hspa4	**Up**	4,12,24h	**Up**	4h	Hsp110
15507	Hspb1	**Up**	4,8,12,18,24 h,4,14d	**Up**	8,12,18h,4,14d	Hsp25/27
15510	Hspd1	**Up**	4,8,12,18,24 h,4,14d	**Up**	8,18h	Hsp60
15528	Hspe1	**Up**	24 h,4,14d			Hsp10
15505	Hsph1	**Up**	2,4h	**Up**	2,4,8h (4d down)	Hsp105/110
18415	Hspa4l	**Up**	24h,4,14d	**Up**	8,12h	
Complement & coagulation cascades pathway						
complement factor						
12261	C1qbp	**Up**	24h			Complement cascade
12260	C1qb	**Down**	18h,4d	**Down**	8h	
50909	C1r	**Down**	18h,4,14d			
50908	C1s	**Down**	18h,4,14d	**Down**	8h	
12263	C2	**Down**	8,12,18,24 h,4,14d	**Down**	8h	
12268	C4b	**Down**	18h,4,14d	**Down**	8h	
230558	C8a	**Down**	18,24h,4,14d			
110382	C8b	**Down**	18,24h,4,14d			
69379	C8g	**Down**	14d			
12279	C9	**Down**	18,24h,4,14d			
12628	Cfh	**Down**	18h,4,14d			
50702	Cfhr1	**Down**	12,18h,14d			
18636	Cfp	**Down**	18h			

Table 11 (cont'd)

GeneID	Symbol	Wy	Time points	Clo	Time points	Functional Description
coagulation factor						
14066	F3	**Up**	12,24h			Coagulation cascade
14067	F5	**Down**	8,18h,4,14d	**Down**	8h	
14068	F7	**Down**	8,12,18,24 h,4,14d	**Down**	8,12h	
109821	F11	**Down**	8,12,18,24 h,4,14d	**Down**	8,12h	
others						
17174	Masp1	**Down**	8,12,18h,4,14d			activation of the lectin pathway
18816	Serpinf2	**Down**	18h			Progression of fibrosis

A

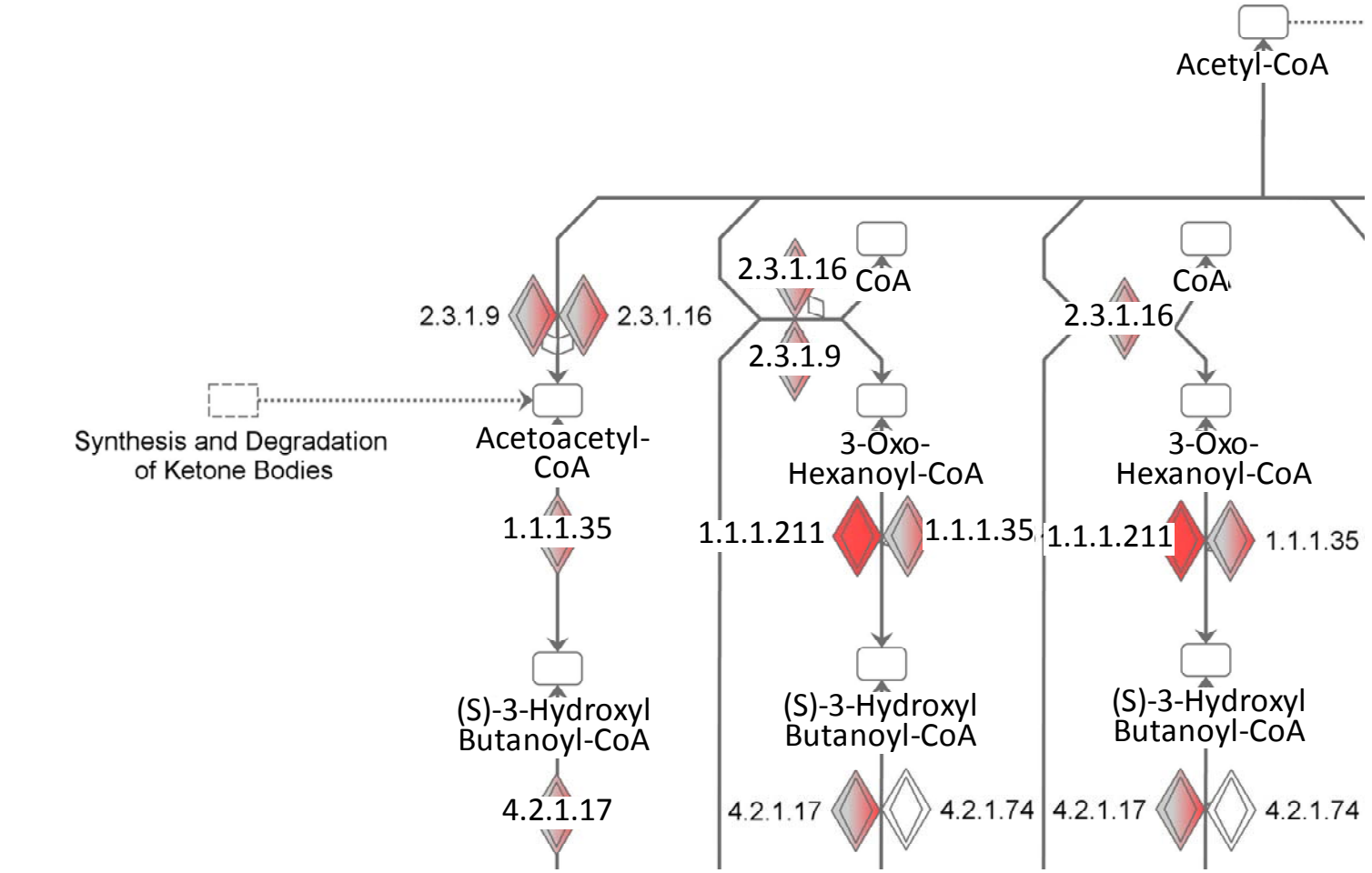

Figure 28. Pathway mapping analysis.
(A) Fatty acid metabolism pathway, (B) Proteasome pathway, (C) Complement & coagulation cascades pathway. Differentially expressed genes by Wy-14,643 were mapped to the targeted pathway using KEGG Mapper pathway mapping tools (http://www.genome.jp/kegg/ mapper.html). Colored genes represent differentially expressed genes. Red: induction, blue: repression.

Figure 28 (Cont'd)
B

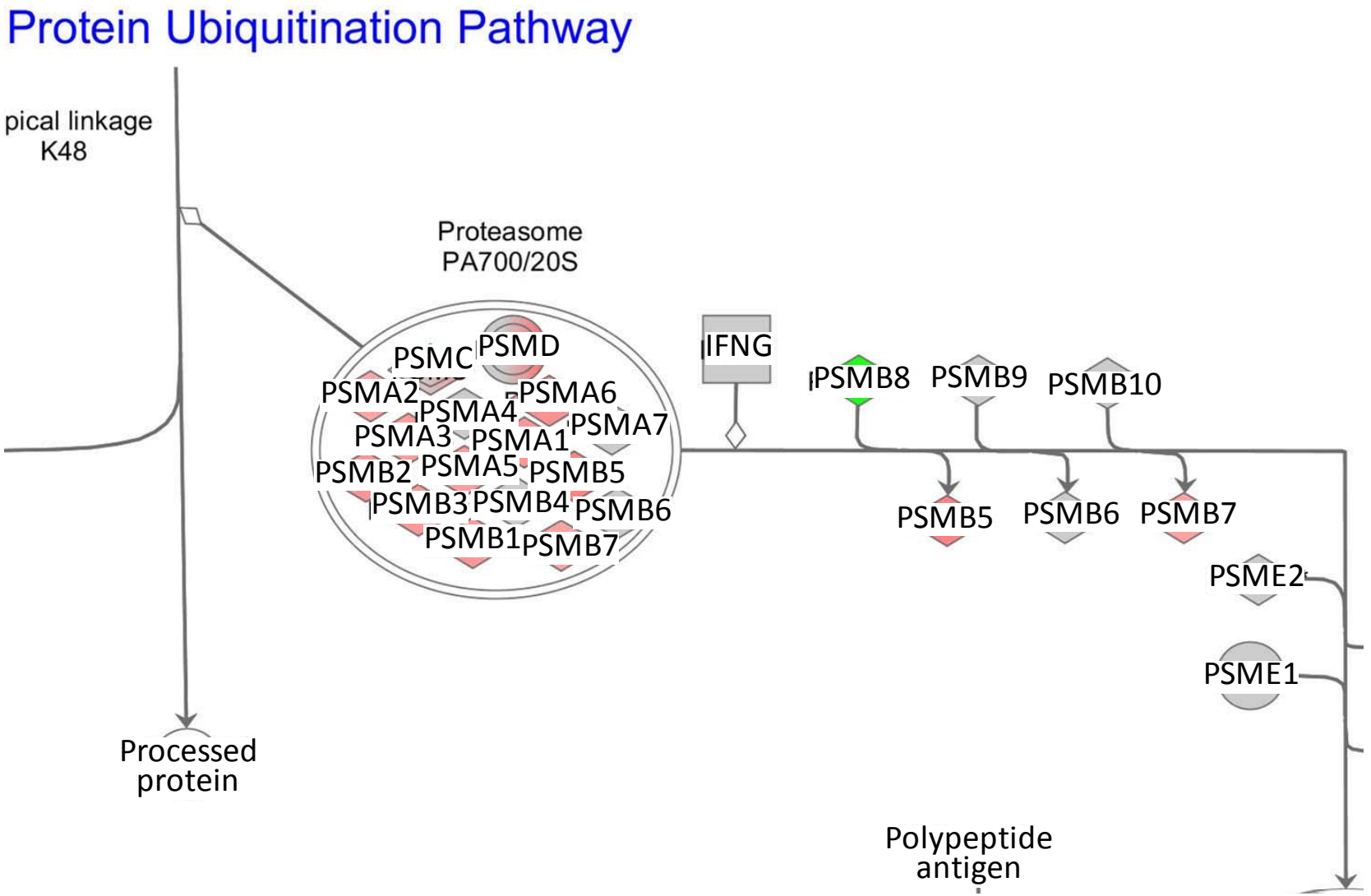

Figure 28 (Cont'd)
C

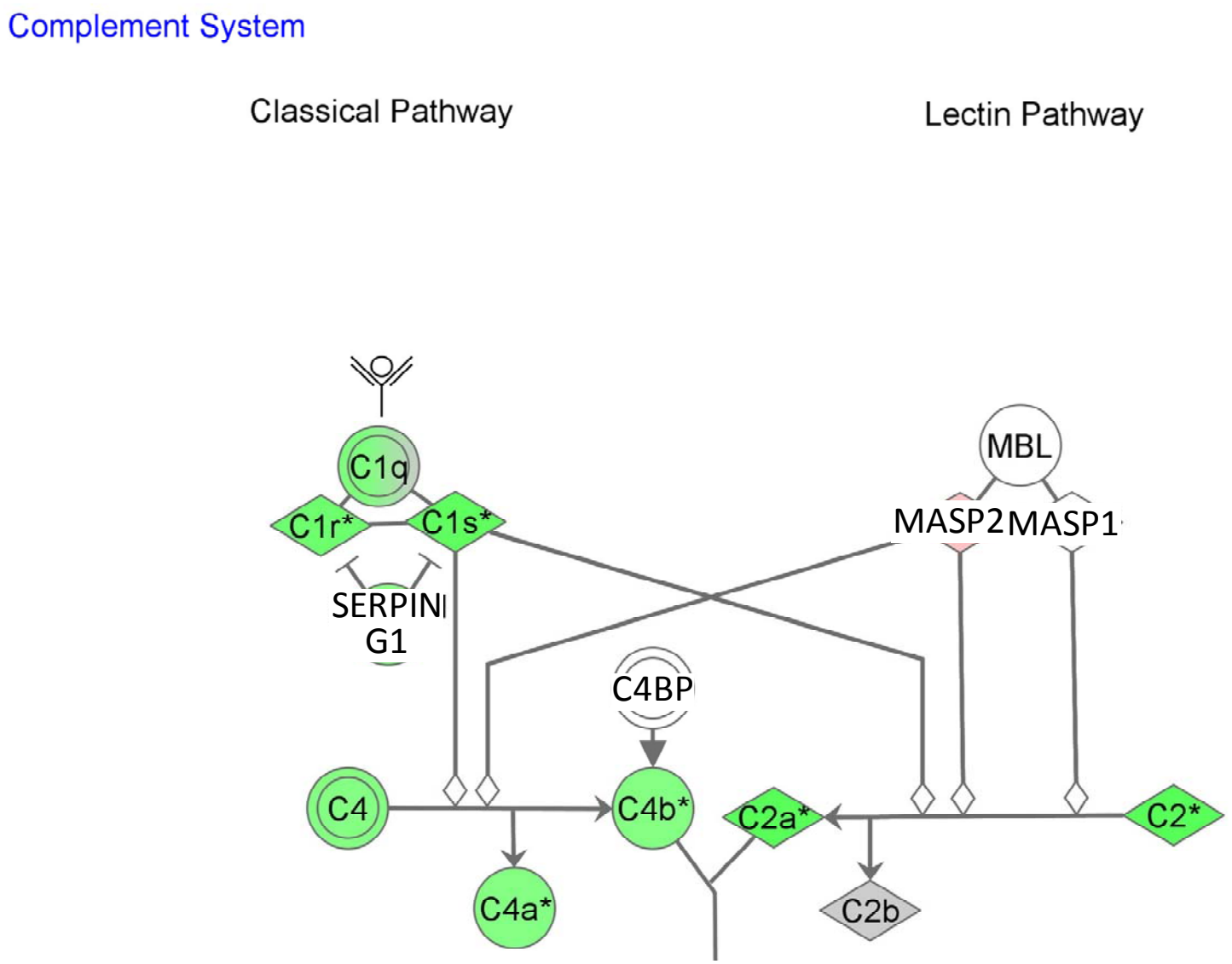

PPs also induced stress modifier genes in mouse liver, which maintain the proteome. Proteome maintenance genes consist of heat shock proteins (Hsps, chaperones) and proteasome components (26S proteosome). Hsps stabilize unfolded proteins preventing aggregation while the ubiquitin-proteasome pathway removes aged, damaged, and misfolded proteins. Induction of proteome maintenance by PPARα suggests a protective role in response to oxidative stress [45], since liver and primary hepatocytes from null mice are more sensitive to chemical induced oxidative stress [46]. In the present study, except alternative β form subunits (Psmb8, 9 and 10) for the immuno-proteasome assembly, most of proteasome subunits were induced. Proteasome inhibitor Psmf1 (PI31) was also induced which interferes with the maturation of immune-proteasome precursor complexes [47]. Moreover, most Hsp genes were induced by PP in mouse liver. In fact, induction of stress responsive genes activation was shown at late time points (8 ~ 24 h), possible due to oxidative stress as a result of fatty acid oxidation from increased peroxisomal activation.

The over-representation of genes associated with cell cycle and apoptosis is consistent with hepatomegaly as well as hyperplastic and hypertrophic hepatocyte growth. The induction of several cell cycle and DNA damage repair genes, such as Chek1, Prkdc, Mcm, and Rad51, by Wy-14,643 is abolished in PPARα null mice [48]. This suggests sustained PPARα activation leads to impaired cell cycle regulation and increased DNA damage by oxidative stress possibly contributing to hepatocarcinogenicity in rodents since Wy-14,643 is considered a non-genotoxic hepatocarcinogen in rodents [38, 39].

In mouse liver, repressed genes were associated with immune and acute inflammatory responses consistent with PP repression reported in cynomolgus monkey [49] and rat [50]. The complement cascade triggers inflammatory responses while the coagulation pathway contributes

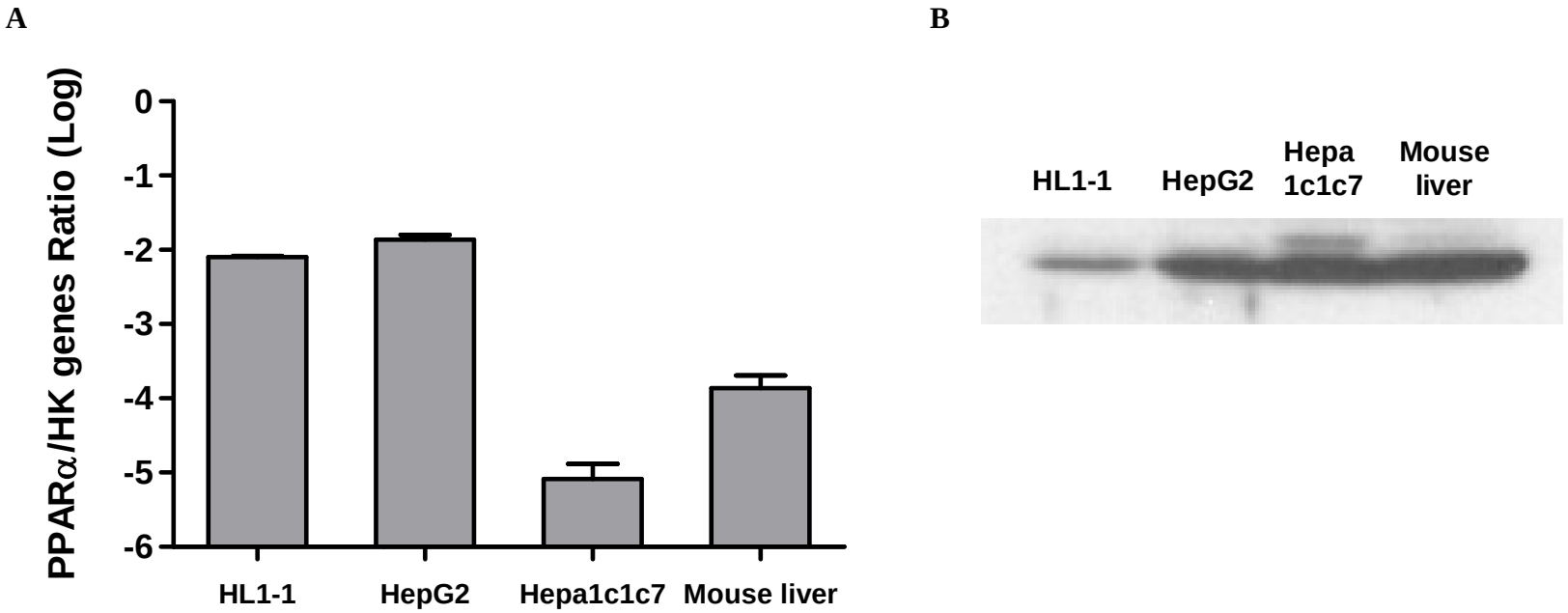

Figure 29. Basal PPARα mRNA and protein levels.
(A) PPARα mRNA levels in HL1-1, HepG2, and Hepa1c1c7 cells as well as C57BL/6 mouse liver were examined by QRT-PCR using species-specific primers. PPARα mRNA levels are normalized to the geometric mean of housekeeping genes (HK) (Hprt, Gapdh and Actb). Bars are mean ± SE, N = 3. (B) Representative Western blot for PPARα.

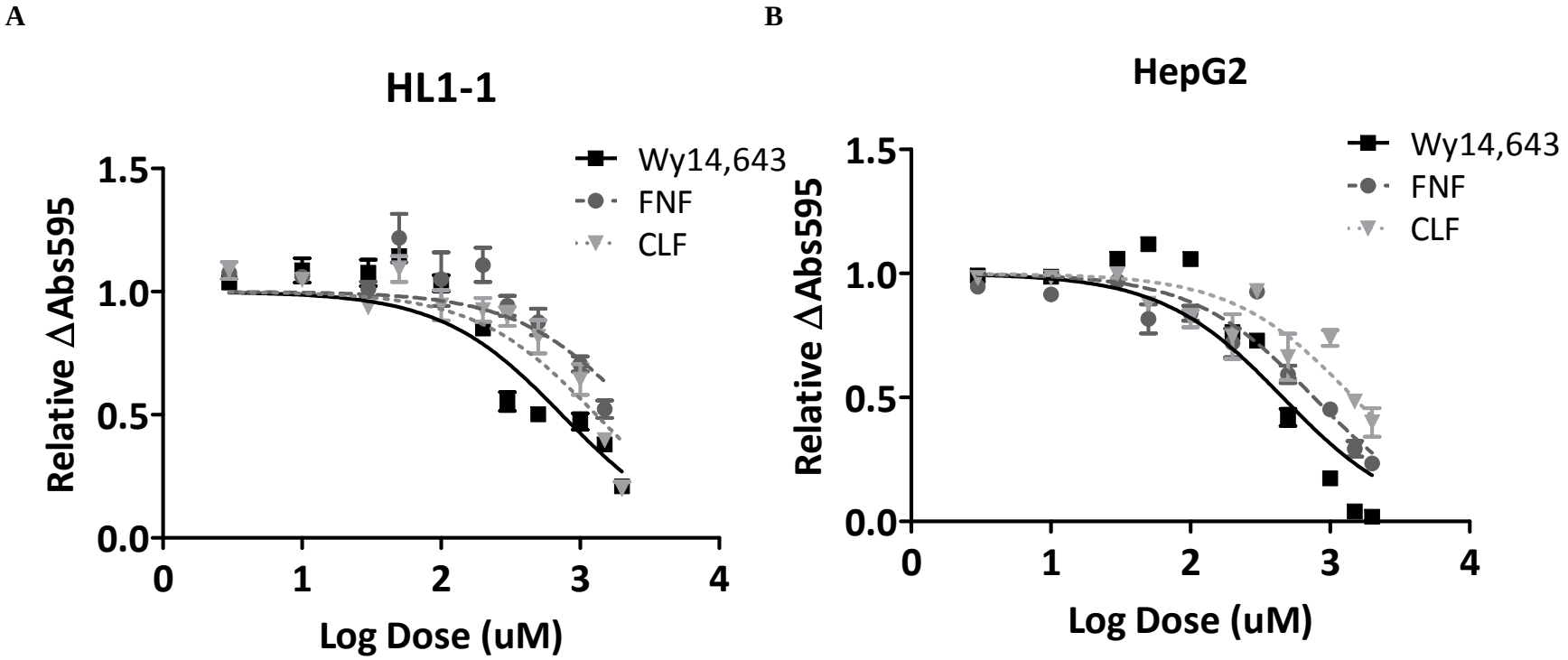

Figure 30. Cytotoxicity testing.
Cytotoxicity of Wy-14,643, fenofibrate (FNF) and clofibrate (CLF) were measured by MTT assay in (A) human liver stem cells HL1-1 and (B) human hepatoma cells HepG2. Bars are mean ± SE, N = 3.

Table 12. Cytotoxicity of PPs in human cell lines

	IC_{50} (μM)	
	HL1-1	HepG2
Wy-14,643	740 ± 141	459 ± 108
fenofibrate	2607 ± 712	767 ± 113
clofibrate	1301 ± 223	1473 ± 233

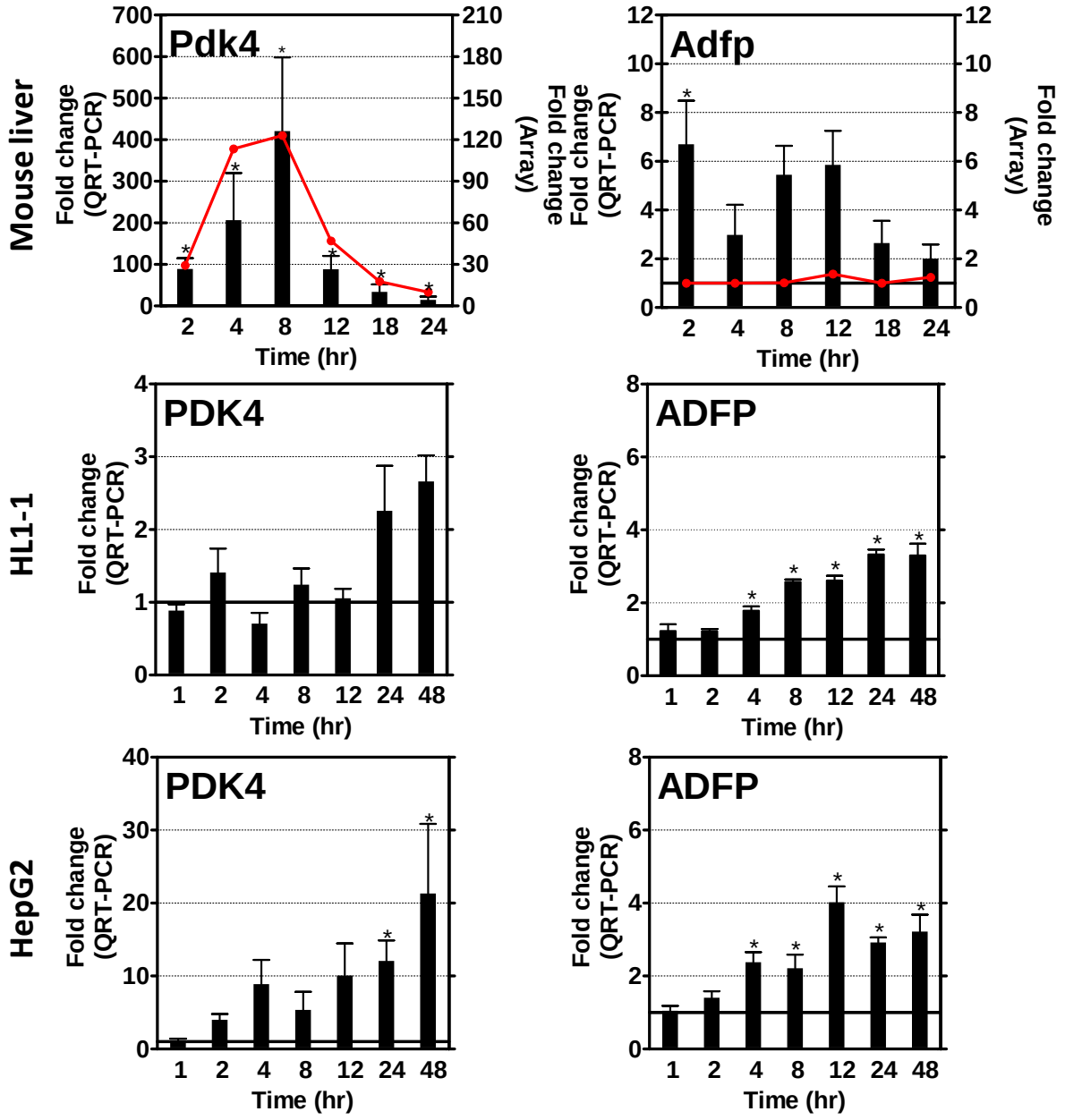

Figure 31. Comparative analysis of *in vivo* mouse liver and *in vitro* human HL1-1 and HepG2 temporal gene expression elicited by Wy-14,643.
Fold changes were calculated relative to time-matched vehicle controls. Bars (left axis) and lines (right axis) represent QRT-PCR and microarray data, respectively. Bars are mean ± SE for the average fold change, *p < 0.05 for QRT-PCR, N = 3.

Figure 31 (Cont'd)

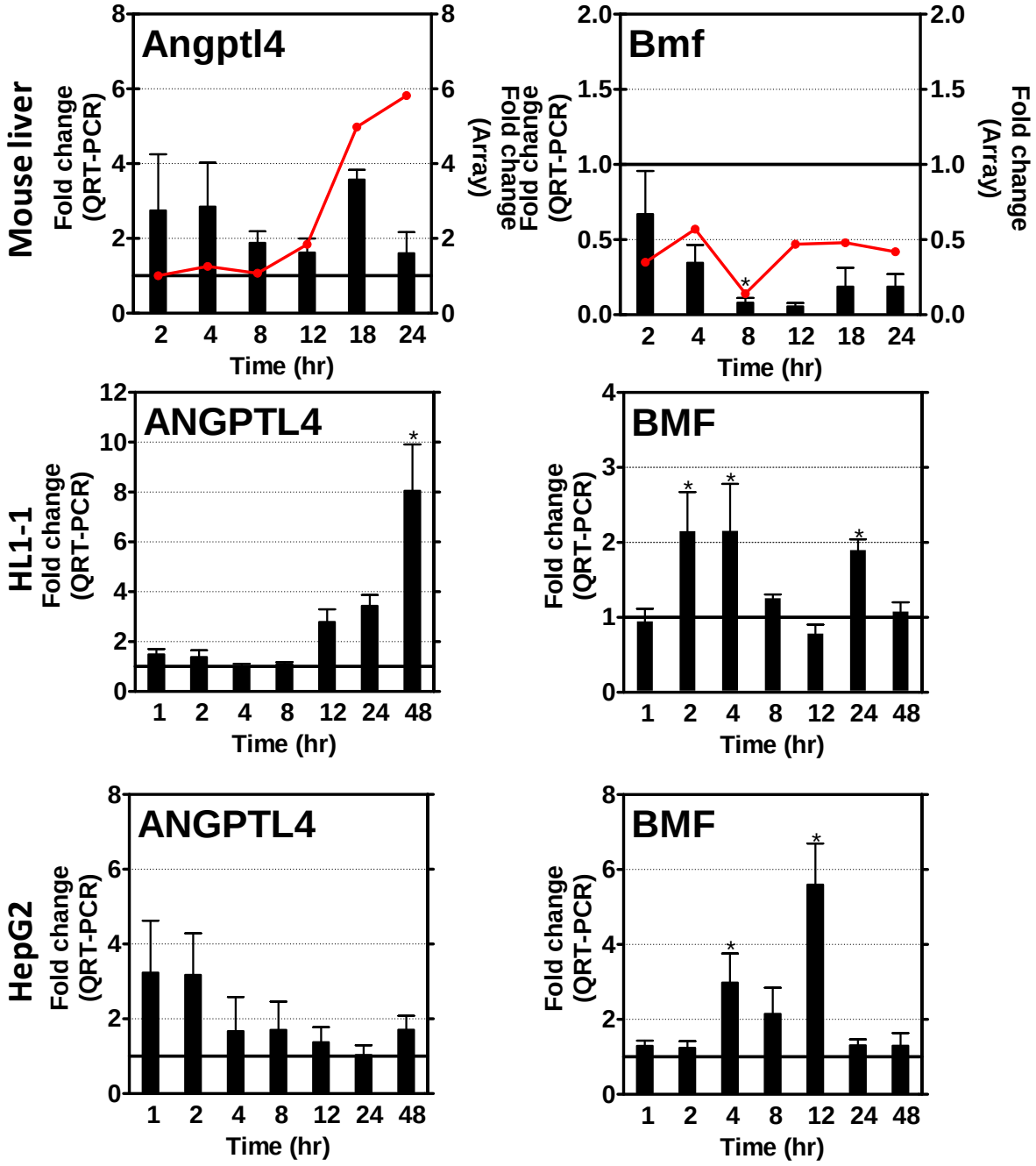

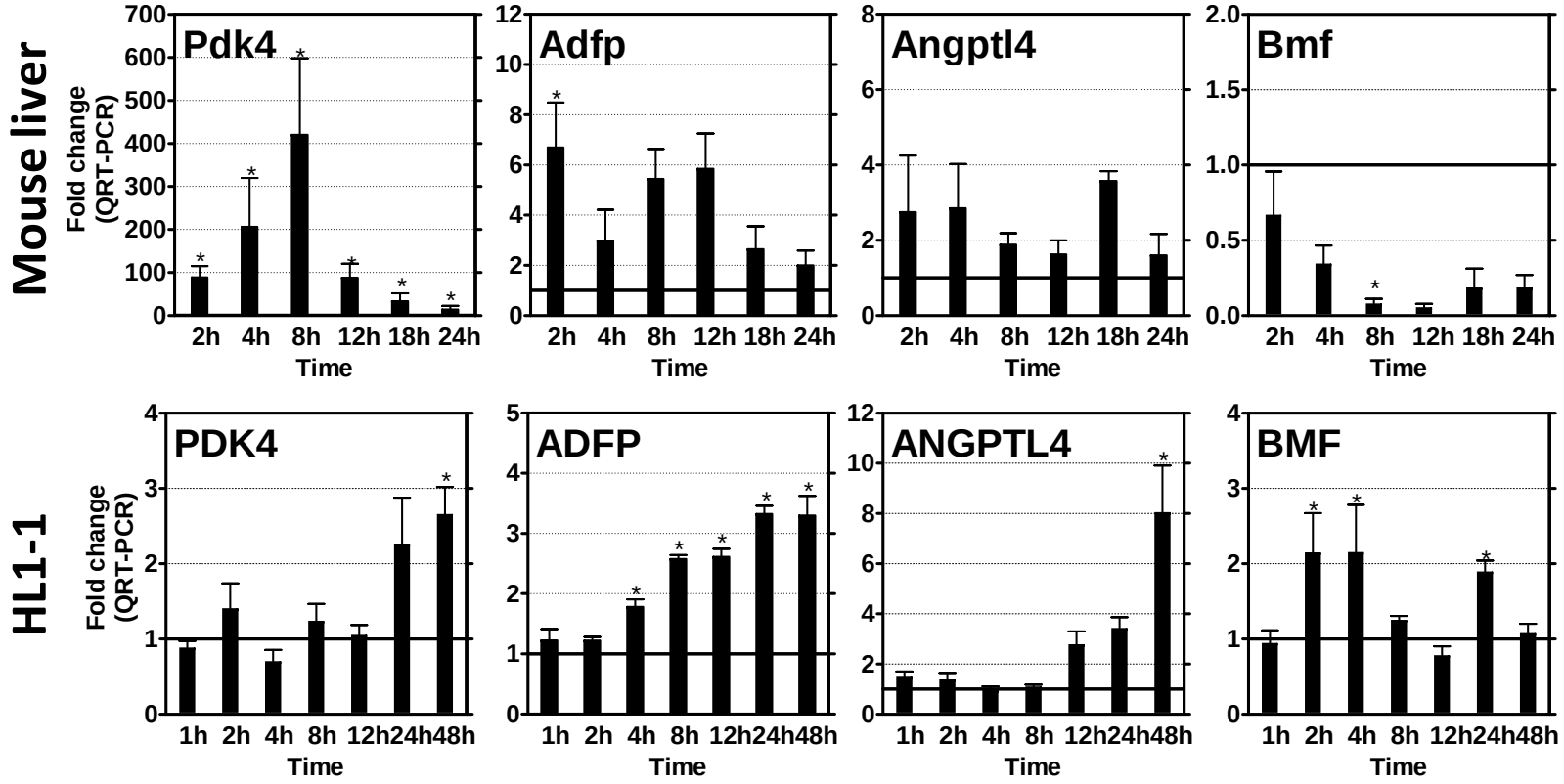

Figure 32. Comparative analysis of *in vivo* mouse liver and *in vitro* human liver stem cell (HL1-1) time course studies with Wy-14,643 treatment.

All fold changes were calculated relative to time-matched vehicle controls. Bars represent QRT-PCR (human *in vitro*) and microarray data (mice *in vivo*), respectively. Bars are mean ± SE for the average fold change, *$p < 0.05$ for QRT-PCR, N = 3.

Figure 32 (Cont'd)

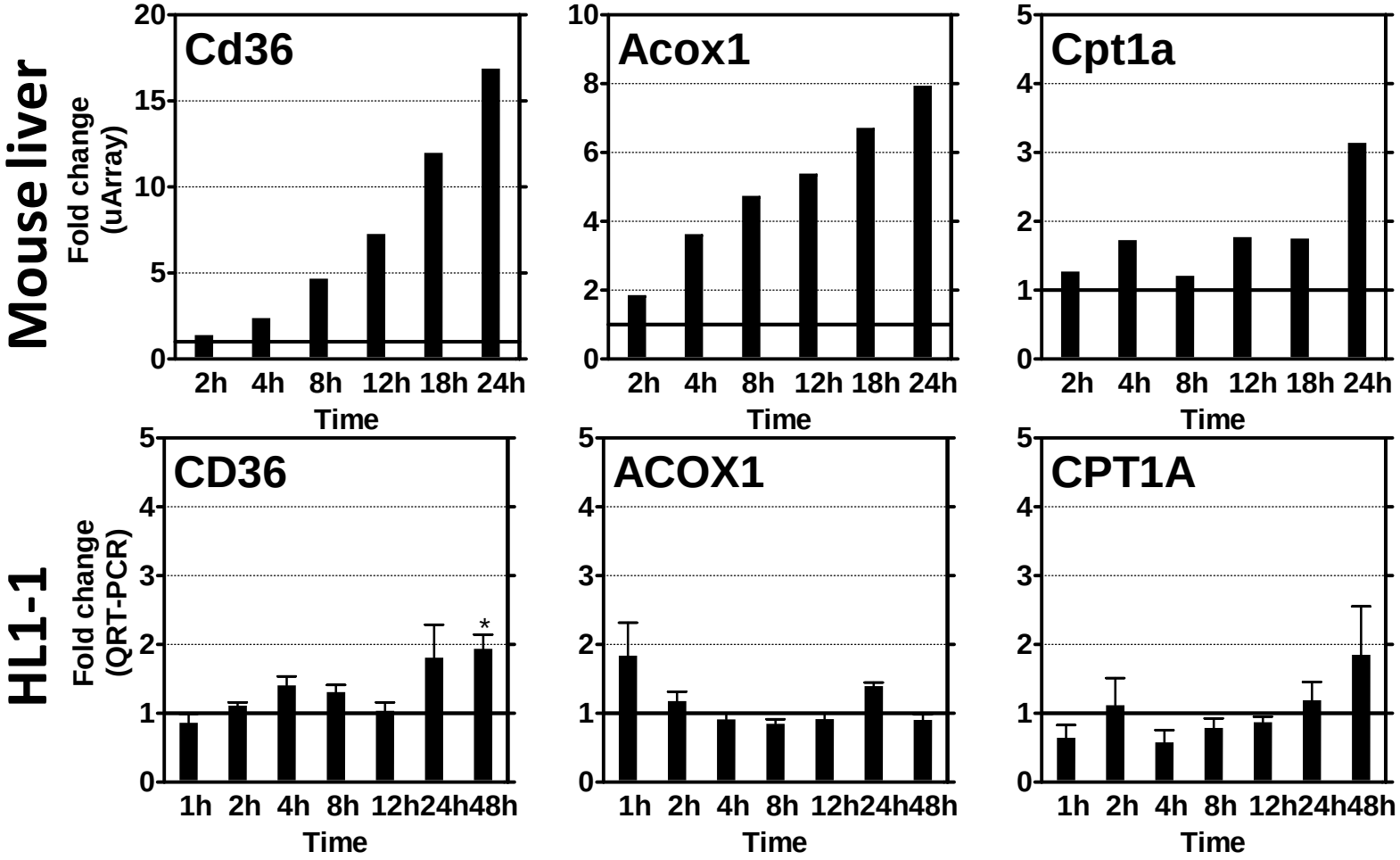

Figure 32 (Cont'd)

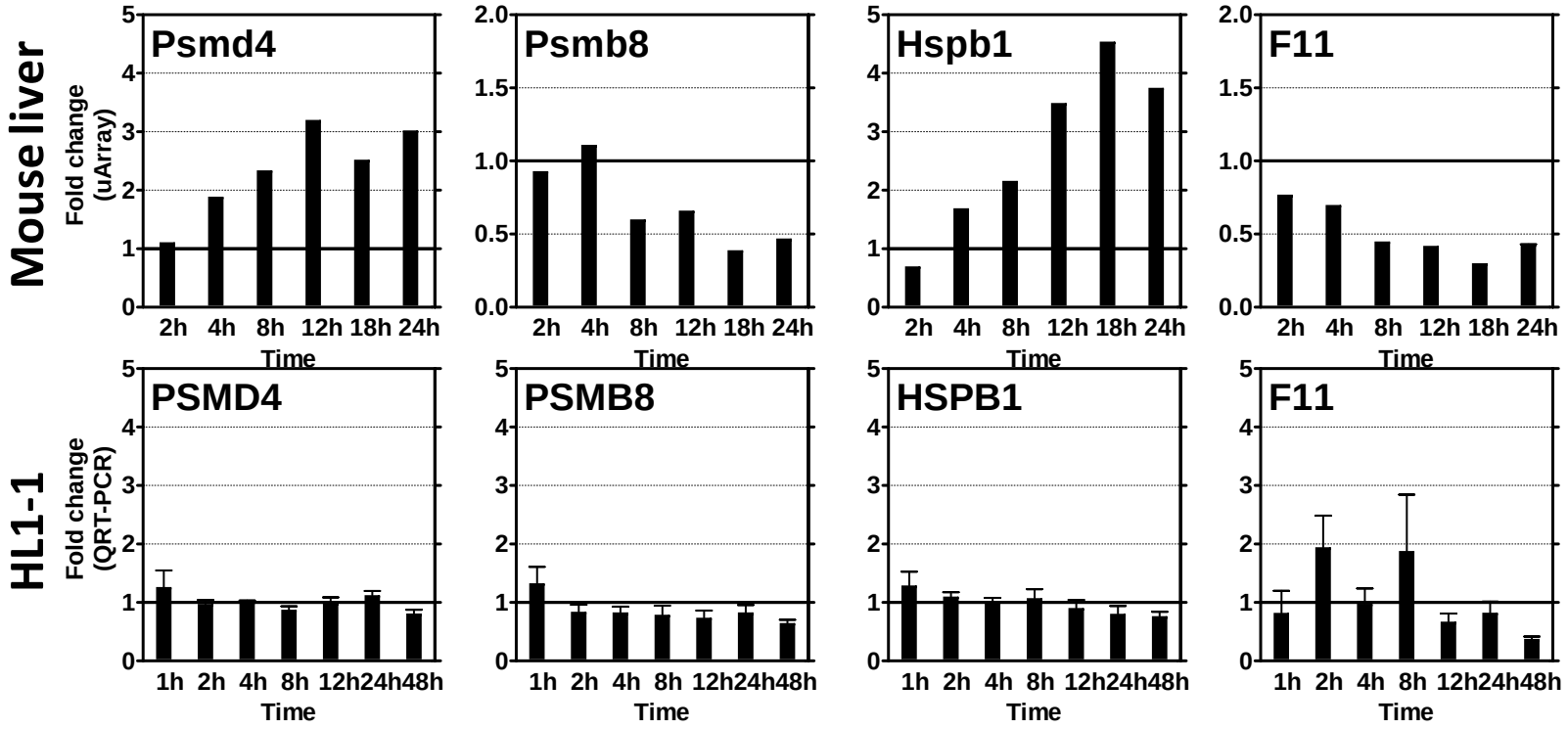

to the innate immune system. The PP-induced anti-inflammatory response inhibits nuclear translocation of nuclear factor-kB (NF-kB) p65 subunit and phosphorylation of the activator protein-1 (AP-1) c-jun subunit [51], which reduces pro-inflammatory signals such as interleukin-1 (IL-1), tumor necrosis factor-α (TNF-α), and inducible nitric oxide synthase (iNOS) as well as cyclooxygenase-2 (COX-2) expression [51-53]. PPARα also induces anti-inflammatory genes such as interleukin-1 receptor antagonist (IL-1ra) [54]. Moreover, leukotriene B4 (LTB4), a powerful chemotactic inflammatory eicosanoid and endogenous PPARα ligand, triggers feedback inhibition through activation of the β- and ω-oxidation pathways that degrade LTB4. PPARα null mice also have a prolonged inflammatory response when compared to wild-type controls [55]. The anti-inflammatory response and improved lipid profiles elicited by PPs have also been investigated in methionine and choline deficient (MCD) diet-induced steatohepatitis in mice [56] and as a dyslipidemia treatment for non-alcoholic fatty liver disease (NAFLD) patients [57, 58].

Comparison of *in vivo* mouse liver and *in vitro* human liver cell (i.e., HL1-1 and HepG2) responses elicited by Wy-14,643 identified common as well as divergent responses. In HL1-1 cells, lipid trafficking and metabolism related genes including CD36, PDK4, ADFP and ANGPTL4 were induced, but ACOX1 and CPT1A, which regulate fatty acid oxidation, were not affected by PP. In addition, the differential expression of lipid metabolism related genes was generally lower in HL1-1 cells compared to mouse liver. In addition, proteasome maintenance and coagulation factor genes were also unresponsive to Wy-14,643 in HL1-1 cells. Some of these species-specific responses can be explained by differences in PPARα expression levels, ligand activation, and biological responses [20, 43, 59, 60]. For example, primates and humans appear to be resistant to PP-mediated peroxisome proliferation induction and hepatocarcinoma

development due to lower PPARα expression levels [18, 61] and the expression of splice variants [62]. Differences in the promoter regions of PPARα target genes may also account for some species-specific response [63]. Furthermore, the expression of different coactivator proteins (i.e. PBP/MED1) necessary for PPARα-mediated transactivation between species may be a contributing factor [19, 64, 65]. The lack of exogenous soluble factors, extracellular matrix components, and cell-cell interactions can also affect *in vitro* cellular functions [66]. For example, HL1-1 cells lack communication with other hepatic non-parenchymal sub-populations such as Kupffer, biliary, endothelial and stellate cells that likely affect responsiveness and function.

The species–specific expression of the tumor suppressor Bmf is intriguing since PPARα agonists increase hepatocellular replication and inhibit apoptosis in rodents, but induce apoptosis in human models [67, 68]. The Bcl-2 family of proteins, can be either pro-apoptotic or anti-apoptotic regulators in cell proliferation/differentiation and contribute to tumorigenesis when their balance is altered. Bmf, a Bcl-2 family member, is pro-apoptotic gene which is repressed by Wy-14,643 in mouse liver, but is induced in human cell models. It binds and neutralizes anti-apoptotic Bcl-2 proteins triggering Bax/Bak activation and caspase-mediated cell apoptosis [69]. Moreover, rodent-specific peroxisomal β-oxidation induction produces hydrogen peroxide, and the potential for oxidative damage. Overall, β-oxidation related gene changes are greater in rodent than human models and consistent with rodent-specific tumorigenesis elicited by PPs. The species-specific divergent regulation of Bmf may be another factor contributing to PP carcinogenicity in rodents but not humans.

In summary, Wy-14,643 elicited gene expression responses highly overlapped with clofibrate-mediated responses and reflected PPARα-mediated regulation of fatty acid metabolism,

proteome maintenance, cell cycle, immune suppression and anti-inflammatory responses. HL1-1 human liver stem cells expressed functional PPARα and some prototypical PPARα response genes were differentially expressed by Wy-14,643 treatment. However there are many mouse response genes which were not responding or differentially regulated in HL1-1. This study also provides insight into key events that may contribute to the species-specific tumorigenic effects of PPs that warrant further investigation.

REFERENCES

REFERENCES

1. Desvergne, B. and W. Wahli, *Peroxisome proliferator-activated receptors: nuclear control of metabolism.* Endocr Rev, 1999. **20**(5): p. 649-88.

2. Pyper, S.R., et al., *PPARalpha: energy combustion, hypolipidemia, inflammation and cancer.* Nucl Recept Signal, 2010. **8**: p. e002.

3. Ahmed, W., et al., *PPARs and their metabolic modulation: new mechanisms for transcriptional regulation?* J Intern Med, 2007. **262**(2): p. 184-98.

4. Peraza, M.A., et al., *The toxicology of ligands for peroxisome proliferator-activated receptors (PPAR).* Toxicol Sci, 2006. **90**(2): p. 269-95.

5. Berger, J.P., T.E. Akiyama, and P.T. Meinke, *PPARs: therapeutic targets for metabolic disease.* Trends Pharmacol Sci, 2005. **26**(5): p. 244-51.

6. Lalloyer, F. and B. Staels, *Fibrates, glitazones, and peroxisome proliferator-activated receptors.* Arterioscler Thromb Vasc Biol, 2010. **30**(5): p. 894-9.

7. Auboeuf, D., et al., *Tissue distribution and quantification of the expression of mRNAs of peroxisome proliferator-activated receptors and liver X receptor-alpha in humans: no alteration in adipose tissue of obese and NIDDM patients.* Diabetes, 1997. **46**(8): p. 1319-27.

8. Thorp, J.M. and W.S. Waring, *Modification of metabolism and distribution of lipids by ethyl chlorophenoxyisobutyrate.* Nature, 1962. **194**: p. 948-9.

9. Reddy, J.K., D.L. Azarnoff, and C.E. Hignite, *Hypolipidaemic hepatic peroxisome proliferators form a novel class of chemical carcinogens.* Nature, 1980. **283**(5745): p. 397-8.

10. Lee, S.S., et al., *Targeted disruption of the alpha isoform of the peroxisome proliferator-activated receptor gene in mice results in abolishment of the pleiotropic effects of peroxisome proliferators.* Mol Cell Biol, 1995. **15**(6): p. 3012-22.

11. Peters, J.M., R.C. Cattley, and F.J. Gonzalez, *Role of PPAR alpha in the mechanism of action of the nongenotoxic carcinogen and peroxisome proliferator Wy-14,643.* Carcinogenesis, 1997. **18**(11): p. 2029-33.

12. IARC, *Peroxisome Proliferation and Its Role in Carcinogenesis.* IARC Technical Report, 1995(No. 24.).

13. Ashby, J., et al., *Mechanistically-based human hazard assessment of peroxisome proliferator-induced hepatocarcinogenesis.* Hum Exp Toxicol, 1994. **13 Suppl 2**: p. S1-117.

14. Cattley, R.C., et al., *Do peroxisome proliferating compounds pose a hepatocarcinogenic hazard to humans?* Regul Toxicol Pharmacol, 1998. **27**(1 Pt 2): p. 47-60.

15. Cheung, C., et al., *Diminished hepatocellular proliferation in mice humanized for the nuclear receptor peroxisome proliferator-activated receptor alpha.* Cancer Res, 2004. **64**(11): p. 3849-54.

16. Morimura, K., et al., *Differential susceptibility of mice humanized for peroxisome proliferator-activated receptor alpha to Wy-14,643-induced liver tumorigenesis.* Carcinogenesis, 2006. **27**(5): p. 1074-80.

17. Tugwood, J.D., et al., *Peroxisome proliferator-activated receptors: structures and function.* Ann N Y Acad Sci, 1996. **804**: p. 252-65.

18. Palmer, C.N., et al., *Peroxisome proliferator activated receptor-alpha expression in human liver.* Mol Pharmacol, 1998. **53**(1): p. 14-22.

19. Yu, S. and J.K. Reddy, *Transcription coactivators for peroxisome proliferator-activated receptors.* Biochim Biophys Acta, 2007. **1771**(8): p. 936-51.

20. Ammerschlaeger, M., et al., *Characterization of the species-specificity of peroxisome proliferators in rat and human hepatocytes.* Toxicol Sci, 2004. **78**(2): p. 229-40.

21. Yang, Q., et al., *The PPAR alpha-humanized mouse: a model to investigate species differences in liver toxicity mediated by PPAR alpha.* Toxicol Sci, 2008. **101**(1): p. 132-9.

22. Rakhshandehroo, M., et al., *Comparative analysis of gene regulation by the transcription factor PPARalpha between mouse and human.* PLoS One, 2009. **4**(8): p. e6796.

23. Patrawala, L., et al., *Side population is enriched in tumorigenic, stem-like cancer cells, whereas ABCG2+ and ABCG2- cancer cells are similarly tumorigenic.* Cancer Res, 2005. **65**(14): p. 6207-19.

24. Visvader, J.E. and G.J. Lindeman, *Cancer stem cells in solid tumours: accumulating evidence and unresolved questions.* Nat Rev Cancer, 2008. **8**(10): p. 755-68.

25. Alison, M.R., S. Islam, and S. Lim, *Stem cells in liver regeneration, fibrosis and cancer: the good, the bad and the ugly.* J Pathol, 2009. **217**(2): p. 282-98.

26. Crisafulli, C., et al., *PPAR-alpha contributes to the anti-inflammatory activity of 17beta-estradiol.* J Pharmacol Exp Ther, 2009. **331**(3): p. 796-807.

27. Boverhof, D.R., et al., *Temporal and dose-dependent hepatic gene expression patterns in mice provide new insights into TCDD-Mediated hepatotoxicity.* Toxicol Sci, 2005. **85**(2): p. 1048-63.

28. Kopec, A.K., et al., *Comparative toxicogenomic examination of the hepatic effects of PCB126 and TCDD in immature, ovariectomized C57BL/6 mice.* Toxicol Sci, 2008. **102**(1): p. 61-75.

29. Kopec, A.K., et al., *PCB153-elicited hepatic responses in the immature, ovariectomized C57BL/6 mice: comparative toxicogenomic effects of dioxin and non-dioxin-like ligands.* Toxicol Appl Pharmacol, 2010. **243**(3): p. 359-71.

30. Kopec, A.K., et al., *Automated dose-response analysis and comparative toxicogenomic evaluation of the hepatic effects elicited by TCDD, TCDF, and PCB126 in C57BL/6 mice.* Toxicol Sci, 2010. **118**(1): p. 286-97.

31. Kim, S., et al., *Comparative analysis of AhR-mediated TCDD-elicited gene expression in human liver adult stem cells.* Toxicol Sci, 2009. **112**(1): p. 229-44.

32. Eckel, J.E., et al., *Empirical bayes gene screening tool for time-course or dose-response microarray data.* J Biopharm Stat, 2004. **14**(3): p. 647-70.

33. Burgoon, L.D. and T.R. Zacharewski, *dbZach toxicogenomic information management system.* Pharmacogenomics, 2007. **8**(3): p. 287-91.

34. Saeed, A.I., et al., *TM4: a free, open-source system for microarray data management and analysis.* Biotechniques, 2003. **34**(2): p. 374-8.

35. Dennis, G., Jr., et al., *DAVID: Database for Annotation, Visualization, and Integrated Discovery.* Genome Biol, 2003. **4**(5): p. P3.

36. Rozen, S. and H. Skaletsky, *Primer3 on the WWW for general users and for biologist programmers.* Methods Mol Biol, 2000. **132**: p. 365-86.

37. Vandesompele, J., et al., *Accurate normalization of real-time quantitative RT-PCR data by geometric averaging of multiple internal control genes.* Genome Biol, 2002. **3**(7): p. RESEARCH0034.

38. Reddy, J.K., et al., *Mitogenic and carcinogenic effects of a hypolipidemic peroxisome proliferator, [4-chloro-6-(2,3-xylidino)-2-pyrimidinylthio]acetic acid (Wy-14, 643), in rat and mouse liver.* Cancer Res, 1979. **39**(1): p. 152-61.

39. Suzuki, T., et al., *Evaluation of in vivo liver genotoxic potential of Wy-14,643 and piperonyl butoxide in rats subjected to two-week repeated oral administration.* Arch Toxicol, 2010. **84**(6): p. 493-500.

40. Cayen, M.N., *Disposition, metabolism and pharmacokinetics of antihyperlipidemic agents in laboratory animals and man.* Pharmacol Ther, 1985. **29**(2): p. 157-204.

41. NTP, *NTP Technical Report on the Toxicity Studies of Wy-14,643 (CAS No. 50892-23-4) Administered in Feed to Sprague-Dawley Rats, B6C3F1 Mice, and Syrian Hamsters.* Toxicity Report Series, 2007. **no. 62**(NIH Publication no. 08-4419).

42. Willson, T.M., et al., *The PPARs: from orphan receptors to drug discovery.* J Med Chem, 2000. **43**(4): p. 527-50.

43. Klaunig, J.E., et al., *PPARalpha agonist-induced rodent tumors: modes of action and human relevance.* Crit Rev Toxicol, 2003. **33**(6): p. 655-780.

44. Blanquart, C., et al., *Peroxisome proliferator-activated receptor alpha (PPARalpha) turnover by the ubiquitin-proteasome system controls the ligand-induced expression level of its target genes.* J Biol Chem, 2002. **277**(40): p. 37254-9.

45. Ren, H., et al., *Regulation of Proteome Maintenance Gene Expression by Activators of Peroxisome Proliferator-Activated Receptor alpha.* PPAR Res, 2010. **2010**: p. 727194.

46. Anderson, S.P., et al., *The transcriptional response to a peroxisome proliferator-activated receptor alpha agonist includes increased expression of proteome maintenance genes.* J Biol Chem, 2004. **279**(50): p. 52390-8.

47. Zaiss, D.M., et al., *PI31 is a modulator of proteasome formation and antigen processing.* Proc Natl Acad Sci U S A, 2002. **99**(22): p. 14344-9.

48. Qu, A., et al., *PPARalpha-dependent activation of cell cycle control and DNA repair genes in hepatic nonparenchymal cells.* Toxicol Sci, 2010. **118**(2): p. 404-10.

49. Cariello, N.F., et al., *Gene expression profiling of the PPAR-alpha agonist ciprofibrate in the cynomolgus monkey liver.* Toxicol Sci, 2005. **88**(1): p. 250-64.

50. Kramer, J.A., et al., *Transcription profiling distinguishes dose-dependent effects in the livers of rats treated with clofibrate.* Toxicol Pathol, 2003. **31**(4): p. 417-31.

51. Ramanan, S., et al., *PPARalpha ligands inhibit radiation-induced microglial inflammatory responses by negatively regulating NF-kappaB and AP-1 pathways.* Free Radic Biol Med, 2008. **45**(12): p. 1695-704.

52. Delerive, P., et al., *Peroxisome proliferator-activated receptor alpha negatively regulates the vascular inflammatory gene response by negative cross-talk with transcription factors NF-kappaB and AP-1.* J Biol Chem, 1999. **274**(45): p. 32048-54.

53. Delerive, P., et al., *Induction of IkappaBalpha expression as a mechanism contributing to the anti-inflammatory activities of peroxisome proliferator-activated receptor-alpha activators.* J Biol Chem, 2000. **275**(47): p. 36703-7.

54. Stienstra, R., et al., *The Interleukin-1 receptor antagonist is a direct target gene of PPARalpha in liver.* J Hepatol, 2007. **46**(5): p. 869-77.

55. Devchand, P.R., et al., *The PPARalpha-leukotriene B4 pathway to inflammation control.* Nature, 1996. **384**(6604): p. 39-43.

56. Ip, E., et al., *Administration of the potent PPARalpha agonist, Wy-14,643, reverses nutritional fibrosis and steatohepatitis in mice.* Hepatology, 2004. **39**(5): p. 1286-96.

57. Madej, A., et al., *Effects of fenofibrate on plasma cytokine concentrations in patients with atherosclerosis and hyperlipoproteinemia IIb.* Int J Clin Pharmacol Ther, 1998. **36**(6): p. 345-9.

58. Fernandez-Miranda, C., et al., *A pilot trial of fenofibrate for the treatment of non-alcoholic fatty liver disease.* Dig Liver Dis, 2008. **40**(3): p. 200-5.

59. Lawrence, J.W., et al., *Differential gene regulation in human versus rodent hepatocytes by peroxisome proliferator-activated receptor (PPAR) alpha. PPAR alpha fails to induce peroxisome proliferation-associated genes in human cells independently of the level of receptor expresson.* J Biol Chem, 2001. **276**(34): p. 31521-7.

60. Gonzalez, F.J. and Y.M. Shah, *PPARalpha: Mechanism of species differences and hepatocarcinogenesis of peroxisome proliferators.* Toxicology, 2007.

61. Walgren, J.E., D.T. Kurtz, and J.M. McMillan, *Expression of PPAR(alpha) in human hepatocytes and activation by trichloroacetate and dichloroacetate.* Res Commun Mol Pathol Pharmacol, 2000. **108**(1-2): p. 116-32.

62. Gervois, P., et al., *A truncated human peroxisome proliferator-activated receptor alpha splice variant with dominant negative activity.* Mol Endocrinol, 1999. **13**(9): p. 1535-49.

63. Varanasi, U., et al., *Identification of a peroxisome proliferator-responsive element upstream of the human peroxisomal fatty acyl coenzyme A oxidase gene.* J Biol Chem, 1996. **271**(4): p. 2147-55.

64. Jia, Y., et al., *Transcription coactivator PBP, the peroxisome proliferator-activated receptor (PPAR)-binding protein, is required for PPARalpha-regulated gene expression in liver.* J Biol Chem, 2004. **279**(23): p. 24427-34.

65. Matsumoto, K., et al., *Critical role for transcription coactivator peroxisome proliferator-activated receptor (PPAR)-binding protein/TRAP220 in liver regeneration and PPARalpha ligand-induced liver tumor development.* J Biol Chem, 2007. **282**(23): p. 17053-60.

66. Guillouzo, A., *Liver cell models in in vitro toxicology.* Environ Health Perspect, 1998. **106 Suppl 2**: p. 511-32.

67. Kubota, T., et al., *Fenofibrate induces apoptotic injury in cultured human hepatocytes by inhibiting phosphorylation of Akt.* Apoptosis, 2005. **10**(2): p. 349-58.

68. Martinasso, G., et al., *Involvement of PPARs in Cell Proliferation and Apoptosis in Human Colon Cancer Specimens and in Normal and Cancer Cell Lines.* PPAR Res, 2007. **2007**: p. 93416.

69. Puthalakath, H., et al., *Bmf: a proapoptotic BH3-only protein regulated by interaction with the myosin V actin motor complex, activated by anoikis.* Science, 2001. **293**(5536): p. 1829-32.

CHAPTER 6

CHAPTER 6

CONCLUSIONS AND FUTURE RESEARCH

The preceding studies have established and evaluated human liver stem cells as a novel human *in vitro* model for toxicogenomic studies. Human liver HL1-1 stem cells were shown to express functional AhR and PPARα, and their gene expression profiles were identified using a toxicogenomic approach. Responses of HL1-1 cells were compared with human hepatoma cells HepG2 and mouse *in vivo* hepatic expression to elucidate molecular mechanisms of receptor-mediated toxicity. Receptor activation elicited complex temporal and species-conserved and -specific gene expression responses, which could be related to physiological and toxicological outcomes of exposure. Many cross-species, cross-model conserved response genes were consistent with previously reported receptor-mediated physiological outcomes such as tumor development and alterations in lipid metabolism. Although some common pathways are affected, the data suggest that species-specific receptor-mediated gene expression profiles imply species-specific regulons and provide insight into key events that may contribute to the species-specific effects which warrant further investigation. However, new research opportunities have also been identified that warrant further exploration in order to further elucidate species-specific receptor-mediated mechanisms of toxicity as outlined below.

COMPARATIVE STUDIES FOR FURTHER EVALUATION

Data presented in Chapter 4 and 5 provide baseline quantitative response data on the human liver stem cells and mouse liver following treatment with TCDD (AhR ligand) and Wy-14,643 (PPARα ligand), which can be used in future comparative studies. Functional

categorization of response genes a significant overlap between lipid metabolism related genes regulated by AhR and PPARα. These data suggest a possible AhR/PPARα cross-talk in lipid metabolism modulation which is in agreement with previously published interactions [1, 2]. Co-treatment studies using AhR and PPARα inducers could further elucidate potential AhR/PPARα cross-talk mechanisms involved in lipid metabolism modulation.

Freshly isolated primary hepatocytes from intact liver tissues are often referred as the gold *in vitro* model standard for evaluating hepatic metabolism and toxicity testing [3]. TCDD toxicogenomic studies utilizing primary hepatocytes from human, mouse and rat were recently conducted in this lab (Forgacs *et al*., in preparation). To further assess human liver stem cells as an *in vitro* model, the results from human primary hepatocytes should be compared to human liver stem cells from Chapter 4, which will expand the understanding of AhR-mediated molecular level responses in human. Additionally, the same approach could be applied to PPARα-mediated gene expression profiles using comparative analysis with recently published human primary hepatocytes data [4].

MODEL SYSTEM IMPROVEMENTS AND FURTHER APPLICATION OF HUMAN LIVER STEM CELLS

The development of immortalized HLhT1 cell line and their AhR- and PPARα-mediated gene expression responses comparison with parental HL1-1 cell was described in Chapter 3. Basal expression level of receptors and their responses are comparable to parental cell, as confirmed using a subset of responsive genes (CYP1A1, CYP1B1, SLC7A5 and ALDH1A3). Immortalized human liver stem cells are a very promising alternative model, which is amenable to high-throughput and mechanistic studies. However, further characterization including whole-genome gene expression profiling is required.

In Chapter 3, the development of hepatocyte differentiation methods was suggested which may re-establish the expression of PXR and other hepatic metabolizing enzymes. Liver stem cells give rise to both hepatocytes and bile duct epithelial cells also known as cholangiocytes. The growth and differentiation of hepatoblasts is regulated by various extrinsic signals and complex regulatory mechanisms [5, 6]. However, hepatocyte differentiation methods development from ES (embryonic stem) cells, MSC (mesenchymal stem cells) and even IPS (induced pluripotent stem) cells have been attempted by many groups [7, 8]. A major limitation of differentiated stem cell application in standardized high-throughput studies is the prominent heterogeneity of cell types. However, transgenic molecular enrichment and selection, and over-expression of transcription factors facilitate enhancement of the purity of the targeted differentiated cells [9].

Two dimensional *in vitro* cultures on plastic surfaces and growing in log phase in high oxygen tension, unlike *in vivo* situation, may cause non-relevant responses. To develop cell culture conditions closely mimicking the *in vivo* conditions, application of structural material resembling the complex extracellular environment such as Matrigel and three dimensional organoids co-cultured with their normal stromal cells providing specific organ-requiring micro-environmental factors has been proposed [10]. Additionally, clinical application of liver stem cells to regeneration of the liver parenchyma as a therapeutic option of end-stage liver disease (cirrhosis) is being investigated as an alternative approach to liver repair and regeneration [11].

ALTERNATIVE TECHNOLOGIES FOR TOXICOGENOMICS

Microarrays are limited in terms of probe coverage due to integrity and completion of sequence information and gene annotation. Additionally, the data from microarrays could be affected by probe affinity to target genes and non-specific hybridization. Recently, genome-wide

sequencing has been enabled in biomedical research with the development of modern NGS (next generation sequencing). ChIP (Chromatin immunoprecipitation)-sequencing and RNA-sequencing analysis with NGS can be utilized for motif finding, assessment of differential gene expression, novel target gene discovery, splice isoform expression, and SNP (single-nucleotide polymorphism) annotations with their functional relation [12]. Application of NGS should be considered in future studies to provide more comprehensive analyses.

Because of the limited intra-laboratory resources, -omics data from public repositories such as GEO (www.ncbi.nlm.nih.gov/geo), ArrayExpress (www.ebi.ac.uk/arrayexpress), CEBS (http://cebs.niehs.nih.gov), and DrugMatrix (https://ntp.niehs.nih.gov/drugmatrix) could also be used for comparative analyses. The growth of publicly available -omics data sets will increasingly drive integrated computational meta-analysis. Meta-analysis allows merging of several -omics data sets such as genomics, proteomics and metabolomics into knowledge through cross-examination of data and network reconstruction. Additional integrative analyses with RNA interference perturbations will provide more definitive evidence of functionally important connections and relationships within regulatory pathways. Systems integration of different experimental data into a consistent meta-analysis will guide more closely to the true biology involved in toxicity.

REFERENCES

REFERENCES

1. Villard, P.H., et al., *PPARalpha transcriptionally induces AhR expression in Caco-2, but represses AhR pro-inflammatory effects.* Biochem Biophys Res Commun, 2007. **364**(4): p. 896-901.

2. Shaban, Z., et al., *AhR and PPARalpha: antagonistic effects on CYP2B and CYP3A, and additive inhibitory effects on CYP2C11.* Xenobiotica, 2005. **35**(1): p. 51-68.

3. Madan, A., et al., *Effects of prototypical microsomal enzyme inducers on cytochrome P450 expression in cultured human hepatocytes.* Drug Metab Dispos, 2003. **31**(4): p. 421-31.

4. Rakhshandehroo, M., et al., *Comparative analysis of gene regulation by the transcription factor PPARalpha between mouse and human.* PLoS One, 2009. **4**(8): p. e6796.

5. Tanaka, M., et al., *Liver stem/progenitor cells: their characteristics and regulatory mechanisms.* J Biochem, 2011. **149**(3): p. 231-9.

6. Gaudio, E., et al., *New insights into liver stem cells.* Dig Liver Dis, 2009. **41**(7): p. 455-62.

7. Ochiya, T., Y. Yamamoto, and A. Banas, *Commitment of stem cells into functional hepatocytes.* Differentiation, 2009.

8. Gallicano, G.I. and L. Mishra, *Hepatocytes from induced pluripotent stem cells: a giant leap forward for hepatology.* Hepatology, 2010. **51**(1): p. 20-2.

9. Ahuja, Y.R., V. Vijayalakshmi, and K. Polasa, *Stem cell test: a practical tool in toxicogenomics.* Toxicology, 2007. **231**(1): p. 1-10.

10. Trosko, J.E. and C.C. Chang, *Factors to consider in the use of stem cells for pharmaceutic drug development and for chemical safety assessment.* Toxicology, 2010. **270**(1): p. 18-34.

11. Zhao, Q., et al., *Stem/progenitor cells in liver injury repair and regeneration.* Biol Cell, 2009. **101**(10): p. 557-71.

12. Werner, T., *Next generation sequencing in functional genomics.* Brief Bioinform, 2010. **11**(5): p. 499-511.